



universität  
wien

# DIPLOMARBEIT

Titel der Diplomarbeit

mTor signalling in primary human lung fibroblasts in 3D cultures

angestrebter akademischer Grad

Magistra der Naturwissenschaften (Mag. rer. nat)

|  |                                    |
|--|------------------------------------|
| Verfasserin / Verfasser:                             | Nina Kramer                        |
| Matrikel-Nummer:                                     | 0445068                            |
| Studienrichtung /Studienzweig<br>(lt. Studienblatt): | Biologie/ Anthropologie            |
| Betreuer:  | Priv. Doz. Mag. Dr. Helmut Dolznig |

Wien, im Dezember 2010



## **Acknowledgements**

I would like to thank Univ. Prof. Mag. Dr. Markus Hengstschläger for giving me the opportunity to work on my diploma thesis in his laboratory and for putting me in touch with Priv. Doz. Mag. Dr. Helmut Dolznig.

I owe thanks to Priv. Doz. Mag. Dr. Helmut Dolznig for teaching me the “spheroid invasion assay”, his support and his never-ending patience.

A special thank goes to Margit Rosner for her technical support, all the productive and interesting discussions and her comments regarding this thesis.

Further thanks go to all labmembers especially to Christiane Fuchs for her help and support.

Finally I want to thank my family, my husband and my friends for all their support and encouragement to help me find my way!





## Summary

3D cell culture is supposed to mimick a tissue-like environment found *in-vivo* and it is used to study molecular and biochemical aspects of many physiologic functions under *in-vitro* conditions. A key regulatory pathway of important cellular functions such as ribosomal biosynthesis, proliferation, metabolism and cell size is the mammalian target of rapamycin (mTOR) pathway. It was previously extensively studied using monolayer culture, however mTOR signalling has not been studied very well in cells cultivated in 3D. Since the environment and the shape of cells can determine its behaviour and gene expression, we wanted to identify differences between 2D and 3D culture in respect to mTOR signalling. Furthermore we were interested in the invasion potential of fibroblasts in collagen gels under these experimental settings. After establishing culture conditions for IMR-90 lung fibroblasts in collagen gels and a harvesting protocol, cells from 2D and 3D culture were subjected to FACS analysis and DNA content and cell size was determined. Spheroid invasion assays were performed in the presence of the specific mTOR inhibitor rapamycin and siRNA mediated knockdowns of raptor- and rictor, two components of different mTOR multiprotein complexes. Immunofluorescence analyses were done with antibodies for mTOR pathway components,  $\alpha$ -phospho Histone H3 and  $\alpha$ -cleaved caspase-3. We found a massive cell size reduction, less proliferation and changes in the granularity in fibroblasts cultivated in 3D as compared to cells in 2D. Altered cell size and cell cycle distribution indicate changes in the mTOR pathway, however immunofluorescence analyses did not show significant differences in the amount or activity of the proteins. Some mTOR pathway components were altered in respect to localisation, e.g. pAKT (S473) displayed a more vesicular like distribution and total AKT protein was upregulated within the nuclei in fibroblasts cultivated in 3D. Furthermore cells cultured in collagen gels displayed reduced invasion after treatment with rapamycin and transfection with raptor and rictor siRNA. The invasive properties of the IMR-90 cells were profoundly reduced upon rictor knockdown, whereas raptor knockdown displayed an intermediate effect. Immunofluorescence analysis showed induction of apoptosis in rapamycin treated spheroids as demonstrated by an increase in the proportion of early apoptotic (cleaved caspase-3<sup>+</sup>) and late apoptotic (cleaved caspase<sup>+</sup>/condensed nuclei<sup>+</sup>) fibroblasts.

In summary we found profound alterations in fibroblasts cultivated in 3D as compared to 2D and an influence of mTOR signalling in the invasive properties of IMR-90 fibroblasts, however, further quantitative evaluation of the mTOR pathway (e.g. by Western blot analysis) is needed to determine the molecular events leading to reduced cell cycle progression and size as well as to a decrease in invasive capacity upon mTOR inhibition.

## **Zusammenfassung**

3D-Zellkultur wird verwendet, um eine gewebeähnliche Umgebung, wie sie *in-vivo* zu finden ist, nachzuahmen. Ein weiterer Verwendungszweck ist die Untersuchung von molekularen und biochemischen Aspekten vieler physiologischer Funktionen unter *in-vitro* Bedingungen. Der „mammalian target of rapamycin (mTOR)-pathway“ ist ein wichtiger Signalweg der Zellen, der essentielle Funktionen wie ribosomale Biosynthese, Zellteilung, Stoffwechsel und Zellgröße kontrolliert. Dieser wurde bisher ausführlich in Monolayerkulturen untersucht, jedoch nicht in Zellen in 3D Kultur. Da die Form und die Umgebung der Zellen ihr Verhalten und ihre Genexpression bestimmen können, wollten wir Unterschiede zwischen Fibroblasten aus 2D- und 3D-Kultur, in Bezug auf den mTOR-Signalweg, identifizieren. Weiters waren wir an ihrem Invasionspotenzial innerhalb der Kollagen-Gele interessiert. Nachdem wir die Kulturbedingungen für IMR-90 Fibroblasten in Kollagen-Gelen und ein Isolations-Protokoll etablierten, wurde der DNA-Gehalt und die Zellgröße von Zellen aus 2D- und 3D-Kultur mit Hilfe von FACS-Analyse bestimmt. „Spheroid invasion assays“ wurden unter Anwesenheit des spezifischen mTOR Inhibitors Rapamycin und siRNA vermittelter knock-downs von Raptor und Rictor, den Komponenten zweier unterschiedlicher mTOR Multiproteinkomplexe, durchgeführt. Immunfluoreszenz-Analysen wurden mit Antikörpern gegen mTOR Komponenten, phospho Histone H3 und cleaved caspase-3 durchgeführt. Im Unterschied zu 2D fanden wir in Fibroblasten aus 3D- Kultur eine massive Reduktion der Zellgröße, geringere Zellteilung und Veränderungen in der Granularität. Veränderte Zellgröße und Zellzyklusverteilung weisen auf Änderungen des mTOR-Signalweges hin, Immunfluoreszenzanalysen zeigten jedoch keine signifikanten Unterschiede in der Menge oder der Aktivität der beteiligten Proteine. Einige Komponenten des mTOR-Signalweges waren in Bezug auf ihre Lokalisation in den Fibroblasten verändert, z. B. pAKT (S473), welches eine vesikulärere Verteilung zeigte und das Totalprotein AKT, das innerhalb der Kerne in 3D Kultur hochreguliert war. Weiters zeigten in Kollagen-Gelen kultivierte Zellen reduzierte Invasion nach Behandlung mit Rapamycin und Transfektion mit Raptor und Rictor siRNA. Die invasiven Eigenschaften von IMR-90 Zellen wurden nach Behandlung mit Rictor siRNA hochgradig reduziert, während die Transfektion mit Raptor siRNA eine mittelgradige Wirkung zeigte. Immunfluoreszenz-Analyse zeigte eine Induktion von Apoptose in Rapamycin behandelten Sphäroiden durch einen erhöhten Anteil von früh (cleaved caspase-3<sup>+</sup>) und spät apoptotischen (cleaved caspase-3<sup>+</sup>/kondensierten Kernen<sup>+</sup>) Fibroblasten.

Zusammenfassend stellten wir Veränderungen in Fibroblasten aus 3D-Kultur verglichen mit 2D-Kultur fest. Weiters fanden wir Einflüsse des mTOR-Signalweges auf die invasiven Eigenschaften von IMR-90 Fibroblasten, allerdings werden noch weitere quantitative Auswertungen des mTOR-Signalweges (zB durch Western-Blot-Analyse) benötigt, um die molekularen Mechanismus, die zu reduzierter Zellgröße und Zellzyklus Verteilung, sowie zu einem Rückgang der invasiven Kapazität durch mTOR-Hemmung führen, zu bestimmen.



## Table of contents

|   |           |
|---|-----------|
| <b>1 INTRODUCTION</b>   | <b>11</b> |
| <b>1.1 WHAT ARE FIBROBLASTS?</b>  | <b>12</b> |
| 1.1.1 FIBROBLAST ORIGIN AND FUNCTION                                    | 12        |
| 1.1.2 FIBROBLAST MORPHOLOGY   | 12        |
| 1.1.3 FETAL LUNG DEVELOPMENT  | 13        |
| <b>1.2 3D CELL CULTURE</b>  | <b>14</b> |
| 1.2.1 FIBROBLASTS IN 3D   | 15        |
| 1.2.2 3D CULTURE METHODS  | 16        |
| 1.2.3 CELL INVASION ASSAYS  | 18        |
| 1.2.4 3D CO-CULTURE METHODS   | 20        |
| <b>1.3 mTOR PATHWAY</b>   | <b>21</b> |
| 1.3.1 mTOR  | 21        |
| 1.3.2 mTORC1 AND mTORC2 ASSEMBLY  | 22        |
| 1.3.3 DOWNSTREAM TARGETS OF mTORC1                                      | 23        |
| 1.3.4 DOWNSTREAM TARGETS OF mTORC2                                      | 23        |
| 1.3.5 UPSTREAM REGULATORS   | 24        |
| 1.3.6 NEGATIVE FEEDBACK-LOOP  | 26        |
| 1.3.7 TREATMENT WITH RAPAMYCIN  | 26        |
| 1.3.8 mTOR ASSOCIATED DISEASE AND CANCER                                | 27        |
| <b>2 MATERIAL AND METHODS</b>   | <b>29</b> |
| <b>2.1 CELL CULTURE</b>   | <b>30</b> |
| 2.1.1 CELLS   | 30        |
| 2.1.2 GENERAL ISSUES  | 30        |
| 2.1.3 BUFFERS AND SOLUTIONS   | 31        |
| 2.1.4 TRYPSINISATION  | 32        |
| 2.1.5 CELL PASSAGING  | 32        |
| 2.1.6 CELL FREEZING FOR STORAGE   | 32        |
| 2.1.7 CELL THAWING  | 33        |
| <b>2.2 THREE-DIMENSIONAL COLLAGEN GEL ASSAY</b>                         | <b>34</b> |
| 2.2.1 BUFFERS AND SOLUTIONS   | 34        |
| 2.2.2 ESTABLISHING A PROTOCOL FOR THE 3D COLLAGEN GEL ASSAY WITH IMR-90 | 35        |
| 2.2.3 SPHEROID ASSAY  | 35        |
| 2.2.4 3D-COLLAGEN GELS WITH SINGLE-CELL SUSPENSION                      | 38        |
| <b>2.3 siRNA KNOCKDOWNS OF SPECIFIC PROTEINS</b>                        | <b>39</b> |
| 2.3.1 BUFFERS AND SOLUTIONS   | 39        |
| 2.3.2 CELL PREPARATION  | 39        |
| 2.3.3 PREPARATION OF siRNA STOCK SOLUTIONS                              | 39        |
| 2.3.4 TRANSFECTION  | 40        |
| 2.3.5 PREPARATION OF CELLS FOR 3D-COLLAGEN GELS                         | 40        |
| <b>2.4 WESTERN BLOT ANALYSIS</b>  | <b>41</b> |
| 2.4.1 BUFFERS AND SOLUTIONS   | 41        |
| 2.4.2 PROTEIN EXTRACTION  | 45        |
| 2.4.3 PROTEIN PREPARATION   | 45        |
| 2.4.4 SDS-PAGE  | 46        |
| 2.4.5 WESTERN BLOT  | 47        |
| 2.4.6 PROTEIN DETECTION   | 48        |
| 2.4.7 REPROBING   | 48        |
| 2.4.8 ANTIBODIES  | 49        |
| 2.4.9 DENSITOMETRIC EVALUATION OF X-RAY FILMS                           | 49        |

|   |            |
|---|------------|
| <b>2.5 FLOW CYTOMETRY</b>   | <b>50</b>  |
| 2.5.1 BUFFERS AND SOLUTIONS   | 50         |
| 2.5.2 CELL FIXATION AND STAINING OF TISSUE CULTURE CELLS                      | 51         |
| 2.5.3 ESTABLISHING A HARVESTING PROTOCOL FOR 3D COLLAGEN GELS                 | 51         |
| 2.5.4 HARVESTING CELLS FROM 3D COLLAGEN GELS                                  | 52         |
| 2.5.5 ANALYSIS  | 52         |
| <b>2.6 MICROSCOPIC ANALYSIS</b>   | <b>53</b>  |
| 2.6.1 BUFFERS AND SOLUTIONS   | 53         |
| 2.6.2 IMMUNOFLOURESCENCE STAININGS  | 54         |
| 2.6.3 IMMUNOFLOURESCENCE STAININGS OF COLLAGEN GELS                           | 55         |
| 2.6.4 MICROSCOPIC ANALYSIS  | 55         |
| 2.6.5 ANTIBODIES  | 56         |
| <b>2.7 RAPAMYCIN AND CVT-313 TREATMENT</b>                                    | <b>58</b>  |
| <b>2.8 STATISTIC ANALYSIS</b>   | <b>58</b>  |
| <b>3 RESULTS</b>  | <b>59</b>  |
| <b>3.1 ESTABLISHING CULTURE CONDITIONS FOR IMR-90 IN COLLAGEN GELS</b>        | <b>60</b>  |
| <b>3.2 ESTABLISHMENT OF A HARVESTING PROTOCOL FOR FLOW CYTOMETRY ANALYSIS</b> | <b>63</b>  |
| <b>3.3 IMR-90 IN DIFFERENT CULTURE CONDITIONS</b>                             | <b>65</b>  |
| <b>3.4 EFFECT OF RAPAMYCIN ON SPHEROID INVASION</b>                           | <b>67</b>  |
| 3.4.1 TREATMENT AFTER COLLAGEN GEL POLYMERIZATION                             | 67         |
| 3.4.2 TREATMENT THREE HOURS BEFORE HARVESTING SPHEROIDS                       | 68         |
| 3.4.3 OVER NIGHT TREATMENT BEFORE SPHEROID AGGREGATION                        | 70         |
| <b>3.5 COLLAGEN GELS WITH siRNA TREATED CELLS</b>                             | <b>72</b>  |
| <b>3.6 COMPARISON OF THE INVASION RATES</b>                                   | <b>75</b>  |
| <b>3.7 DETECTION OF APOPTOSIS UPON mTOR INHIBITION</b>                        | <b>76</b>  |
| <b>3.8 IMMUNOFLOURESCENCE STAININGS</b>                                       | <b>78</b>  |
| 3.8.1 SECONDARY ANTIBODY CONTROL  | 78         |
| 3.8.2 mTOR  | 78         |
| 3.8.3 pAKT S473   | 79         |
| 3.8.4 AKT   | 80         |
| 3.8.5 pS6 S240/244  | 81         |
| 3.8.6 4E-BP1  | 82         |
| 3.8.7 p-H3 S10  | 82         |
| 3.8.8 CLEAVED CASPASE-3   | 83         |
| <b>4. DISCUSSION</b>  | <b>85</b>  |
| <b>4.1 SETUP OF A 3D MODEL SYSTEM</b>   | <b>86</b>  |
| <b>4.2 CELL CYCLE DISTRIBUTION AND CELL SIZE OF IMR-90 CELLS IN 3D</b>        | <b>87</b>  |
| <b>4.3 DOES mTOR SIGNALLING ALTER INVASION?</b>                               | <b>89</b>  |
| 4.3.1. CELL DEATH AND APOPTOSIS   | 91         |
| 4.3.2 EXPRESSION AND LOCALISATION OF mTOR PATHWAY COMPONENTS IN IMR-90 IN 3D  | 92         |
| <b>4.4 PERSPECTIVES</b>   | <b>94</b>  |
| <b>5 REFERENCES</b>   | <b>95</b>  |
| <b>6 APPENDIX</b>   | <b>103</b> |
| <b>6.1 REAGENTS</b>   | <b>104</b> |
| <b>6.2 EQUIPMENT</b>  | <b>107</b> |
| <b>6.3 USED siRNA-POOLS</b>   | <b>109</b> |
| <b>6.4 BUFFERS AND SOLUTIONS</b>  | <b>110</b> |
| <b>6.5 LIST OF ABBREVIATIONS</b>  | <b>114</b> |
| <b>6.6 CURRICULUM VITAE</b>   | <b>119</b> |



## **1 Introduction**

## **1.1 What are fibroblasts?**

### **1.1.1 Fibroblast origin and function**

Fibroblasts are mesenchymal cells, mostly residing in connective tissue, which consists in addition to fibroblasts of fat cells, macrophages, eosinophilic granulocytes, lymphocytes, melanocytes and mast cells embedded in extracellular matrix (ECM). Connective tissue encloses organ structures (then called stroma) and is located throughout the whole body. ECM itself consists of basic components (hyaluronic acids, proteoglycans, glycoproteins), collagen and elastin fibres [1]. Fibroblasts are responsible for the synthesis of collagen in the ECM and are concomitantly regulated by changes in the composition of ECM, leading to interactions with integrins stimulating fibrogenesis (cell proliferation, migration, ECM deposition). Further functions are implicated in i) wound healing, which is a universal response to injury-following inflammation, ii) regulation of epithelial differentiation and iii) inflammation regulation ([2]; reviewed in [3, 4]). During wound healing after cutaneous injuries, fibroblasts migrate quickly to the wound environment, thereafter start to proliferate and produce ECM proteins (collagen and fibronectin) [3]. Fibroblasts are connected with various diseases like fibrosis [3, 5], keloid formation [6], diseases caused by deficient or abnormal collagen (scurvy [7], Ehlers-Danlos syndrome [8]) and cancers (cancer-associated fibroblasts, reviewed in [4]).

### **1.1.2 Fibroblast morphology**

Fibroblasts display a spindle-shaped pattern *in-vivo*, cultured on plastic surfaces of tissue culture plates they show a dendritic morphology, with large and euchromatic nuclei. They are characterised as non-vascular, non-epithelial and non-inflammatory cells, defined by the lack of certain markers for other cell lines, such as epithelial, smooth muscle, endothelial, perineural and histiocytic cells (reviewed in [4, 9-11]). There are well-established markers for fibroblasts, but none of these are expressed exclusively or in all fibroblasts. E.g. vimentin is found in all fibroblasts and in neurons, endothelial and myoepithelial cells or desmin, which is only present in skin fibroblasts and in other cell lines like muscle and vascular smooth muscle cells (reviewed in [4]).

The cells, which were used for the experiments in this study, are primary human lung fibroblasts. They are derived from a human female fetus with a gestation age of 16 weeks [12]. At this time the fetal lung transits from the pseudoglandular to the canalicular stage



(see below). The fibroblasts reside in a dense three-dimensional (3D) ECM, surrounding the developing alveoli (see Figure 1.1 and chapter 1.1.3).

Fibroblasts possess a topographic memory. This was demonstrated using fibroblasts from different sites of various donors and full genome covering cDNA microarrays [9]. Unsupervised hierarchical cluster analysis showed that fibroblasts were grouped according to their sites of origin rather than depending on the individual they are derived from. Also different passages were grouped together, showing that the gene expression patterns are stable under culture conditions [9]. These results let us hypothesize that the fibroblasts used for the experiments in our study display very similar expression patterns as compared to the *in-vivo* situation.

### **1.1.3 Fetal lung development**

Lung development can be classified in four histological stages, the pseudoglandular, the canalicular, the terminal saccular and the alveolar stage [13]. The first one is the pseudoglandular stage from 5-17 weeks of human pregnancy (E9.5-16.6 days in mouse embryo). During this stage branching morphogenesis of epithelial tubes generates terminal bronchioles and epithelial gland-like structures are formed, which are embedded in a rapidly proliferating mesenchyme (or stroma) containing predominantly fibroblasts (see Figure 1.1). In the canalicular stage from 16-25 weeks (E16.6-17.4 days) the respiratory tree undergoes further size expansion accompanied by vascularisation and angiogenesis within the surrounding stroma, leading to a massive increase of capillaries. The airway epithelial cells differentiate into peripheral squamous cells and proximal cuboidal cells and the terminal bronchioles divide into respiratory bronchioles and alveolar ducts. This stage partially overlaps with the pseudoglandular stage, due to the faster developing cranial part of the lung. The terminal saccular stage, from 24 weeks to late fetal period (E17.4 to postnatal day 5 (P5)), is accompanied by thinning of the interstitium due to further differentiation of mesenchymal cells and apoptosis. The capillaries grow into the mesenchyme and form a dense network. At the end of this stage air-exchange is possible. The last part of fetal lung development is the alveolar stage from the late fetal period to childhood (P5-P30), it is characterised by alveolarisation, where the largest part of surface for gas-exchange is formed (reviewed in [13]).

The adult lung interstitium contains fibroblasts, collagen type I and III and elastin, whereas alveolar and lung basement membranes (BM) predominantly consist of collagen type IV and laminin [3].

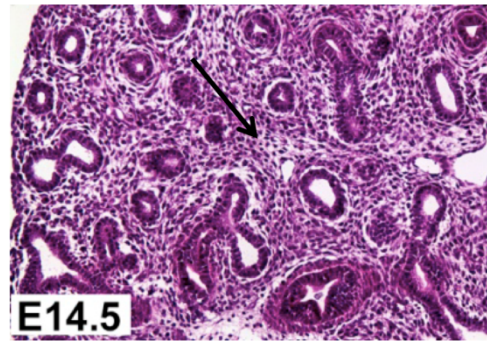


Figure 1.1: The image shows the pseudoglandular stage of a mouse embryonic lung (E14.5). The arrow marks the rapidly proliferating mesenchyme, which educes fibroblasts. (Picture taken from [13])

## 1.2 3D cell culture

3D cell culture is a useful tool to study physiological aspects of many cellular features e.g. biomechanical functions, like cell-matrix interactions, under *in-vitro* conditions. It is supposed to allocate a tissue like environment mimicking the ECM features, which are found *in-vivo*, since the environment and the shape of a cell can determine behaviour and gene expression [14]. There are many examples for the more physiologic behaviour of cells cultured in a 3D environment, a few of which will be described below. T47D breast epithelial cells cultured in monolayer are not able to differentiate into duct-like tubules until they are transferred into floating collagen gels and subsequently undergo tubulogenesis [15]. *In-vivo* nutrient exchange in epithelial cells occurs normally through their basolateral surface, cultivation on tissue culture plates restrict this access due to the attachment of the basal side of the cells with the culture dish and the presence of tight-junctions and desmosomes between the cells. Whereas the culture of epithelial cells on microporous membranes allow metabolic processes, like they occur *in-vivo* through their basal membrane and result in a more differentiated phenotype of the cells [16-18]. Mouse mammary gland cells cultured on uncoated or collagen coated tissue culture plates synthesise only minor amounts of  $\beta$ -casein (a major milk protein), whereas those cells cultivated on top of a floating collagen gel regain their *in-vivo* morphology and expression of  $\beta$ -casein caused by stimulation of BM formation, leading to upregulation of  $\beta$ -casein synthesis. The same effect occurs when cells are cultivated directly on a BM gel. (reviewed by [19]). Cells from a metastatic melanoma cultured as monolayer on 2D display profound modifications of the gene expression compared to cells cultivated in multicellular spheroids [20]. Two gene products (CXCL1 (GRO- $\alpha$ ) and IL-8), which are

involved in melanoma progression and metastatic processes, are significantly upregulated in spheroid culture [20]. 3D cell culture enables co-cultivation of different cell types, and cells in different states like proliferating, nonproliferating and necrotic cells (reviewed in [21]).

### **1.2.1 Fibroblasts in 3D**

Fibroblasts can also be cultivated under more physiologic conditions than on plastic surfaces. When fibroblasts are embedded in collagen gels, they adopt morphologies varying from bipolar spindle forms to dendritic forms [11]. This depends on the matrix tension and stiffness. Fibroblasts in floating collagen gels (gels, which are released from a solid support, mostly the plastic surface onto which they have been poured, after cells are embedded) start to remodel the ECM due to their motile activity. The cells do not show stress fibers and a dendritic phenotype, this morphology can be observed *in-vivo* during quiescence and apoptosis. In attached collagen gels the matrix stiffness is higher than in released ones. Cells show a bipolar pattern with actin stress fiber development and cytoskeletal reorganization, which also occur during the process of wound healing [14, 22].

When fibroblasts are cultured in a collagen gel, the cells contract the ECM. The resulting gel is dense, has an opaque body and is less than 1/10 of the original size [11]. The collagen density can increase from 1.5 mg/ml to 20 mg/ml, which is equal to the density of collagen in tissue [23]. Collagen gels without cells do not shrink even after a week of cultivation, indicating that the reason for the contraction is only the presence of fibroblasts. Experiments showed that the rate of contraction is dependent on the amount of cells, which are embedded in the gel [24].

Culturing of fibroblasts in cell aggregates leads to a programmed activation of a pathway called nemosis. This results in activation of growth factor secretion and the induction of proinflammatory and proteolytic responses that cause a programmed necrosis-like cell death (reviewed in [25]). After 24 hours of cultivation fibroblast spheroids start to decompose, the volume decreases and after 120 hours only remnants of dead cells and debris are left [26]. Ultrastructural features are compatible with necrosis, like the pyknotic nuclei whereas the loss of nuclear membrane integrity is lacking. The main difference to necrosis is that nemosis does not occur accidentally but seems to be executed in a programmed manner like apoptosis. Differences to apoptosis are that nemosis is executed without caspase-3 activation and DNA fragmentation (reviewed in [25]).

Cells, which undergo necrosis, show a massive induction of cyclooxygenase-2 (COX-2), which is usually absent in most normal tissues but has been shown to increase the metastatic potential in colon cancer cells. COX-2 shows an even expression throughout the spheroid, showing that nutrient deprivation and hypoxia in the centre are not the reasons for its increase (reviewed in [25]). Experiments showed that the caspase inhibitor Z-VAD-FMK reduces COX-2 expression and inhibits membrane damage, this suggests that necrosis is not executed caspase-independently [26].

### **1.2.2 3D culture methods**

There are different methods to cultivate cells in a 3D environment. The appropriate method to use depends on the scientific question, since not all problems can be addressed with the same model [15, 27]. In the following chapters different methods for 3D cell culture, tumour cell culture and co-culture of tumour cells and stromal cells are summarised.

#### *Spontaneous cell aggregation*

This method uses non-adherent culture plates, which prevent cell-surface attachment. Within this cultivation tumourigenic cells show a much higher self-aggregation rate to form sphere like structures (spheroids) than non-transformed cells [28].

#### *Liquid overlay culture*

For this method cell culture tissue plates with a layer of agar, agarose or reconstituted BM like Matrigel® are used to avoid cell attachment to the plastic surface. Cells are thereafter seeded on top of the surface of the coated dishes, which induces the formation of spheroids. For studying individual spheroids this method is widely used ([29]; reviewed in [21]). Under these conditions primary cells from a mouse lung and tumour cells are able to form aggregates; but only tumour cell aggregates are capable to grow, unlike these primary lung cells, which break apart after three days [29].

#### *Filter well inserts*

Filter well inserts are microporous filter membranes inserted in culture vessels like 24-well plates forming an upper and lower compartment filled with growth medium [18]. Cultivation of epithelial cells on these membranes allows the apical and also the basal membrane to interact with the environment, whereas this interaction of the basal

membrane is not possible in normal tissue culture plates [16]. This metabolic process recapitulates the *in-vivo* situation more likely than in 2D [18].

#### *Spinner flask culture, gyratory rotation culture, rotating-wall vessel culture*

For cultivation of greater numbers of spheroids suspension cultures in spinner flasks, gyratory rotation incubators and rotating-wall vessels are used. The main advantage of suspension cultures is a good diffusion; that means the spheroids are supplied with nutrients and by-products are removed efficiently ([29]; reviewed in [21]).

In spinner flasks growth medium is stirred continuously by impeller mixing, this constant movement prevents the attachment of the cells with the walls and the bottom of the flask ([29]; reviewed in [21]). A similar culture method uses Erlenmeyer flasks containing a tumour cell suspension, which is then placed on a gyratory rotation incubator for spheroid aggregation and further growth (reviewed in [21]).

Rotating-wall vessels are horizontally rotating vessels, which are completely filled with cell-suspension. Due to the constant rotation the cells never reach the bottom and cell-surface attachment is prevented. The lack of air bubbles minimizes fluid turbulences and shear forces on the cells; this is an advantage especially for fragile cells ([30]; reviewed in [21]).

#### *Microcarrier beads*

Cells, which do not aggregate spontaneously and need attachment to form aggregates, can be cultured on microcarrier beads. They are manufactured carriers, which are available in a great variety of coatings, like collagen-coated beads; composite materials, like dextran; and sizes. This method is used for studying cell-cell and cell-substratum interactions. Usually this method is combined with rotating-wall vessel culture, which allows up to 1000-fold greater cell densities, than possible with conventional monolayer cultures. This is a system with the potential for high-throughput screenings ([30]; reviewed in [21]).

#### *Scaffold based culture*

Within this method cells attach to prefabricated scaffolds, on which they can migrate, divide and form complex 3D structures. They consist most commonly of collagen I (see below) but also other ECM proteins or synthetic polymers can be used. Growth or regulatory factors can be supplemented. Scaffold culture models are used for long term

studies of growth and differentiation of epithelial cells, neurons, endothelial cells and fibroblasts ([31]; reviewed in [21]).

#### *Collagen gel culture*

For this methods cells are cultured in type I collagen gel, which is covered with growth medium. There are two different possibilities to grow cells in collagen gel, either by using a single-cell suspension or by spheroid culture. For single-cell suspension trypsinised cells are pelleted, resuspended in collagen I solution, which is thereafter induced to polymerize. For spheroid collagen gel culture cells are aggregated to spheroids and embedded into collagen gel. After polymerisation gels can be cultured attached to the surface or released and free-floating in growth medium [15, 32].

Whether using attached or free-floating collagen gels depends on the experiment itself. For instance T47D cells will not form differentiated structures while they are cultured in attached collagen gels, instead they continue to proliferate. When these collagen gels are released, the cells start with tubulogenesis and form structures with lumen, since they become mechanical unloaded which leads to collagen gel contraction and decreased proliferation [15].

### **1.2.3 Cell invasion assays**

The invasion of BM is a contributing factor in metastasis and angiogenesis in tumour development. BM is a specialised ECM remaining at the basolateral side of the cells [4]. Benign tumours do not cross the BM layer, but malign tumours do so and subsequently invade organs and spread over the whole organism (metastasis) [33]. For studying invasive potential of various cell types *in-vitro* different assays are used.

#### *Transwell invasion assay*

This assay is quite the same as the boyden chamber migration assay, which consists of two chambers filled with growth medium separated by a porous filter. Cells are seeded in the upper compartment and can migrate through the filter to the lower chamber, where they can be quantified [34]. The only difference to the invasion assay is that the porous filter of the upper chamber is overlaid with a layer of ECM, like collagen I or Matrigel® before cells are seeded. This prevents non-invasive cells from migrating to the lower chamber. Invasive cells, which reach the lower chamber, can be cultured for further experiments [35]. This assay can be expanded to a chemoinvasion assay by adding

growth factors like VEGF, PDGF or EGF to the lower chamber as chemoattractants to stimulate the cells [33, 35].

To differentiate between cells with a high invasive potential and slow motility and cells with a low invasive potential but high motility it is recommended to calculate the “invasive index”. Therefore an invasion assay and a migration assay have to be performed, evaluated and then the ratio of those two determines the invasive index [33].

#### *Platypus invasion assay*

This invasion assay is also a modification of a migration assay. For the migration assay 96-well plates are used which are equipped with small silicone stoppers. A cell-suspension is added and after attachment of the cells the stoppers are removed leaving a round exclusion zone, in which the cells migrate. For the invasion assay the bottom of the 96-well plate is coated with basement membrane extract (BME), which has to polymerise. Thereafter the silicone stoppers are fitted, cell suspension is added and the cells adhere to the BME. Now the stoppers are removed leaving a cell-free zone. The last step is to overlay the cells and the invasion zone with a thicker layer of BME. Cells start to invade into the middle zone, what can be documented with a microscope [36].

#### *Spheroid collagen gel invasion assay*

Spheroids are defined as multicellular cell aggregates, which are able to mimic the in-vivo situation of primary tumour clusters. Meaning, that cells located at the outlying area are proliferating, compared to cells in the innermost, which become quiescent and undergo apoptosis or necrosis, due to the lack of oxygen and nutrients and accumulation of lactate in the inner spheroid [27].

Multicellular spheroids can be produced by hanging drop cell cultivation, spinner flask culture, gyratory rotation culture, rotating-wall vessel culture and by cultivating cells in non-adherent 96-well plates in methylcellulose-/agar-growth medium suspension [27, 37, 38].

These spheroids can thereafter be embedded into collagen I or BME gels. Tumour cell lines, endothelial cell lines and mesenchymal cell lines such as fibroblasts start to invade the surrounding gel in a “starburst” like outgrowth. This outgrowth can be followed with a microscope and quantified. These collagen gels can be treated with inhibitors and growth factors, also cells treated with siRNA can be embedded [38, 39]. By using this

method the requirement of cancer cells for the membrane-anchored metalloproteinase MT1-MMP for invasion was investigated [39].

In our experiments we produced multicellular spheroids using 96-well plates with a methylcellulose-cell suspension mixture. After 6 hours the spheroids are harvested, to prevent the cells from necrosis. The spheroids are then embedded in collagen I gels and a mesh is added to avoid collagen gel contraction, otherwise we could not be able to observe and quantify the outgrowth.

#### *Nested collagen matrices*

This method is akin with the spheroid collagen gels. The only difference is that the cells, predominantly fibroblasts, are not aggregated to multicellular spheroids. The cells are embedded in collagen I gel and incubated over night, so that the fibroblasts contract the gel to 1-2 mm diameter, which are called dermal equivalents. These are then embedded in the middle of fresh collagen gel. After polymerisation the cells start to invade the surrounding gel, this can be observed with a microscope and quantified [40]. It is used to study wound healing contraction and cell-matrix interactions [41].

### **1.2.4 3D co-culture methods**

#### *Confrontation assay*

This assay is used for co-culture of tumour cells and stromal cells or other cell lines. This culture method is for example used to mimic scirrhous breast tumours. Therefore one fibroblast spheroid is transferred into each well of an agarose-coated 96-well plate and co-cultured with one tumour cell aggregate. Experiments show that co-cultures of breast tumour cells with normal skin fibroblasts mirror early stages during breast tumour development; in contrast co-cultures with tumour-derived fibroblasts reflect advanced scirrhous breast tumours due to differentiation of fibroblasts to myofibroblasts [42]. Another possibility is to transfer one spheroid of the individual tumour cells and stromal cells onto a poly-D-lysine-coated cover slip where they are co-cultivated. The spheroids can be thereafter fixed and analysed with a microscope [43].

#### *Artificial skin model*

This assay is used for studying interactions between tumour spheroids and fibroblasts. Therefore tumour spheroids were produced for instance in non-adherent 96-well plates in methylcellulose medium suspension. The spheroids were thereafter transferred into a



microcentrifuge tube; fibroblasts were trypsinised and transferred into the tube as well. Afterwards the spheroids and cells were agitated with collagen gel and transferred into casting devices for polymerisation. Further cultivation was proceeded in medium-containing 24-well plates (Dolznig et al, submitted to American Journal of Pathology).

### **1.3 mTOR pathway**

For our analysis we chose the mammalian target of rapamycin (mTOR) pathway, due to its involvement in many important cellular functions as regulating mRNA translation, ribosomal biosynthesis, proliferation, metabolism and cell size via its downstream targets (reviewed in [44]). Another reason is that this pathway was previously extensively studied using monolayer cultures of IMR-90 in our lab [45, 46]. However, mTOR signalling has not been studied very well in fibroblasts cultivated in 3D so far. Recently in synovial fibroblasts mTOR expression and their invasive properties after Rapamycin treatment were studied using Western blot analysis and transwell invasion assay. Reduced phosphorylation of mTOR, p70 S6K and 4E-BP1 was found, confirming mTOR inhibition. Furthermore after treatment with Rapamycin the invasiveness of the cells is specifically lower than in the controls [47]. In a study of human skin fibroblasts in collagen lattices cell cycle distribution was analysed with flow cytometry. They observed decreased proliferation with better biological viability [48].

#### **1.3.1 mTOR**

mTOR is a member of the PIKK (phosphoinositide 3-kinase related kinase) family of protein kinases and is part of two distinct complexes called mammalian TOR complex 1 and 2 (mTORC1/mTORC2) (reviewed in [49]). In the early 1970s the bacterial strain *Streptomyces hygroscopicus* was isolated on the island of Rapa Nui. It excreted an antifungal macrolide, which was then called rapamycin [50]. It was used as an immunosuppressant to prevent graft rejection and with its help mTOR was discovered. Rapamycin is a specific and potent inhibitor of mTOR, by interacting with FK506-binding protein 12 (FKBP12) to assemble a FKBP12/rapamycin complex [51]. This complex interacts with the FKBP12-rapamycin binding (FRB) domain of mTOR kinase, causing a decrease of proliferation, mRNA translation and ribosomal biosynthesis [52]. In this way mTORC1 was discovered in 1994 [51, 53, 54] and mTORC2 in 2004 [55, 56].

### 1.3.2 mTORC1 and mTORC2 assembly

mTORC1 consists of mTOR, raptor, PRAS40, Gβ1/mLST8 and DEPTOR (see Figure 1.2 A). Compared to mTORC2 it is a rapamycin-sensitive complex, since rapamycin destabilises the connection between mTOR and raptor leading to a decrease of mTORC1 activity. Raptor means regulatory associated protein of mTOR and is a scaffold protein, which connects mTORC1 downstream targets, containing the TOR signalling (TOS) motif, with the mTOR kinase ([53]; reviewed in [44, 49]). The proline-rich AKT substrate of 40 kDa (PRAS40) is a tumour suppressor protein, which interacts with raptor to inhibit mTORC1 activity [57]. Gβ1/mLST8 binds to the mTOR kinase domain and provides the assembly and the signalling of the complex [54]. DEPTOR is an inhibitor and can be found in both complexes like Gβ1/mLST8 ([58]; reviewed in [59]).

mTORC2 contains besides Gβ1/mLST8 and deptor also rictor, mSin1 and PRR5/protor (see figure 1.2 B). The rapamycin-insensitive companion of mTOR (rictor) [55] and mSIN1 provide mTORC2 assembly and signalling [60], the function of PRR5/protor is not clear at the moment (reviewed in [44]).

mTORC1 is directly responsible for linking environmental cues with protein synthesis, cell growth, cell proliferation and cell metabolism via its downstream targets. These functions are promoted by growth factors and nutrients ([61]; reviewed in [44, 49]).

mTORC2 controls whole body growth, cytoskeleton, metabolism and cell survival [55, 56, 62].

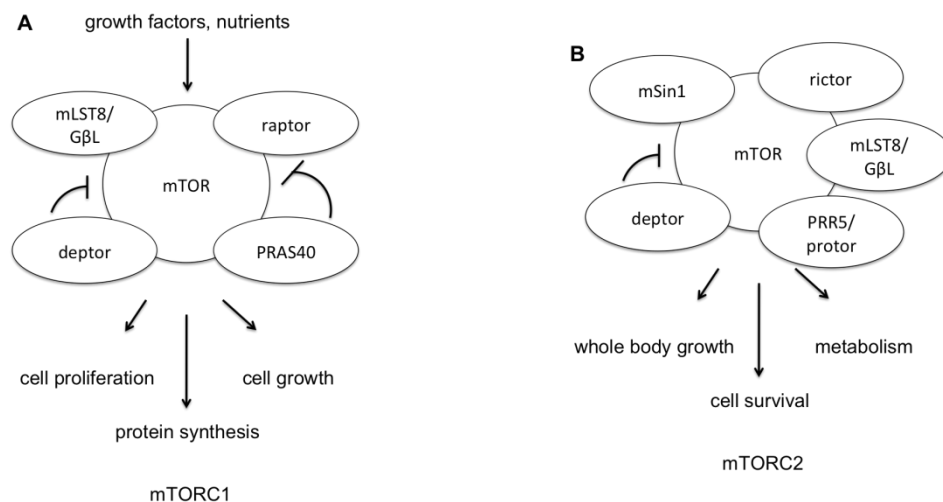


Figure 1.2: Scheme shows mTORC1 assembly. Its kinase activity is promoted by growth factor and nutrient stimulation and leads to increased cell proliferation, cell growth and protein synthesis. B mTORC2 assembly leads to whole body growth, cell survival and metabolism regulation.

### 1.3.3 Downstream targets of mTORC1

The main downstream targets of mTORC1 are ribosomal S6 kinase 1 and 2 (S6K1, S6K2) and eukaryotic initiation factor 4 E (eIF4E) binding protein 1 (4E-BP1), all three components of the translation machinery (reviewed in [49]). The mTOR/raptor mediated phosphorylation of p70S6K1 takes place at the hydrophobic motif site threonine 389 (T389) [63]. One substrate of p70S6K1 is among others ribosomal protein S6, which is phosphorylated at S240/244 and S235/236 [64]. 4E-BP1 is phosphorylated at T37/46, T70, S65 to inhibit its function and support its dissociation from eIF4E, which promotes the assembly of the eIF4E complex (eIF4F) for initiation of mRNA translation ([65]; reviewed in [44]). Phosphorylation of S6 and 4E-BP1 are dependent on activated mTORC1 signalling, meaning that translation and subsequent cell growth and proliferation are regulated by growth factor and nutrient stimulation ([65]; reviewed in [44]).

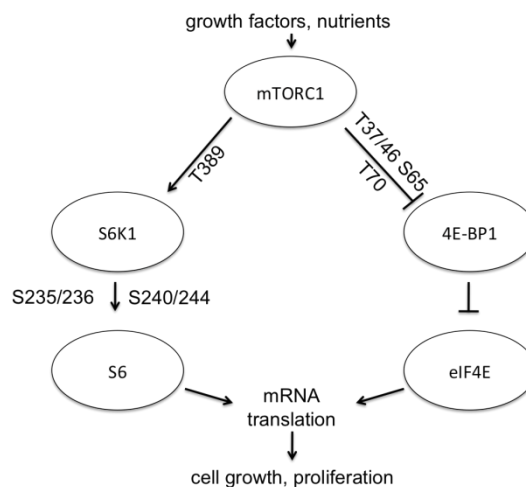


Figure 1.3: S6K1 and 4E-BP1 are the main downstream targets of mTORC1. It phosphorylates S6K1 at T389 guiding its activation and subsequently its phosphorylation of S6 at S240/244 and S235/236. Inhibitory phosphorylations of 4E-BP1 by mTORC1 occurs at multiple sites (T37/46, S65, T70). 4E-BP1 inhibits eIF4E to initiate mRNA translation.

### 1.3.4 Downstream targets of mTORC2

One of mTORC2's substrates is the proto-oncogene AKT. It controls metabolic processes, cell migration, cell survival and cell proliferation. mTORC2 directly phosphorylates AKT at the turn motif site T450, to stabilise newly synthesised proteins. In addition it is phosphorylated at S473 by mTORC2 ([66]; reviewed in [44]). For full AKT activation a second phosphorylation besides S473 at T308 is necessary, which is a target of phosphoinositide-dependent kinase 1 (PDK1), a downstream target of PI3K (reviewed in [44]).

Fully activated AKT phosphorylates tuberous sclerosis complex gene 2 (TSC2) and PRAS40 guiding their inhibition to increase mTORC1 activity. AKT has been demonstrated to phosphorylate and thereby active or inhibit multiple targets such as the transcription factor FOXO, the apoptosis regulator Bcl-2-associated death promoter (BAD) and others ([67]; reviewed in [68]).

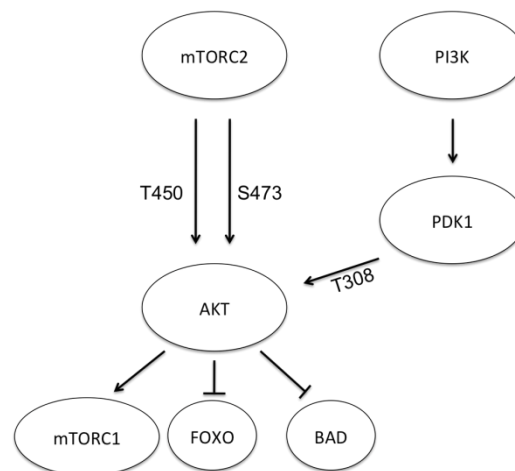


Figure 1.4: This figure shows mTORC2's downstream target AKT. Newly synthesised AKT is first phosphorylated at T450 by mTORC2, when full activation is needed AKT is phosphorylated by mTORC2 at S473 and also by PDK1 at T308. AKT controls mTORC1 activity, apoptosis, cell metabolism and a variety of other processes.

### 1.3.5 Upstream regulators

#### mTORC1

The main upstream regulators of mTORC1 are the tuberous sclerosis complex genes TSC1 and TSC2, encoding hamartin and tuberin respectively. They form a heterodimer (tuberous sclerosis complex, TSC) and are classified as tumour suppressor proteins. TSC1/TSC2 complex suppresses mTORC1 activity by inhibiting its activator ras-homologue enriched in brain (Rheb). TSC2 possesses a GTPase activating protein (GAP) activity, which converts the GTP-bound active state of Rheb into a GDP-bound inactive state. However the biochemical mechanism by which mTORC1 is activated via Rheb, is not defined yet ([69, 70]; reviewed in [44, 71]).

TSC itself can be phosphorylated by AKT through the PI3K pathway. Therefore AKT is activated by PDK1 (T308) and by mTORC2 (S473). Thereafter the targeting sites S939, S981 and T1462 of TSC2 are phosphorylated by AKT, which leads to an activation of mTORC1 (see Figure 1.5) ([72]; reviewed in [44]).

PRAS40 is another phosphorylation substrate of AKT, which is stimulated by insulin through the PI3K pathway leading to the dissociation of PRAS40 from mTORC1. This relieves its inhibitory function and enhances mTORC1 signalling towards S6K1 and 4E-BP1 (see figure 1.5) ([57, 73]; reviewed in [49]).

Another activating effect of mTORC1 is mediated by the Ras/ERK pathway. It inhibits TSC2 through an inhibitory phosphorylation at S664 (promoted by ERK) and S1798 (promoted by RSK) (see figure 1.5) ([74]; reviewed in [49, 75].)

Nutrient deprivation and cellular stress like hypoxia and genotoxic stress leads to an elevation of AMP and of the AMP/ATP ratio, causing phosphorylation of AMP-activated protein kinase (AMPK) through the tumour-suppressor serine-threonine kinase 1 (LKB1). AMP then binds to a subunit of AMPK to prevent its dephosphorylation. Its main function is to activate ATP-generating pathways and to inhibit ATP-consuming functions like the mTOR pathway. This kinase phosphorylates TSC2 on S1345 to enhance its GAP activity towards Rheb-GTP, leading to mTORC1 inhibition. Another substrate of AMPK is raptor, which is directly phosphorylated at S792 and S722, enabling 14-3-3 binding and initiates its degradation. This prevents cells from energy deprivation-induced apoptosis (see Figure 1.5) ([69, 76]; reviewed in [44, 49]).

## mTORC2

Upstream regulators of mTORC2 remain almost unknown. Probably PI3K lies upstream as it promotes phosphorylation of Akt (S473) via mTORC2 [68, 75] and its inhibition reduces mTORC2's activity ([77]; reviewed in [44]).

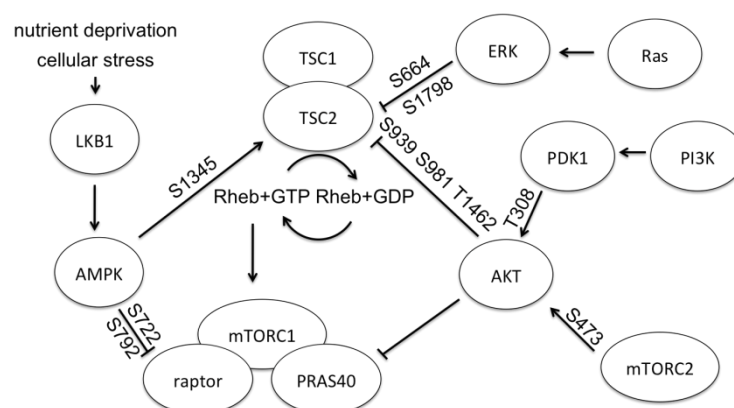


Figure 1.5: Scheme illustrating the upstream regulators of mTORC1. AKT phosphorylates TSC2 at S939, S981 and T1462 and activating mTORC1. AKT also phosphorylates PRAS40 resulting in increased mTORC1 activity. Nutrient deprivation and cellular stress activates AMPK, which inhibits raptor and enhances TSC2 for decreased mTORC1 activity.

### 1.3.6 Negative feedback-loop

Activated mTORC1 leads to an inhibitory feedback loop to insulin receptor substrate (IRS). This is mediated by an inhibitory phosphorylation of IRS through S6K1, guiding its release from PI3K, that shows decreased signalling towards AKT, TSC2 and PRAS40 reducing mTORC1 activity (see Figure 1.6 A). Furthermore raptor itself binds the SAIN domain of IRS leading to its inhibition [78]. When this negative feedback loop does not operate properly, an excess of nutrients can lead to increased mTORC1 activity, what may result in insulin resistance and type II diabetes ([79]; reviewed in [44, 49]).

In another feedback loop p70S6K1 phosphorylates rictor on T1135, which stimulates 14-3-3 binding to rictor, resulting in a decrease in AKT S473 phosphorylation to enhance GAP activity of TSC2 towards Rheb for reduced mTORC1 activity (see Figure 1.6 B) ([80]; reviewed in [44]).

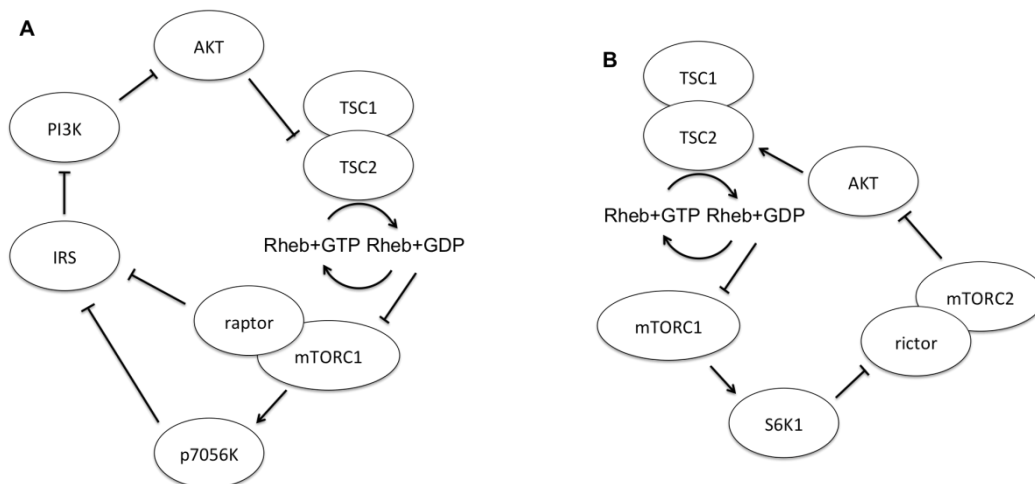


Figure 1.6 A Negative feedback loop of S6K1 towards IRS, guiding its dissociation of PI3K and reduction of AKT activity resulting in enhanced TSC2 and decreased mTORC1 activity. B Phosphorylation of rictor by S6K1 leads to decreased mTORC2 and AKT activity, stimulating TSC2 GAP activity towards mTORC1.

### 1.3.7 Treatment with rapamycin

mTORC1 is inhibited by rapamycin, which interacts with FKBP12 to assemble a FKBP12/rapamycin complex [51], enhancing the dissociation of raptor from mTOR and reduced substrate binding [81]. This results in decreased mRNA translation, smaller cell size and cell cycle arrest through dephosphorylation of 4E-BP1 [82], p70 S6K1 at T389 and subsequent S6 dephosphorylation of S240/244. Concomitantly treatment with rapamycin activates protein phosphatase A (PP2A) leading to dephosphorylation of p70

S6K and 4E-BP1 [83]. This occurs already a few minutes after the application of the drug ([46, 61, 63, 84]; reviewed in [85]).

mTORC2 is known as the rapamycin-insensitive complex. Short-term treatment with rapamycin showed dephosphorylation of rictor and mSIN1 in the cytoplasm with no impact on mTORC2 assembly [45]. The rapamycin/FKBP12 complex cannot bind to mTORC2 itself, but it can compete with its components to bind newly synthesised mTOR to prevent the assembly of new mTORC2 complexes ([55, 56]; reviewed in [86]). Prolonged treatment with rapamycin leads to complete dephosphorylation of rictor and mSin1 and dependent on the transformation status in some cell lines like PC3 and HEK-293T to a decrease of AKT S473 phosphorylation [87]. Diminished AKT S473 phosphorylation does not occur after long-term treatment with 100 nM rapamycin in IMR-90 [45].

Treatment with rapamycin induces AKT activation in a dose dependent manner, due to the loss of the negative feedback loop, in which S6K1 normally inhibits IRS and rictor, respectively. Low rapamycin concentrations lead to increased AKT activation, whereas high concentrations inhibit its phosphorylation. ([84, 88]; reviewed in [85]).

### **1.3.8 mTOR associated disease and cancer**

Since the mTOR pathway consists of many proto-oncogenes like AKT or Ras and tumour-suppressors as TSC1, TSC2 and LKB1, it is not astonishing that mutations cause a variety of cancers and other disease.

Genetic inactivation of TSC1 or 2 leads to an increase of mTORC1 activity with augmented protein synthesis and cell growth, causing tuberous sclerosis complex (TSC) and other related disease. TSC is an autosomal dominant disorder, but the majority of mutations occur *de novo* in either TSC1 or TSC2. Tuberous sclerosis is characterised by the formation of hamartomas in the kidneys, heart, skin and brain ([89]; reviewed in [52, 71, 90]).

Lymphangioleiomyomatosis (LAM) is associated with mutations in TSC2. It is characterised by benign lesions of smooth muscle-like cells in the lung and affects almost exclusively woman ([91, 92]; reviewed in [90]).

The autosomal dominant polycystic kidney disease (ADPKD) is a result of mutations in the PKD1 gene, which encodes polycystin-1 and the PKD2 gene encoding polycystin-2. Patients suffer from renal cysts, which lead to a replacement of normal renal tissue and a significant overall growth of the organs ([93]; reviewed in [90]).

Mutations in the tumour-suppressor gene LKB1 causes Peutz-Jeghers syndrome, resulting in gastrointestinal hamartomatous polyps. Patients show also an increased risk of malignant tumours in the intestine and elsewhere ([94]; reviewed in [52, 90]).

mTOR hyperactivation can occur in various tumours by dysfunction of various components of the mTOR/PI3K/ERK pathway. For instance oncogenic Ras can activate the mitogen-activated protein kinase (MAPK)/ERK pathway, leading to phosphorylation of TSC2 with following upregulation of p70S6K and 4E-BP1 (reviewed in [74, 90]). Another way is through the PI3K pathway, where mutations in upstream elements can lead to enhanced AKT signalling and inhibition of TSC2 (reviewed in [90]).



## **2 Material and methods**

## **2.1 Cell culture**

### **2.1.1 Cells**

Normal diploid human lung fibroblasts (IMR-90, CCL-186) obtained from the American Type Culture Collection (ATCC) were used for this study. These primary fibroblasts were isolated from a 16-week old female fetus in 1975 by Nichols [12]. IMR-90 are primary cells, which are nontransformed and nonimmortalised displaying a limited proliferation capacity of 58 population-doublings before the onset of senescence [12]. The cells display an elongated fibroblastoid phenotype and adhere to standard plastic cell culture dishes. The cells were kept in DMEM high glucose (4.8 g glucose/l) supplemented with 10% fetal calf serum, 30 mg/l penicillin, 50 mg/l streptomycin sulphate and 2 mM l-glutamine. Cells used in the entire study were from passages 16-19, in order to avoid artefacts due to the onset of senescence.

### **2.1.2 General issues**

All cell culture procedures were performed in laminar flow hoods (MSc Advantage biological safety cabinet from Thermo Scientific, Waltham, MA, USA). Furthermore all surfaces, gloves and instruments, like tweezers or pipettes, were wiped with 96% Ethanol (EtOH) periodically. 1.5 ml microcentrifuge tubes (VWR, West Chester, PA, USA, 211-0015 (Europe)/ 20170-038 (North America)) and pipette-tips (Starlab, Ahrensburg, Germany, 0,1-10 µl S1111-3000 / 1-200 µl S1111-1006 / 101-1000 µl S1111-2021) were sterilized in an autoclave at 121°C for 20 min. Growth medium, 1x PBS and TE were always prewarmed in a 37°C water bath and the outside of the flasks were afterwards sterilized with EtOH before use.

Cells were cultured in 100 mm tissue culture plates (Iwaki, Asahi Glass Co LTD, Tokyo, Japan, 3020-100) in Heraeus BBD 6220 incubators (Thermo Scientific, Waltham, MA, USA) at 37°C, 5% CO<sub>2</sub> and 80% rH (relative humidity).

### 2.1.3 Buffers and solutions

#### Trypsin-EDTA solution (TE):

- 2200 U trypsin
- 2% Na EDTA pH 7.4
- 1x PBS

For TE 1g trypsin (2.2 U/mg) was dissolved in 245 ml of 1x PBS supplemented with 5 ml of Na EDTA (1% solution, pH 7.4); the resulting solution was mixed by agitation. Afterwards it was filtered with a sterile filtration unit with 0.2 µm pore size (Sarstedt, Nümbrecht, Germany, 83.1822.001), aliquoted in 10 ml portions and stored at -20°C. After thawing for use it was stored at 4°C.

#### Antibiotics stock solution:

- 10 g/l streptomycin sulfate
- 6 g/l penicillin
- 10% 10x PBS

Antibiotics were prepared by dissolving 1 g of streptomycin sulfate and 0,6 g of penicillin in 10 ml of 10x PBS. H<sub>2</sub>O<sub>dest.</sub> was added to a final volume of 100 ml. After sterile filtration with 0.2 µm pore size 5 ml aliquots in 15 ml centrifuge tubes were stored at -20°C.

#### DMEM with 10% FCS:

- DMEM high glucose (4.8 g glucose/l)
- 10% FCS
- 60 mg/l penicillin
- 100 mg/l streptomycin sulfate
- 2 mM l-glutamine

Growth medium was prepared by thawing of a 50 ml aliquote of fetal calf serum, of a 5 ml aliquote of a 200 mM stock l-glutamine and of a 5 ml aliquote of antibiotics at 37°C in a watherbath. Afterwards the surfaces of these flasks and of a 500 ml flask of DMEM high glucose (4.8 g glucose/l) were wiped. In a laminar flow hood 50 ml of serum, 5 ml of l-glutamine and 5 ml of antibiotics was pipetted in the flask with DMEM and mixed gently by agitation. The concentration of fetal calf serum in DMEM was 10%, of l-glutamine 2 mM, of penicillin 60 mg/l and of streptomycin sulfate 100 mg/l. Complete growth medium was stored at 4°C and was depleted within 2 weeks. ö

#### **2.1.4 Trypsinisation**

When cells reached 90-95% confluency they were splitted in a ratio of about 1:3-1:4. Higher splitting ratios are not recommended. Growth medium was removed from a 100 mm tissue culture plate and was rinsed with 5 ml of 1x PBS to remove residual serum containing growth medium that may inhibit the enzymatic activity of trypsin. For tissue culture plates with a diameter of 100 mm 500µl of TE was added and the dishes were incubated at 37°C in the incubator with periodical microscopic examination until all cells were detached. Thereafter 5 ml of complete growth medium (DMEM +10% serum) was added and cells were resuspended carefully by pipetting. Tissue culture plates were incubated at 37°C in the incubator.

#### **2.1.5 Cell passaging**

Cells were trypsinised as described in 2.1.4. When all cells were detached, they were resuspended in 8 ml of fresh growth medium and 4 new tissue culture plates were filled with 2 ml cells suspension each. Afterwards 8 ml growth medium was added, cells were resuspended carefully and equally distributed all over the plate. Thereafter the tissue culture plates were incubated at 37°C in the incubator.

#### **2.1.6 Cell freezing for storage**

Cells were usually frozen when they were about 75% confluence. Cells were trypsinised as described, resuspended with 5 ml of complete growth medium, transferred into 15 ml centrifuge tubes (Sarstedt, Nümbrecht, Germany, 62.554.502) and centrifuged at 1000 rpm for 3 min. at room temperature in a centrifuge (Thermo Scientific Multifuge X3 FR). Thereafter the supernatant was discarded and the pellet was resuspended in 900 µl of fresh DMEM and slowly dropped into CryoTubes™ (Nalge Nunc International, Naperville, IL, USA, 343958) containing 100 µl of DMSO during very soft swaying. After closure the tube was inverted 3 times and immediately cooled on ice for 20 min. Thereafter the tube was frozen at -80°C over night in a 1 cm thick polystyrene box in order to reach a cooling rate of approximately 1°C/minute. Afterwards it was transferred into a liquid nitrogen tank at -196°C for long-term storage.

### **2.1.7 Cell thawing**

100 mm tissue plates with 10 ml of complete growth medium were prewarmed. The frozen cells in Cryo-Tube™ vials were taken off the liquid nitrogen tank and thawed in a 37°C water bath right away until the last ice crystals disappeared. Afterwards the tube was wiped with 75% EtOH and the cells were resuspended in 10 ml fresh prewarmed medium and seeded into the prepared plate and incubated at 37°C in the incubator. After 24 hours the growth medium was removed and fresh medium was added.

## 2.2 Three-dimensional collagen gel assay

### 2.2.1 Buffers and Solutions

#### Methylcellulose (MC):

- 1.5% (w/v) *Methylcellulose*
- *DMEM supplemented with 2 mM l-glutamine*

Methylcellulose was used for cell aggregation and for the preparation of collagen gels, therefore it was needed to be sterile. After autoclaving only sterile DMEM was used and all procedures like opening the flask and adding of DMEM were done in laminar flow hoods.

In a 1 l glas flask 15 g of methylcellulose was weighed, a magnetic stirrer was added and the not firmly closed flask was autoclaved for 20 min. at 121°C. Thereafter 500 ml of preheated DMEM (60°C) was filled in the flask and dissolved by stirring for 20 min. using the containing autoclaved magnetic stirrer afterwards. Another 500 ml DMEM with room temperature and 10 ml of the aliquoted 200 mM l-glutamine stock solution were added and stirring was continued over night at 4°C. The solution was thereafter aliquoted in 50 ml centrifuge tubes, centrifuged for 2 h with 5000g at room temperature. The clear highly viscous supernatant was transferred into fresh 50 ml centrifuge tube and the rest was discarded. MC was stored at -20°C. The solution had a concentration of 1.5% (w/v) methylcellulose and 2 mM l-glutamine.

#### Antibiotics stock solution:

- 10 g/l *streptomycin sulfate*
- 6 g/l *penicillin*
- 10% (v/v) 10x *PBS*

Antibiotics were prepared by dissolving 1 g of streptomycin sulfate and 0,6 g of penicillin in 10 ml of 10x PBS. H<sub>2</sub>O<sub>dest.</sub> was added to a final volume of 100 ml. After sterile filtration with 0.2 µm pore size 5 ml aliquots in 15 ml centrifuge tubes were stored at -20°C.

#### DMEM with 2% FCS:

- *DMEM high glucose (4.8 g glucose/l)*
- *2% FCS*
- *60 mg/l penicillin*
- *100 mg/l streptomycin sulfate*
- *2 mM l-glutamine*

Growth medium was prepared by thawing of a 50 ml aliquote of fetal calf serum, of a 5 ml aliquote of a 200 mM stock l-glutamine and of a 5 ml aliquote of antibiotics at 37°C in a waterbath. Afterwards the surfaces of these flasks and of a 500 ml flask of DMEM high glucose (4.8 g glucose/l) were wiped. In a laminar flow hood 1 ml of serum, 0.5 ml of l-glutamine and 0.5 ml of antibiotics was pipetted in the flask with DMEM and mixed gently by agitation. The concentration of fetal calf serum in DMEM was 2%, of l-glutamine 2 mM, of penicillin 60 mg/l and of streptomycin sulfate 100 mg/l. Complete growth medium was stored at 4°C and was depleted within 2 weeks.

#### **2.2.2 Establishing a protocol for the 3D collagen gel assay with IMR-90**

The basic steps for all preliminary experiments were the same as described in chapter 2.2.3. Only the following parameters were changed to find the best conditions: aggregation time, cell number per spheroids and spheroid number per gels.

#### **2.2.3 Spheroid assay**

##### 2.2.3.1 Cell aggregation

After cells were trypsinised as described in chapter 2.1.4, they were agitated with 5 ml of complete growth medium (DMEM +10% serum) and were transferred into 15 ml centrifuge tubes. Spheroid aggregation was accomplished by using 96-well plates (Sterillin, Aberbargoed, Caerphilly, UK, microtiter plate 612V96, lid 642000) with a defined amount of cells, for that cells were counted using a Bright-Line hemacytometer (Hausser Scientific, Horsham, PA, USA, 3120). 10 µl of cell suspension and 10 µl of trypan blue were resuspended in 500 µl microcentrifuge tubes (Eppendorf, Hamburg, Germany, 0030 121.023) in order to identify dead cells and to exclude them while counting. The mixture was then pipetted on the hemacytometer and 6 large corner and 2 middle squares were counted with a 10x objective. One big square had a surface area of 1 mm<sup>2</sup> and a depth of 0,1 mm that is a volume of 0,1 mm<sup>3</sup>.

The cell number was calculated with following formula:

$$\text{mean cell number}/0,1 \text{ mm}^3 = \frac{\text{counted cells} \times 2}{8}$$

$$\text{cell number/ml} = \text{mean cell number}/0,1 \text{ mm}^3 \times 10.000$$

2 stands for the dilution factor, 8 for the counted squares and 10.000 is the conversion factor from 0,1 mm<sup>3</sup> to 1 ml.

For easier calculation and in order to avoid an insufficient amount of methylcellulose-cell suspension mixture for the 96-well plates we calculated with 100 wells per plate. Each well was filled with 100 µl of the mixture, so for 1 plate 10 ml were required. 2 ml of methylcellulose (20% v/v) was filled in 50 ml centrifuge tubes. The needed amount of cell suspension was transferred into the tube and remaining cells were transferred in new 100 mm tissue culture plates, which were filled to a total volume of 10 ml with complete growth medium (DMEM +10% serum) and were incubated at 37°C in the incubator. Complete growth medium was added into the 50 ml centrifuge tube to a final volume of 10 ml and mixed well by agitation. It was filled in a v-shaped reservoir (Eppendorf, Hamburg, Deutschland, D5063-85) and 100 µl per well were transferred with a multi-channel pipette. Afterwards the plates were centrifuged at 1000 rpm for 3 min., then incubated at 37°C for no longer than 6 hours in the incubator.

#### 2.2.3.2 Harvesting spheroids

After 6 hours of incubation the content of the 96-well plate was pipetted with a multi-channel pipette completely off and were transferred into v-shaped reservoirs. Afterwards the plate was controlled with a microscope for remaining spheroids. If more than 5% were remaining, 100 µl of growth medium were added in these wells and were pipetted off once more. For 1 collagen gel the spheroids of 2 plates were transferred into a 50 ml centrifuge tube. They were centrifuged at 1000 rpm, 4°C for 5 min. Afterwards growth medium was aspirated by pipetting leaving 1 ml of medium in the tubes; the spheroids were resuspended carefully and transferred into 1.5 ml microcentrifuge tubes and centrifuged again. Then the tubes were put on ice.



### 2.2.3.3 3D-collagen gels with spheroids

*1000 µl collagen gel:* - 400 µl methylcellulose

- 500 µl collagen I

- 100 µl 10x PBS

- 11,5 µl 1M NaOH

A FACS-tube (BD Falcon™, BD Biosciences, Erembodegem, Belgium, 352054) for the collagen gel and all ingredients except 10x PBS were cooled on ice. For a single collagen gel 300 µl of collagen mixture were needed. Due to the high viscosity of methylcellulose a second FACS-tube was prepared, it was used for comparison purpose. For that it was filled with as much water as methylcellulose. Then methylcellulose was transferred in the cooled tube by pipetting until both had the same fluid level. Next collagen I and 10x PBS were added.

The supernatant of the centrifuged spheroids was removed and silicone-forms with a diameter of 1.5 cm and a height of 2 mm were placed into tissue plates. Now as last component 1 M NaOH was added and the tube was shaken thoroughly. After 15-30 min. the gel polymerised completely. The gel was centrifuged in a precooled centrifuge for 15 sec. at 2000 rpm at 4°C. The air bubbles were removed carefully with a pipette-tip and afterwards the gel was cooled on ice again. Then 300 µl of collagen gel was carefully agitated with the spheroids in the microcentrifuge tube and afterwards transferred into the form by pipetting and was evenly distributed with the pipette-tip. A ring-shaped PET mesh with 120 µm mesh size (Bückmann, Mönchengladbach, Germany, PET-100/77-32) was added, so the fibroblasts could not shrink the gel. For proper cell invasion the gels were incubated for 3 min. upside down in order to prevent sinking of the to the ground, otherwise they would behave like cells in tissue plates. Thereafter the plate was turned on the right side and incubated until the gel is polymerised.

Afterwards a few drops of growth medium were added on top of the gels and the silicon forms were removed carefully. The now swimming gels were transferred with a forceps into a 24-well plate containing 1 ml of growth medium (DMEM +2% serum) and incubated at 37°C in the incubator.

#### **2.2.4 3D-collagen gels with single-cell suspension**

Cells were trypsinised as described in chapter 2.1.4. When all cells were detached, 5 ml of complete growth medium was added, cells were agitated and transferred into 15 ml centrifuge tubes. Cell number was determined with a hemacytometer (see chapter 2.2.3.1) and the calculated amount of cell suspension for 300.000 cells was transferred into a 1.5 ml microcentrifuge tube. The remaining cells were seeded in a new 100 mm tissue culture plate, growth medium (DMEM +10% serum) was added to a final volume of 10 ml and it was incubated at 37°C in the incubator. The microcentrifuge tube was centrifuged for 5 min. at 1000 rpm and 4°C. The supernatant was discarded and the tube was held on ice. Then collagen gel was produced as described in chapter 2.2.3.3. Afterwards 300 µl of this gel was transferred into the prepared tube. The cells were agitated carefully by pipetting, due to the high viscosity air bubbles were occurring very easily. Then it was transferred into the silicone form. A mesh was added and the gels were incubated at 37°C in the incubator. When it was polymerised one drop of complete growth medium (DMEM +2% serum) was added on top of the gel, the silicon form was removed and the gel was transferred into a 24-well plate containing 1 ml of growth medium and incubated at 37°C in the incubator.

## 2.3 siRNA knockdowns of specific proteins

### 2.3.1 Buffers and solutions

DMEM with 10% FCS w/o antibiotics:

- *DMEM high glucose (4.8 g glucose/l)*
- *10% FCS*
- *2 mM l-glutamine*

Growth medium was prepared by prewarming a 50 ml flask with 44.5 ml of DMEM high glucose (4.8 g glucose/l) and thawing of a 50 ml aliquote of fetal calf serum and of a 5 ml aliquote of a 200 mM stock l-glutamine at 37°C in a waterbath. Afterwards the surfaces of the flasks were sterilised with EtOH. In a laminar flow hood 5 ml of serum and 0.5 ml of l-glutamine was pipetted in the flask with DMEM and mixed gently by agitation. The concentration of fetal calf serum in DMEM was 10% and of l-glutamine 2 mM. Growth medium was stored at 4°C and was depleted within 2 weeks.

### 2.3.2 Cell preparation

24 hours before transfection cells were trypsinised as described in chapter 2.1.4. When all cells were detached, they were resuspended with 5 ml of growth medium (DMEM +10% serum) and transferred into 15 ml centrifuge tubes. Thereafter 10 µl of cell suspension was mixed with 10 µl of trypan blue and cells were counted as described in chapter 2.2.3.1 in a hemacytometer. Then 150.000 cells were seeded in each well of a 6-well plate (PAA, Pasching, Austria, PAA30006X). Growth medium without antibiotics was added to a final volume of 2 ml. The plate was incubated over night at 37°C in the incubator.

### 2.3.3 Preparation of siRNA stock solutions

The tube containing siRNA was briefly centrifuged to collect the content at the bottom. Then 200 µl of 5x siRNA buffer was diluted with 800 µl of DEPC treated water to 1x siRNA buffer. In a vial with 5 nmol siRNA 250 µl of 1x siRNA buffer was added in order to get a 20 µM stock solution. The vial was mixed thoroughly and placed on an orbital shaker (Rocky® 3D) for 30 min. Afterwards it was centrifuged briefly. The stock solution was aliquoted into volumes of 10 µl in 500 µl microcentrifuge tubes so that the siRNA vials were not thawed too many times and were stored at -20°C.

#### **2.3.4 Transfection**

At first aliquoted OptiMEM I was prewarmed in a 37°C water bath and wiped before use. Then for each single well 245 µl of OptiMEM I was transferred into a 1.5 ml microcentrifuge tube and 5 µl of the 20 µM siRNA-stock solution was added and mixed gently by snapping. Lipofectamine RNAiMAX was mixed and centrifuged briefly. For each transfection 247.5 µl of OptiMEM I was preplaced in a microcentrifuge tube and 2.5 µl of RNAiMax was added. The tube was inverted 3 times. For more than one transfection at a time a bulk solution of Lipofectamine RNAiMAX was prepared. After 5 min. of incubation at room temperature, 250 µl of OptiMEM I-RNAiMAX solution was transferred in one of the prepared siRNA containing microcentrifuge tube. The tube was mixed gently, centrifuged briefly and incubated for 20 min. at room temperature, in order to form siRNA-lipidcomplexes.

In the meantime 500 µl of DMEM was removed from each well of the 6-well plate. After incubation 500 µl of siRNA-lipidcomplex solution was added to the wells, mixed gently by pipetting and incubated for 72 hours at 37°C in the incubator. Each well contains now 50 nM siRNA and 0.125% Lipofectamine RNAiMAX.

#### **2.3.5 Preparation of cells for 3D-collagen gels**

After 72 hours of incubation the growth medium was removed from the 6-well plates, the cells were rinsed with 2 ml of 1x PBS and 200 µl of TE was added. After incubation at 37°C, when all cells were detached, the cells were agitated with 1 ml of complete growth medium (DMEM +10% serum w/o antibiotics) and transferred in a 60 mm tissue plate. 3 ml of growth medium was added; cells were spread and incubated for additional 24 hours. The cells were then trypsinised for aggregation (see chapter 2.2.3.1).

## 2.4 Western blot analysis

### 2.4.1 Buffers and solutions

#### NP40 lysis buffer:

- 40 mM Hepes pH 7.5
- 120 mM NaCl
- 1 mM EDTA pH 8.0
- 10 mM 2-glycerophosphate
- 50 mM NaF
- 0.5mM Na<sub>3</sub>VO<sub>4</sub>
- 1% NP40

In a 15 ml centrifuge tube 0.4 ml of 1 M Hepes (pH 7.5), 1.2 ml of 1 M NaCl, 20 µl of 0.5 M EDTA (pH 8.0), 1 ml of 0.1 M 2-glycerophosphate, 1 ml of 0.5 M NaF, 0.1 ml of 50 mM Na<sub>3</sub>VO<sub>4</sub> and 1 ml of 10% NP40 were added. The solution was filled to a total volume of 10 ml with H<sub>2</sub>O<sub>dest.</sub>. It was mixed by agitation, aliquoted in 490 µl portions and stored at -20°C.

#### PIM:

- 2 µg/ml Leupeptin
- 2 µg/ml Aprotinin
- 0,3 µg/ml Benzamidine chloride
- 10µg/ml Trypsin inhibitor

In a 50 ml centrifuge tube 100 µg of leupeptin, 100 µg of aprotinin, 15 µg of benzamidine chloride and 500 µg of trypsin inhibitor was weighed and filled with H<sub>2</sub>O<sub>dest.</sub> to a total volume of 50 ml. The tube was mixed thoroughly by agitation, aliquoted in 10 µl portions and stored at -20°C.

#### 4x protein sample buffer:

- 200 mM Tris pH 6.8
- 400 mM DTT
- 8% SDS
- 0.4% Bromphenol blue
- 40% Glycerol

In a 50 ml centrifuge tube 5 ml of 2 M Tris (pH 6.8), 20 ml of 1 M DTT and 20 ml of glycerol were added by pipetting and 4 g of SDS and 2 g of bromophenolblue were weighed. The tube was mixed by agitating, H<sub>2</sub>O<sub>dest.</sub> was added to a total amount of 50 ml and aliquots of 1 ml were prepared. They were stored at -20°C.

Buffer B pH 8.8:

- 1.5 M Tris pH 8.8

- 0.4% (v/v) SDS

In a 500 ml glass beaker 90.75 g of Tris was weighed and 20 ml of 10% SDS was added by pipetting. It was filled with H<sub>2</sub>O<sub>dest.</sub> to a volume of 250 ml. While stirring with a magnetic stirrer 37% HCl was added till a pH of 8.8 was achieved and the solution had room temperature. Thereafter it was filled with H<sub>2</sub>O<sub>dest.</sub> to a total volume of 500 ml. This solution was stored at 4°C.

APS:

- 10% (w/v) APS

In a 15 ml centrifuge tube 1 g of ammonium persulfate was dissolved in 10 ml of H<sub>2</sub>O<sub>dest.</sub>. It was stored at 4°C.

Buffer C pH 6.8:

- 0.5 M Tris pH 6.8

- 0.4% (v/v) SDS

In a 500 ml glass beaker 30.25 g of Tris was weighed and 20 ml of 10% (w/v) SDS was added by pipetting. It was filled with H<sub>2</sub>O<sub>dest.</sub> to a volume of 250 ml. While stirring with a magnetic stirrer 37% HCl was added till a pH of 6.8 was achieved and the solution had room temperature. Thereafter it was filled with H<sub>2</sub>O<sub>dest.</sub> to a total volume of 500 ml. This solution was stored at 4°C.

10x electrophoresis buffer:

- 250 mM Tris

- 1.94 M glycine

- 1% (w/v) SDS

In a 1 l glass flask 30.3 g of Tris, 146 g glycine and 10 g SDS was weighed, H<sub>2</sub>O<sub>dest.</sub> was added to a final volume of 1 l and the buffer was stirred with a magnetic stirrer. It was stored at room temperature.

1x electrophoresis buffer:

- 10% (v/v) 10x electrophoresis buffer

In a measuring cylinder 450 ml of H<sub>2</sub>O<sub>dest.</sub> were filled and 50 ml of 10x electrophoresis buffer were added. The cylinder was closed with parafilm and agitated well.

Harlow 1:

- 48 mM Tris

- 386 mM glycine

- 0,1% (w/v) SDS

- 20% (v/v) methanol

In a 5 l glass flask 29 g of Tris, 145 g of glycine and 5 g of SDS was weighed and filled with H<sub>2</sub>O<sub>dest.</sub> to a volume of 4 l. Thereafter 1 l of methanol was added and mixed by stirring with a magnetic stirrer. This buffer was stored at 4°C

10x Ponceau S:

- 2% (w/v) Ponceau S

- 30% (w/v) trichlor acetic acid

- 30% (w/v) sulfosalicylic acid

In a 100 ml flask 2 g of Ponceau S, 30 g of trichlor acetic acid and 30 g of sulfosalicylic acid was weighed and filled with H<sub>2</sub>O<sub>dest.</sub> to a volume of 100 ml. The solution was mixed by stirring with a magnetic stirrer and was stored at room temperature.

1x Ponceau S:

- 10% (v/v) 10x Ponceau S

In a 50 ml centrifuge tube 5 ml of 10x Ponceau S was added to 45 ml of H<sub>2</sub>O<sub>dest.</sub>. The solution was mixed by agitation and stored at room temperature.

10x TBS:

- 1.5 M NaCl

- 0.5 M Tris pH 7.4

In a 2 l glass beaker 175.32 g of NaCl and 121.14 g of Tris was weighed and filled with H<sub>2</sub>O<sub>dest.</sub> to a volume of 1 l, a magnetic stirrer was added. Thereafter the pH was adjusted with 37% HCl while stirring and occasional cooling phases until the solution had room temperature and a pH of 7.4. H<sub>2</sub>O<sub>dest.</sub> was added to a total volume of 2 l and the solution was transferred into a 2 l glass flask by decanting. It was stored at room temperature.

1x TBS-T:

- 10% (v/v) 10x TBS
- 0.1% (v/v) Triton X-100

A 1 l glass flask was filled with 900 ml of H<sub>2</sub>O<sub>dest.</sub>, 100 ml of 10x TBS and a magnetic stirrer were added. While stirring 1 ml of Triton X-100 was added and stirring was continued until it was mixed well. This solution was stored at room temperature.

5% blocking solution:

- 5% (w/v) milk powder
- 1x TBS-T

In a 15 ml centrifuge tube 10 ml of 1x TBS-T was pipetted and 0.5 g of milk powder was added. The tube was agitated until it was dissolved completely. This solution was never stored.

TBS-T, 5% BSA:

- 5% (w/v) bovine serum albumine
- 1x TBS-T

In a 15 ml centrifuge tube 10 ml of 1x TBS-T was pipetted and 0.5 g of bovine serum albumin was added. The tube was agitated until BSA was completely dissolved. It was stored at 4°C.

stripping buffer:

- 60 mM Tris pH 6.7
- 2% SDS
- 0.7% 2-mercaptoethanol

In a 250 ml glass flask 9 ml of Tris (pH 6.7) and 30 ml of 10% SDS was added and filled with H<sub>2</sub>O<sub>dest.</sub> to a volume of 150 ml. Under a fume hood 1 ml of 2-mercaptoethanol was



added and mixed by agitation. Stripping buffer was stored at room temperature but not longer than over night.

#### **2.4.2 Protein extraction**

All further steps were proceeded on ice. Growth medium was discarded and cells were rinsed with 5 ml of cold 1x PBS. After aspiration of 1x PBS cells were trypsinised with 500µl of TE. Tissue culture plates were incubated at room temperature with periodical microscopic examination until all cells were detached. Cells were agitated with 5 ml of cold complete growth medium (DMEM +10% serum) and were transferred into 15 ml centrifuge tubes. After centrifugation with 1000 rpm at 4°C for 10 min. the supernatant was discarded; cells were resuspended with 1 ml of cold 1x PBS by pipetting and transferred into microcentrifuge tubes. After new centrifugation step the supernatant was removed and the cells were washed once more with 1x PBS. The tube was centrifuged again. In the meantime the lysis buffer was prepared. To 490µl of NP40 lysis buffer 5µl of PMSF and 5µl of PIM were added. Depending on the remaining pellet size after the last centrifugation, the double amount of NP40 lysis buffer was added, cells were agitated thoroughly and vortexed before the tube was incubated on ice for 20 min. in a Eppendorf Centrifuge 5417R (Eppendorf, Hamburg, Germany). Thereafter the tube was centrifuged for 20 min. at 4°C with 15.000 rpm. The supernatant was carefully transferred into new microcentrifuge tubes and were stored at -80°C.

#### **2.4.3 Protein preparation**

The protein amount in the extracts was measured with Bradford solution, which was prepared by adding 10 ml of Biorad Protein Assay to 40 ml of H<sub>2</sub>O<sub>dest.</sub>. To 500 µl of Bradford solution 1 µl of the protein sample and NP40 lysis buffer as a reference probe respectively was added in a cuvette (Sarstedt, Nümbrecht, Germany, 67.746), mixed gently by carefully pipetting and incubated for 5 min. at room temperature. The protein amount was measured with a BioPhotometer (Eppendorf, Hamburg, Germany). Then the amounts for 15 µg of protein samples were calculated.

The according amounts were pipetted in new centrifuge tubes and filled with NP40-lysis buffer to a volume of 6 µl. 1.5 µl of 4x protein sample buffer was added, the tubes were vortexed, spinned and boiled at 95°C with a thermomixer (Thermomixer comfort,

Eppendorf, Hamburg, Germany) for 5 min. Afterwards the samples were cooled down to room temperature.

#### 2.4.4 SDS-PAGE

In a measuring cylinder 1x electrophoresis buffer was prepared by adding 50 ml of 10x electrophoresis buffer to 450 ml of H<sub>2</sub>O<sub>dest.</sub> and it was closed with a piece of Parafilm “M”® (American National Can Company, VWR, West Chester, Pa, USA, 52858-032). Afterwards the cylinder was inverted three times and cooled down to 4°C.

For SDS-PAGE the Mini-PROTEAN Tetra Electrophoresis System from BioRad (Hercules, CA, USA, 165-8002) was used, with a 15-slots comb (BioRad, Hercules, CA, USA, 165-3355).

The 0.75 mm spacer plate and a short plate were combined in a casting frame, which was afterwards fastened in a casting stand, so that the gel could not trickle out. Thereafter the acrylamide gel was produced with following amounts of reagents:

| <b>10.5% separating gel</b>       |        | <b>stacking gel</b>               |         |
|-----------------------------------|--------|-----------------------------------|---------|
| acrylamide                        | 4.2 ml | acrylamide                        | 0.5 ml  |
| buffer B                          | 3 ml   | buffer C                          | 0.75 ml |
| H <sub>2</sub> O <sub>dest.</sub> | 4.8 ml | H <sub>2</sub> O <sub>dest.</sub> | 1.75 ml |
| APS                               | 60 µl  | APS                               | 30 µl   |
| TEMED                             | 5 µl   | TEMED                             | 2.5 µl  |

At first the separating gel was produced. For that acrylamide, buffer B and H<sub>2</sub>O<sub>dest.</sub> were pipetted in a 15 ml centrifuge tube, APS and TEMED were added to start polymerisation and the centrifuge tube was mixed thoroughly. Then it was filled between the spacer and short plate by pipetting. To get a smooth edge 1 ml of isopropyl alcohol was added on top of the separating gel. After polymerisation it was poured off, washed three times with H<sub>2</sub>O<sub>dest.</sub> and dried with filter paper. Then the stacking gel containing acrylamide, buffer C, H<sub>2</sub>O<sub>dest.</sub>, APS and TEMED was prepared, mixed thoroughly and pipetted on top of the separating gel. A 15-slot comb was added.

After polymerisation the electrophoresis system was built with either two gels or one with a buffer dam. The chamber was filled with the prepared 1x electrophoresis buffer. Thereafter the comb was carefully removed in order not to damage the gel. The slots were cleaned by pipetting electrophoresis buffer in the slots.

The slots were loaded with 2.5 µl of PageRuler Prestained Protein Ladder and 7.5 µl of sample respectively by pipetting. The equipment was run with 60 V at the beginning, when the samples form a straight line the voltage was raised to 110 V, till the marker front reaches the bottom of the gel.

#### **2.4.5 Western blot**

Preliminary a 8.5 x 6 cm piece of nitrocellulose membrane (Watman, Dassel, Germany, 10401396) was cut. To ensure proper protein transfer the membrane was equilibrated in Harlow buffer for 10 min. We used a Mini Trans-Blot Module (BioRad, Hercules, CA, USA, 170-3935) with the lower buffer tank and the lid from the Mini-PROTEAN Tetra Electrophoresis System for the transfer. Afterwards 2 foam pads, 4 pieces of 3MM Chr sheets (Whatman, Dassel, Germany, 3030 917) with a size of 8 x 10 cm, the lower buffer tank, inserts, a cooling unit and a lid were prepared. When SDS-PAGE was finished the sandwich for the western blot was assembled as follows, all foam pads and 3MM Chr sheets were soaked with Harlow buffer before use: on top of the black side of the insert one foam pad was placed and one Chr sheet was added. The SDS-PAGE gel was taken out of the chamber and the glass plates were parted so that the gel stayed on the short plate. The stacking gel was removed, one filter paper was layed on the gel, which was transferred on the Chr sheet and thereafter laid on the previous Chr sheet on the insert. The nitrocellulose membrane was put on top of it, thereafter 2 Chr sheets and the second foam pad. The insert was closed, put in the chamber, the cooling unit was added and afterwards Harlow buffer was filled to the top of the chamber. The chamber was closed with the lid and the equipment was run for 1 hour at 350 mA or over night at 25 mA. Afterwards the membrane was transferred in a box with  $H_2O_{dest.}$ , which was placed on an orbital shaker for 5 min. to wash Harlow buffer residues away. The membrane was then incubated for 15 min in a box with 10 ml of Ponceau S to stain all proteins on the membrane; the box was put on a rocking platform (VWR, West Chester, Pa, USA, 40000300). To destain the membrane it was swayed in fresh  $H_2O_{dest.}$  untill all lanes were visible and the background was white again. It was scanned and saved. Afterwards it was destained completely in 1x TBS-T and blocked for 1 hour in 10 ml of 5% blocking solution at room temperature or over night at 4°C. The membrane was then washed three times for 10 min. in 1xTBS-T.

#### **2.4.6 Protein detection**

The blot was incubated in first antibody diluted in TBS-T, 5% BSA over night. The various dilution factors for the used antibodies were shown in chapter 2.4.8.1. Next day it was washed three times for 10 min. with 1x TBS-T. Then it was incubated in 10 ml of 5% blocking solution containing secondary antibody with a dilution of 1:10.000 for 1 hour at room temperature. After that the blot was washed three times for 10 min. with 1x TBS-T again. The signals were detected using enhanced chemiluminescence, which was prepared by mixing equal amounts of detection reagent 1 and 2. For membranes with more than 7 lanes 1.5 ml, membranes with 4 to 7 lanes 1 ml and membranes with less than 4 lanes 0.5 ml per reagent were used. The membrane was incubated for 1 min. with ECL, thereafter it was drained on paper towels and wrapped in cling film. The membrane was taped into cassettes and incubated with light-sensitive Amersham Hyperfilms (GE Healthcare, Buckinghamshire, UK, 28906837) and CL-XPosure films (Thermo Scientific, Rockford, IL, USA, 34089). Afterwards the films were fixed and developed using an Kodak Medical X-ray Processor MXP 2000 (Kodak, Carestream Health Inc, Rochester, NY, USA).

#### **2.4.7 Reprobing**

After detection of phosphorylated proteins the membrane was stripped to detect the amount of total protein. A watherbath shaker (Julabo SW22), containing a box with stripping buffer, was preheated to 55°C. After washing the membrane in 1x TBS-T it was incubated in 75 ml of stripping buffer at 55°C. For intense signals of phosphorylated protein the blot was incubated for 15 min., when the signal was weak the incubation time was shortened to 10 min. Afterwards it was washed three times in 1x TBS-T for 10 min. and incubated for 1 hour at room temperature in 10 ml of blocking solution. The detection procedure was repeated with the primary antibodies for the total protein.

## 2.4.8 Antibodies

The following antibodies were used for Western blot detection.

### 2.4.8.1 Primary antibodies

| antibody                  | phosphorylation | source | MW               | dilution | company                   | Lot No.   |
|---------------------------|-----------------|--------|------------------|----------|---------------------------|-----------|
| $\alpha$ -Rictor          | -               | rabbit | 200 kDa          | 1:2000   | Bethyl Laboratories, Inc. | A300-459A |
| $\alpha$ -Raptor          | -               | rabbit | 150 kDa          | 1:2000   | Bethyl Laboratories, Inc. | A300-506A |
| $\alpha$ -p70 S6K (108D2) | threonine 389   | rabbit | 70 kDa<br>85 kDa | 1:1000   | Cell signaling            | #9234     |
| $\alpha$ -p70 S6K         | -               | rabbit | 70 kDa<br>85 kDa | 1:1000   | Cell signaling            | #9202     |
| $\alpha$ -pAkt (D9E)      | serine 473      | rabbit | 60 kDa           | 1:1000   | Cell signaling            | #4060     |
| $\alpha$ -Akt             | -               | rabbit | 60 kDa           | 1:1000   | Cell signaling            | #9272     |

### 2.4.8.2 Secondary antibody

This secondary antibody was conjugated to horseradish peroxidase.

| antibody                       | source | dilution | company                   | Lot No.   |
|--------------------------------|--------|----------|---------------------------|-----------|
| Goat- $\alpha$ -rabbit IgG-h+l | goat   | 1:10.000 | Bethyl Laboratories, Inc. | A120-101P |

## 2.4.9 Densitometric evaluation of X-ray films

After Western blot analysis the developed films were scanned and used for density measurements with ImageJ64 (version 1.64q). The image of the blot was opened and the colour was inverted, thereafter a square was drawn, which had the size of the biggest signal. It was moved to the first sample for measuring the mean intensity; then moved to a free space beneath the signal where the measurement was repeated to get a value for the background. After collecting values for all samples they were copied to Microsoft Excel 2008, where the background was subtracted. Thereafter the intensities were normalised to the control for equal loading to get results, which are directly comparable. The control sample of each antibody was set to 100% and the corresponding percentages of all other samples were calculated. These data sets were presented graphically using GraphPad Prism 4 (GraphPad Software Inc.).

## 2.5 Flow cytometry

### 2.5.1 Buffers and solutions

#### collagenase B:

- 0,10 g/l  $\text{CaCl}_2$
- 0,10 g/l  $\text{MgCl}_2$  hexahydrate
- 0,20 g/l KCl
- 1x PBS w/o  $\text{Ca}^{2+}$ ,  $\text{Mg}^{2+}$ , K

In a 500 ml flask of 1x PBS (w/o  $\text{Ca}^{2+}$ ,  $\text{Mg}^{2+}$ , K) 0,068 g  $\text{CaCl}_2$  dihydrate, 0,05 g  $\text{MgCl}_2$  hexahydrate and 0,1 g KCl were weighed and mixed by stirring with a magnetic stirrer. An aliquot of 10 ml was sterile filtrated with a single-use syringe (B Braun, Bethlehem, PA, USA, 460 6051 V) and a syringe filter with 0,2  $\mu\text{m}$  pore size (Whatman, Dassel, Germany, 6809-2122).

#### RNAse A stock solution:

- 20 mg/ml RNAse A

In a 50 ml centrifuge tube 400 mg of ribonuclease A was weighed, filled with  $\text{H}_2\text{O}_{\text{dest.}}$  to a total volume of 20 ml and was put in a preheated thermomixer with 99°C for 5 min. Afterwards it was aliquoted in 1.25 ml portions, which were stored at -20°C.

#### PI:

- 1.176 mg/ml of trisodiumcitrat
- 0.25 mg/ml of RNAse A
- 0.05 mg/ml of propidium iodide
- 0.1% Triton X-100

In a 250 ml glass beaker 117.6 mg of trisodiumcitrate and 5 mg of propidium iodid were weighed and 98,75 ml of  $\text{H}_2\text{O}_{\text{dest.}}$  was added. While 1.25 ml of 20 mg/ml stock solution of RNAse A and 100  $\mu\text{l}$  of Triton X-100 were added by pipetting the solution was mixed by stirring with a magnetic stirrer. When the solution was mixed thoroughly it was aliquoted in 5 ml and 10 ml aliquots and stored at -20°C. The solutions were not thawed more than twice.

### **2.5.2 Cell fixation and staining of tissue culture cells**

All further steps were proceeded on ice. Growth medium was discarded, cells were rinsed with 5 ml of cold 1x PBS and were trypsinised with 500 µl of TE. Tissue culture plates were incubated at room temperature with periodical microscopic examination until all cells were detached. Cells were agitated with 5 ml of cold complete growth medium (DMEM +10% serum) and were transferred into 15 ml centrifuge tubes. After centrifugation at 1000 rpm for 5 min. at 4°C the supernatant was aspirated and the cells were washed three times with 3 ml of cold 1x PBS. After new centrifugation step supernatant was removed completely. Cells were fixed in 60% ethanol, therefore cells were resuspended with 800 µl of cold 1x PBS by vortexing. During vortexing 1200 µl of absolute ethanol (-20°C) was slowly dropped into the centrifuge tube and afterwards vortexing was continued for additional 15 seconds. Cells were fixed over night at -20°C. The next day it was centrifuged at 1000 rpm for 10 min., the supernatant was discarded and the cell-pellet was air-dried. Then 500 µL PI was added, cells were agitated and incubated for 20 min. on ice in the dark. Afterwards the cell suspension was transferred into a FACS-tube.

### **2.5.3 Establishing a harvesting protocol for 3D collagen gels**

Cells were trypsinised as described in chapter 2.5.2. After the last washing step with 1x PBS cells were centrifuged at 1000 rpm for 5 min. at 4°C. Thereafter half of the cells were resuspended in 150 µl of 1,25 µg/µl collagenase B dissolved in 1x PBS with 0,1 g/l CaCl<sub>2</sub>, 0,1 g/l MgCl<sub>2</sub> and 0,2 g/l KCl, the second half was incubated with 150µl of the same 1x PBS and both were incubated for 60 min. at 37°C in the incubator. Afterwards 1.5 µl of 0.5 M EDTA was added to stop the enzymatic activity of collagenase B, cells were centrifuged, supernatant was discarded and cells were resuspended in 100 µl of cold 1x PBS. Cells were fixed in 60% ethanol, for that cells were resuspended with 800 µl of cold 1x PBS by vortexing. During vortexing 1200 µl of absolute ethanol (-20°C) was slowly dropped into the centrifuge tube and afterwards vortexing was continued for additional 15 seconds. Cells were fixed over night at -20°C. The next day it was centrifuged at 1000 rpm for 10 min., the supernatant was discarded and the cell-pellet was air-dried. Then 500 µL PI was added, cells were agitated and incubated for 20 min. on ice in the dark. Afterwards the cell suspension was transferred into a FACS-tube.

#### **2.5.4 Harvesting cells from 3D collagen gels**

For FACS analysis single-cell suspension assay and spheroid assay was performed, respectively.

The collagen gel is lysed with collagenase B, which is dissolved in 1x PBS with 0,1 g/l  $\text{CaCl}_2$ , 0,1 g/l  $\text{MgCl}_2$  and 0,2 g/l KCl.

The growth medium in the 24-well plate was discarded and the gel was washed with 250  $\mu\text{l}$  of 1x PBS twice for 10 min. After discarding 1x PBS 150  $\mu\text{l}$  of 1,25  $\mu\text{g}/\mu\text{l}$  collagenase B was added and the gel was incubated at 37°C in the incubator until the gel was solubilised and the aggregates and cells were detached. After stopping the enzymatic activity with 1.5  $\mu\text{l}$  of 0,5 M EDTA and transferring the suspension into a vial, it was centrifuged at 1000 rpm for 3 min. The supernatant was discarded, 50  $\mu\text{L}$  of TE was added and the vial was incubated at 37°C until all cells were spread. Then 1 ml of full growth medium (DMEM +10% serum) was added and the vial was centrifuged at 1000 rpm for 5 min.

#### **2.5.5 Analysis**

The samples were measured with a FACSCalibur (Beckton Dickinson, Franklin Lakes, NJ, USA) using Cellquest (Version 6.0 BD Immunocytometry Systems) to acquire the raw data. FlowJo (Version 7.5.5) was used for analysis.

Due to the treatments with collagenase B cells got sticky. For that reason the crude data contains many cell aggregates. For doublet-discrimination we gated our cells in a two-dimensional dot-plot containing DNA content (FL2-A) and cell width (FL2-W). All cells in the quadrant from 0 - 400 were used for further size and cell cycle analysis.



## 2.6 Microscopic analysis

### 2.6.1 Buffers and solutions

#### 4% Paraformaldehyde (PFA) pH 7.4:

- 4% (w/v) PFA
- 1% 1M NaOH
- 10% 10x PBS

In a 500 ml glass beaker 20 g of Paraformaldehyde was weighed, 250 ml of H<sub>2</sub>O<sub>dest.</sub> and 5 ml of NaOH was added. It was stirred at 65°C until PFA was dissolved completely. Thereafter 50 ml of 10x PBS was added and pH of 7.4 was adjusted. The solution was filled to a total volume of 500 ml with H<sub>2</sub>O<sub>dest.</sub>. It was aliquoted in portions of 10 ml and stored at -20°C.

#### 1x TBS-Tween:

- 0.5% Tween-20
- 1x TBS

In a 250 ml glass beaker 25 ml of 10x TBS was pipetted to 225 ml of H<sub>2</sub>O<sub>dest.</sub> and was mixed by agitation. A magnetic stirrer was added and while stirring 1.25 ml of Tween 20 was added by pipetting. The solution was filtered with sterile filtration units with 0.2 µm pore size and was stored at 4°C.

#### 1x PBS-Tween:

- 0.5% Tween-20
- 1x PBS

In a 500 ml flask of 1x PBS 2.5 ml of Tween 20 was added while stirring with a magnetic stirrer. Afterwards it was filtered with sterile filtration units with 0.2 µm pore size and was stored at 4°C.

#### Blocking buffer:

- 5% FCS
- 0.3% Triton X-100
- 1x PBS

In a 50 ml centrifuge tube 23.5 ml of 1x PBS was preplaced by pipetting. While stirring with a magnetic stirrer 1.25 ml of FCS and 75 µl of Triton X-100 was added. The solution was stored at 4°C.

Antibody Dilution Buffer:

- 1% BSA
- 0,3% Triton X-100
- 1x PBS

In a 50 ml centrifuge tube 40 ml of 1x PBS was preplaced and 0.4 g BSA was added. It was dissolved by agitation and afterwards 120 µl of Triton X-100 was added while stirring with a magnetic stirrer. The solution was stored at 4°C.

## **2.6.2 Immunofluorescence stainings**

Cells were trypsinised as described in chapter 2.2.3. Then 10 µl of cell suspension was agitated with 10 µl of trypan blue and cell number was determined with a hemacytometer (see chapter 2.2.3.1). The amount of cell suspension for 75.000 cells was transferred into each well of a 4-well chamber slide (Lab-Tek®, Nalge Nunc International, Naperville, IL, USA, 177437) and complete growth medium (DMEM +10% serum) was added to a final volume of 1 ml. Slides were incubated at 37°C in the incubator at least over night. During incubation cells were treated as desired.

After previous treatment growth medium was discarded and 500 µl of 4% PFA was added and incubated at room temperature for 15 min. Afterwards 4% PFA was discarded, 1 ml 1x PBS was added and the chamber slide was closed tightly with parafilm. At this point the chamber slides could be stored at 4°C for weeks.

Next step was rinsing the cells twice with 1 ml of 1x TBS-Tween for 10 min. each, then twice in 1x PBS-Tween for 10 min. and afterwards blocked in 30 µl of blocking buffer per well for 1 hour at room temperature. Then the wells were washed three times for 10 min. with 1 ml of 1x PBS-Tween again. The chambers and the adhesive were carefully removed. From now on all washing and incubation steps were performed in a humid chamber. 30 µl/well of primary antibody in antibody dilution buffer was added and incubated over night at 4°C. For double labelling both primary antibodies were diluted in the same tube with antibody dilution buffer. For the used primary antibodies and dilution factors see chapter 2.6.6.

Next day cells were rinsed three times with 1ml of 1x PBS-Tween for 5 min. Cells were incubated with 30 µl/well of secondary antibody (dilution factor 1:500) in antibody

dilution buffer for two hours at room temperature in the dark. For double labelling both secondary antibodies were diluted in the same tube with antibody dilution buffer. Afterwards slides were washed with 1 ml of 1x PBS-Tween three times for 5 min., 50 µl/well of 2 µg/ml DAPI with 0,6µl of Alexa Fluor® 546 phalloidin (dilution factor 1:80) was added and chamber slides were incubated for 45 min. at room temperature in the dark.

At last cells were rinsed with 1 ml of 1x PBS-Tween, mounting medium was dropped on the slides and cover slides were added. They were stored at 4°C and protected from light.

### **2.6.3 Immunofluorescence stainings of collagen gels**

For microscopic analysis the spheroid assay was performed with 1,500 cells per spheroid. The basic steps of this protocol were the same as described in chapter 2.6.2 only the following parameter were changed.

After removing growth medium the collagen gels were fixed with 1 ml 4% PFA for 30 min. at room temperature in the same 24-well plates they were incubated with. Like chamber slides the collagen gel could be stored with 1 ml 1x PBS.

After washing steps the gels were blocked for 1½ hour with 30 µl of blocking buffer at room temperature. The following washing steps were the same as above. A piece of parafilm was placed in a humid chamber and drops of 1x PBS-Tween were preplaced. Then the gel was cut into pieces, containing parts of the mesh and each one was laid down on a drop, so that the gel unwinds.

After the last washing step, for each gel fragment a drop of mounting media was preplaced on a glass slide (Thermo Scientific, Waltham, MA, USA, DXD-10143560) and the parts were transferred. Then a cover slide (Thermo Scientific, Waltham, MA, USA, DXD-10143263 24x60 mm #1) was added and the slides were stored at 4°C, protected from light.

### **2.6.4 Microscopic analysis**

#### **2.6.4.1 Light microscopic analysis**

We used an Olympus IX51 microscope with the camera XC50 and CellF for image capturing. Invasion area of spheroids in collagen gels was measured using the software CellID. All invasive cells outside the spheroid were surrounded with the function “closed polygon”. After a complete turn the spheroid size itself was measured, these two results

were subtracted. Examined spheroid pictures were saved as new 8-bit files with scale bars, the calculated size was used for further analysis in GraphPad Prism 4 and Microsoft Excel 2008 (see chapter 2.8).

#### 2.6.4.2 Confocal microscopic analysis

All samples were analysed on a Zeiss LSM5 Exciter confocal microscope (Carl Zeiss, Oberkochen, Germany).

For the analysis of cleaved caspase-3 stained collagen gels, five optical sections through randomly chosen spheroids were captured, which were then merged to one picture using the projection tool of ImageJ64. Within the spheroids condensed nuclei could be observed. Cleaved caspase-3 positive cells, normal shaped nuclei and condensed nuclei were thereafter counted with the cell counter tool. These results were analysed using Microsoft Excel 2008 and GraphPad Prism 4 (see chapter 2.8).

### **2.6.5 Antibodies**

#### 2.6.5.1 primary antibodies

| antibody                                  | phosphorylation | source | dilution | company        | Cat No. |
|---|-----------------|--------|----------|----------------|---------|
| $\alpha$ -pS6                             | serine 240/244  | rabbit | 1:100    | Cell Signaling | #2215   |
| $\alpha$ -pAKT (D9E)                      | serine 473      | rabbit | 1:200    | Cell Signaling | #4060   |
| $\alpha$ -mTOR                            | -               | rabbit | 1:200    | Cell Signaling | #2972   |
| $\alpha$ -AKT                             | -               | rabbit | 1:200    | Cell Signaling | #9272   |
| $\alpha$ -4E-BP1                          | -               | rabbit | 1:200    | Cell Signaling | #9452   |
| $\alpha$ -p-H3                            | serine 10       | rabbit | 1:100    | Cell Signaling | #9701   |
| $\alpha$ -fibrillarin (C13C3)             | -               | rabbit | 1:400    | Cell Signaling | #2639   |
| $\alpha$ -cleaved caspase-3 (D175) (5A1E) | -               | rabbit | 1:200    | Cell Signaling | #9664   |

#### 2.6.5.2 secondary antibodies

| antibody                                | source | dilution | company    | Cat No. |
|---|--------|----------|------------|---------|
| Goat- $\alpha$ -rabbit Alexa Fluor® 488 | goat   | 1:500    | Invitrogen | A 11034 |
| Goat- $\alpha$ -mouse Alexa Fluor® 594  | goat   | 1:500    | Invitrogen | A 11032 |

#### 2.6.5.3 others

| name                        | target  | dilution | company       | Cat No. |
|-----------------------------|---------|----------|---------------|---------|
| DAPI                        | DNA     | 1:500    | Sigma-Aldrich | 32670   |
| Alexa Fluor® 546 phalloidin | F-actin | 1:80     | Invitrogen    | A 22283 |

## **2.7 Rapamycin and CVT-313 treatment**

The mTOR pathway inhibitor rapamycin and the cdk-2 inhibitor CVT-313 [95], both dissolved in DMSO, were added to the medium of the cells 24 hours before harvesting them for further experiments. The final concentration of rapamycin was 100 nM [46] and 2.5  $\mu$ M of CVT-313 in the growth medium. To exclude an effect of the solvent, control cells were treated at the same time with an equal amount of DMSO. The concentrations of the rapamycin stock solutions was 100  $\mu$ m and of CVT-313 it was 2.5 mM. They were stored at -20°C

## **2.8 Statistic analysis**

For statistic analysis we used GraphPad Prism 4 and Microsoft Excel 2008. Boxplots were created with GraphPad Prism 4. The box indicates the middle 50% of the data, which is from the lower (Q1) to the upper quartile (Q3); the line indicates the median (Q2); the whiskers show the smallest and largest observations.

Bar graphs were created with Microsoft Excel 2008. All graphs are presented with standard deviations.

Comparisons between different groups were calculated using a t-test (two tailed, paired), statistical significance is given with p-values  $\leq 0.05$ .

## **3 Results**

### **3.1 Establishing culture conditions for IMR-90 in collagen gels**

IMR-90 lung fibroblasts have not been cultured in collagen gels in our lab. Therefore we had to establish appropriate culture conditions. We decided to use either single-cell suspension cultures in collagen gel or to use spheroid collagen gel invasion assays. We kept the collagen gel I composition as well as the culture medium the same, whereas we varied cell number per spheroid, spheroid number per collagen gel and the duration of aggregation into spheroids to determine the most suitable conditions to follow outgrowth of the cells from the spheroids into the collagen I matrix.

In a pilot experiment, we used spheroids containing 1000 cells each, which we let aggregate for 24 hours prior to seeding 300 spheroids into one collagen gel. In this experiment it took 8 days until only a minority of the cells were invading into the collagen gel (Figure 3.1 a). It is known in the literature that fibroblasts undergo a process called nemosis, when they are cultivated in spheroids for extended time periods (Figure 3.2). Nemosis is described as a phenomenon, which display features of necrosis and apoptosis at the same time and has so far been observed only in vitro (for further informations on nemosis see chapter 1.2.1). Since we wanted to establish a system in which we can measure and quantify the outgrowth of cells into collagen gels, we strictly wanted to avoid dying cells. Therefore, we reduced the spheroid aggregation time to 14 hours. In addition we varied the amount of spheroids embedded into one collagen gel from 100 to 200 or 300 (Figure 3.1 b-d). Using these conditions, cells started to migrate from the spheroids into the collagen gel even on the first day, indicating that the shorter aggregation time was beneficial for the survival of the cells in the spheroids. However, when 100 spheroids were seeded only a few cells invaded the collagen gel. In the collagen gels harbouring 200 or 300 spheroids, many cells were exiting the spheroid and invading into the collagen gel. It appeared that with increasing amounts of spheroids seeded the amount of cells invading increased. With 300 spheroids/gel there were so many invading cells after only two days, which resulted in an intermingling of migrating cells between neighbouring spheroids, which hindered accurate quantification. Despite the presence of invading cells the spheroid cores looked very condensed and appeared as very dark structures, which indicated still dying cells in the sphere.

Based on these results we decided to let the cells undergo a shorter aggregation time and to use 200 spheroids per collagen gel. In a next experiment we used 1,500 cells per spheroid, 200 spheroids in one collagen gel and only 6 hours of aggregation (Figure 3.1 e). With these parameters we got the best results, the cells looked vital and the spheroids



did not appear as condensed and dark structured as before, indicating that the number of dead cells decreased. We decided to use 1500 cells per spheroid, aggregated for 6 hours and 200 spheroids per gel as our standard condition for microscopic analysis and quantification of invasive structures. For flow cytometry (see chapter 3.2-3.3) we used 300 spheroids per collagen gel and 3000 cells per spheroid to get a higher yield of cells. Single-cell suspension collagen gels were another 3D culture condition we used. Therefore, cells grown on tissue culture plates were trypsinised and 300,000 cells were embedded in collagen I gel (Figure 3.1 f). The lack of spheroid aggregation prevents cells from dying due to necrosis, even after a week of cultivation cells within these gels look vital. The only disadvantage is that a quantification of invasiveness is not possible.

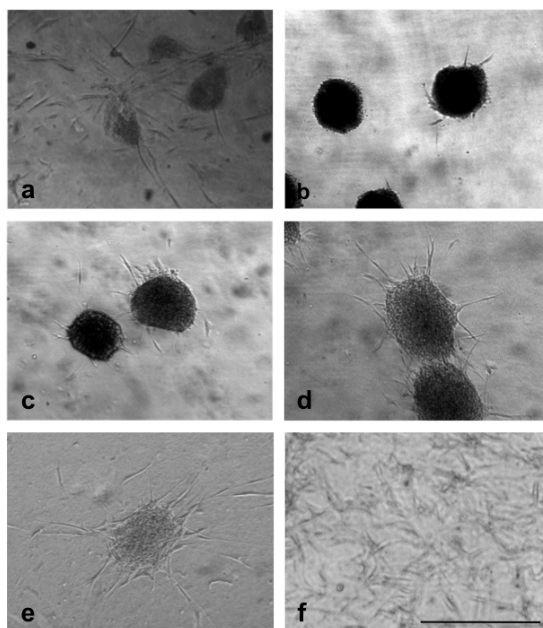


Figure 3.1: Establishing culture conditions for IMR-90 in collagen gels. **a** Pilot experiment with spheroids containing 1,000 cells each after 24 hours aggregation time. Thereafter 300 spheroids were embedded in collagen I gel. This picture shows the outgrowth after 8 days of cultivation. **b** Spheroids contained 3,000 cells after 14 hours of aggregation, 100 spheroids were embedded for this experiment and the picture was taken after one day. **c** 200 spheroids with 3,000 cells each were embedded in collagen gel after 14 hours of aggregation and pictures were taken after day one. **d** 300 spheroids with 3,000 cells each were embedded after 14 hours aggregation time; outgrowth was documented after one day. **e** Standard conditions for microscopic analyses are 200 spheroids each containing 1,500 cells after 6 hours of aggregation. This picture was taken after two days of cultivation. **f** For single-cell suspension collagen gels 300,000 cells were embedded in collagen gel, the picture was taken after two days. Scale bar represents 500  $\mu\text{m}$ .

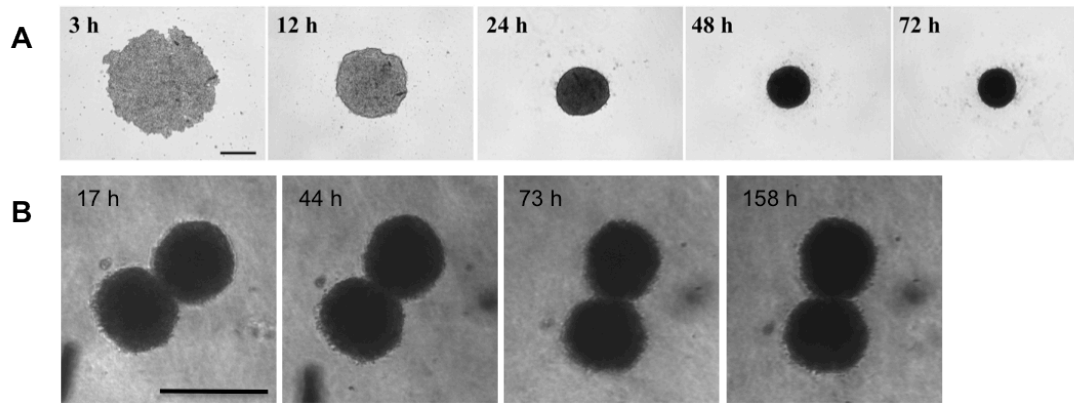


Figure 3.2: **A** Time course of human neonatal foreskin fibroblasts cultured as spheroids with 10,000 cells for 72 hours in agarose-coated wells. Scale bar represents 100  $\mu\text{m}$ . (figure taken from [25]) **B** Individual spheroids consist of 1,000 cells aggregated for 24 hours in non-adherent 96-well plates in methylcellulose-medium suspension. Thereafter 200 spheroids were embedded into collagen gel and images were taken for additional 7 days. Scale bar represents 250  $\mu\text{m}$ .

### **3.2 Establishment of a harvesting protocol for flow cytometry analysis**

Our next intent was to set up a protocol for the analysis of the DNA content and the cell size distribution of IMR-90 for cell cycle analysis by flow cytometry. Therefore, the cells had to be isolated from the collagen gels and be available as single cell suspensions. We used collagenase B to enzymatically digest the collagen I network of the gels in order to release the spheroid structures and the invading cells.

First of all we had to test, if the collagenase B treatment per se had any effects on our cells. Cells grown on tissue culture plates were trypsinised, washed with 1x PBS and divided into two aliquots. The cells in one sample were treated for 1 hour with 1.25 µg/µl collagenase B in PBS supplemented with  $\text{Ca}^{2+}$ ,  $\text{Mg}^{2+}$  and K, the other cells were resuspended in the incubation buffer without collagenase. Afterwards the cells were fixed in ethanol over night and stained with PI and analysed for DNA content and cell size distribution by flow cytometry. The collagenase treatment had no effect on the cell cycle distribution and the cell size as demonstrated by DNA content and forward/side scatter (size) analysis (Figure 3.3)

After testing the collagenase B effect on cells, we set up a standard harvesting protocol. Collagen gels were washed twice with 1x PBS to remove residual growth medium and thereafter, incubated with 1.25 µg/µl collagenase B in PBS supplemented with  $\text{Ca}^{2+}$ ,  $\text{Mg}^{2+}$  and K. As soon as the collagen I network was enzymtically resolved after about two hours collagenase B activity was stopped with 0.5 M EDTA. The cells were transferred into a microcentrifuge tube and immediately put on ice. Cells derived from a single-cell collagen gel were centrifuged and fixed in ethanol over night, whereas, cells harvested from spheroid-assay gels were centrifuged and incubated in TE additionally to dissolve spheroid structures. Thereafter the cells were resuspended in growth medium to inhibit further enzymatic activity of TE, centrifuged and fixed over night in ethanol. All samples were stained with PI and analysed by flow cytometry.

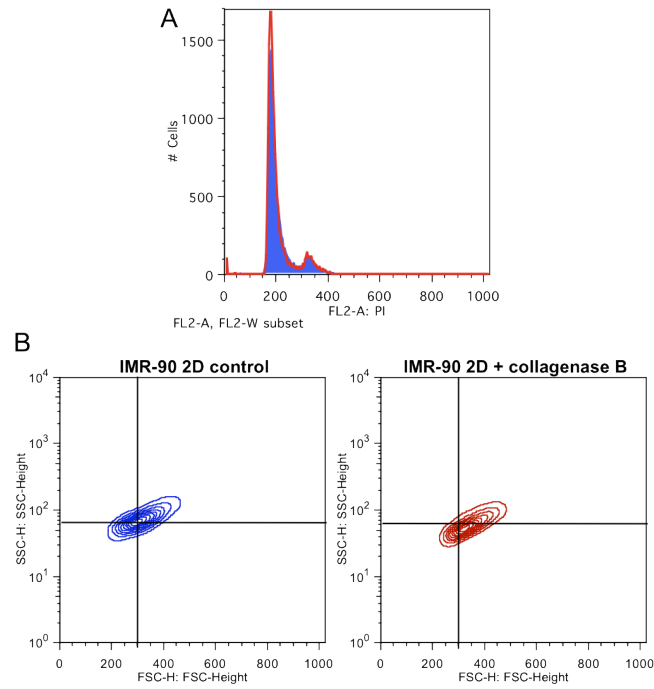


Figure 3.3: Comparison of collagenase B treated and untreated cells. Trypsinised cells grown on tissue culture plates were washed with 1x PBS and divided into two aliquots. One sample was treated with 1.25  $\mu\text{g}/\mu\text{l}$  collagenase B dissolved in PBS supplemented with  $\text{Ca}^{2+}$ ,  $\text{Mg}^{2+}$  and K for one hour. The other sample was incubated for one hour with 1x PBS supplemented with  $\text{Ca}^{2+}$ ,  $\text{Mg}^{2+}$  and K for control purpose. Cells were fixed in ethanol, stained with PI and analysed by flow cytometry. **A** The overlay of both DNA contents shows the control sample in blue and the collagenase B treated cells in red. **B** Comparison of forward/side scatter contour plots of the control sample in blue and the treated sample in red.

### 3.3 IMR-90 in different culture conditions

After we established a protocol for IMR-90 culture in collagen gels and a method to isolate cells from the gels as single cell suspensions for further analysis, we wanted to figure out whether IMR-90 grown in collagen gels, which represent the more *in-vivo* like situation, display a different phenotype compared to cells cultured on tissue plates. We were predominantly interested in differences in cell cycle distribution and cell size therefore FACS-analysis was our method of choice, because we could analyse both parameters in one step.

IMR-90 cells from the same passage number were cultivated as spheroids (IMR90-sph), spheroids embedded into collagen gels (IMR90-sph-CG), single-cell suspension collagen gels (IMR90-cell-CG), sparse (IMR90-2D-sparse) and dense 2D cultures (IMR90-2D-dense) on conventional plastic dishes. The spheroids were harvested after 6 hours of aggregation, one of two collagen gels with spheroids after one hour (IMR90-sph-CG-1h) and the second one like the single-cell collagen gel after two days of cultivation (IMR90-sph-CG-2d). The sparse tissue culture plate was harvested the day after seeding, whereas the dense plate was harvested when cells reached 95% confluence.

Before harvesting cell morphology was documented by microscopic pictures of the cells under all conditions. After fixation all samples were stained with PI and analysed by flow cytometry (Figure 3.4 A).

The DNA-content profiles show that IMR90-2D-sparse shows a higher fraction of S (26.5%) and G2 phase (14.1%) cells than in all other conditions (Figure 3.4 B). As expected, IMR90-2D-dense display a cell cycle arrest in G1 (73.3%) with reduced S (20%) and G2 phase (3.26%). IMR90-single-CG display 8.6% S phase cells and 11.8% G2 phase cells. IMR90-sph and IMR90-sph-CG-1h show also a higher S phase (13.3%, 13.8%) than IMR90-sph-CG-2d with 4.9%. IMR90-sph-CG-2d displays about 10% G2 phase cells.

Interestingly we found that forward scatter/side scatter profiles show that the granularity of the cells did not change significantly within IMR90-2D-sparse, IMR90-2D-dense, IMR90-cell-CG, IMR90-sph and IMR90-sph-CG-1h, whereas in IMR90-sph-CG-2d it is reduced (SSC) (Figure 3.4 C) concomitantly all cells cultured in collagen gels are smaller than cells grown on tissue culture plates (FSC) (Figure 3.4 D,E). IMR90-sph and IMR90-sph-gel-1h display the same size, IMR90-single-gel is slightly smaller than the two mentioned before. IMR90-sph-gel-2d display a dramatic decrease in cell size as compared to cells grown on plastic; in addition they are also smaller than IMR90-single-gel.

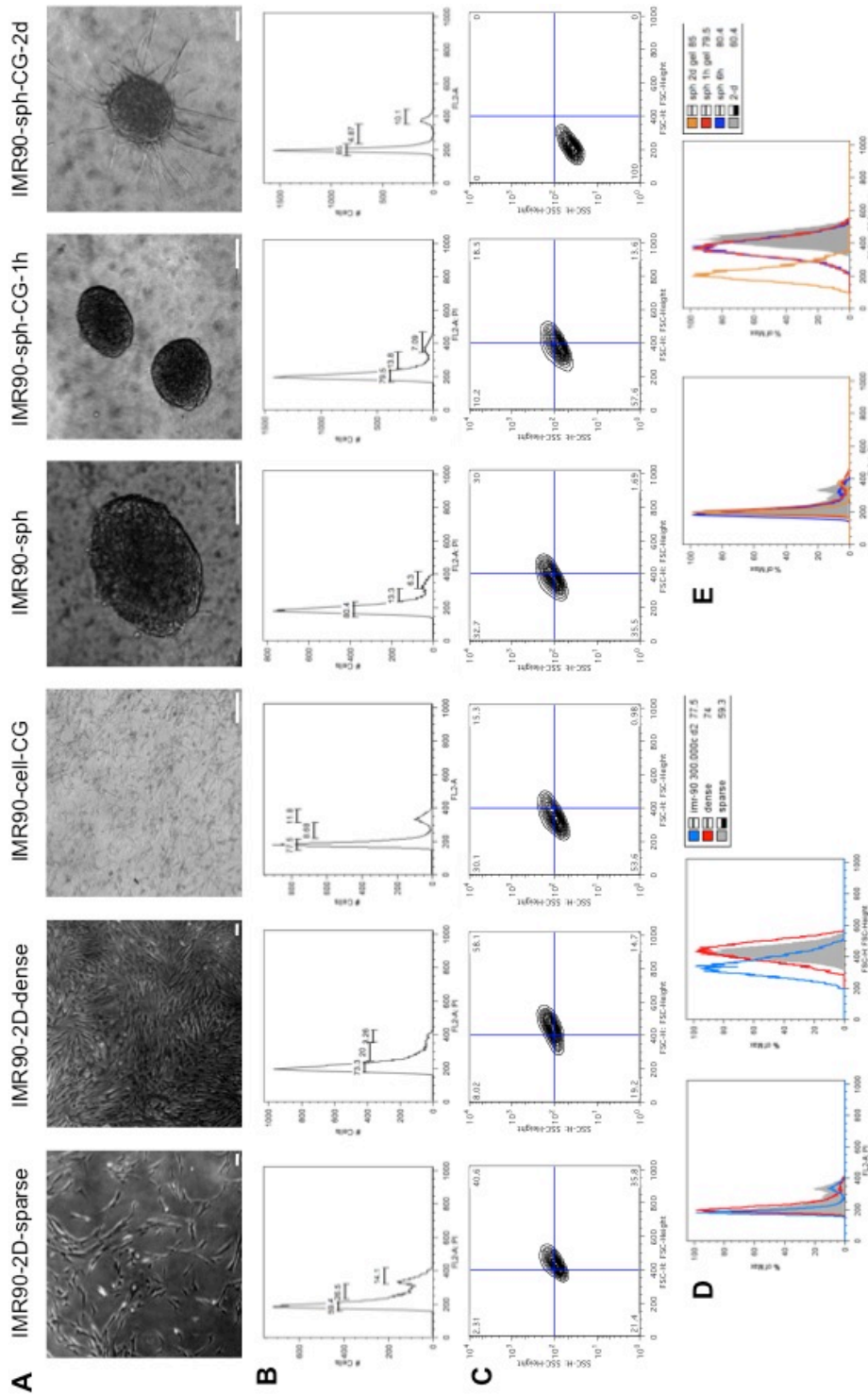


Figure 3.4: Comparison of different culture conditions concerning DNA content, cell size and cell granularity. For the individual conditions cells from the passage number were used. **A** Microscopic images of the individual culture conditions before harvesting. Scale bar represents 100 µm. **B** DNA content profiles of the individual conditions. **C** Forward/side scatter contour plots showing the size and granularity of the cells. **D** Overlay of IMR90-2D-sparse (gray), IMR90-2D-dense (red) and IMR90-cell-CG (light blue) showing DNA content profiles on the left side and forward scatter on the right. **E** Overlay of IMR90-2D-sparse (gray), IMR90-sph (dark blue), IMR90-sph-CG-1h (red) and IMR90-sph-CG-2d (orange) showing DNA content profiles on the left and forward scatter profiles on the right side.

### 3.4 Effect of rapamycin on spheroid invasion

Next we asked whether the invasive potential of IMR-90 cells is dependent on the mTOR pathway. Therefore we incubated spheroids embedded in collagen gels with 100 nM of rapamycin [46]. Furthermore we used CVT-313, a specific cdk-2 inhibitor, which inhibits cell cycle progression in late G1, to determine whether cell proliferation is a prerequisite for the invasiveness of the fibroblasts. The inhibitors were added at three different time points. First, the inhibitors were added after the spheroids were embedded into the collagen gel. Second, rapamycin and CVT-313 were added during the course of spheroid aggregation (3 hours before harvesting spheroids) and third we pre-incubated the cells with the inhibitors on 2D one day before spheroid formation.

#### 3.4.1 Treatment after collagen gel polymerization

When spheroids were embedded in collagen gel they were transferred into 24-well plates containing 1 ml of growth medium supplemented with 100 nM rapamycin, 2,5  $\mu$ M CVT-313 and DMSO as a control, respectively. After 3 hours, 24 hours and 42 hours the morphology was documented by microscopic pictures of the spheroids and invading cells. These pictures were afterwards analysed using Cell<sup>D</sup>, a program that contains image acquisition tools and measurement functions (Figure 3.5 A). For determining the invasive area of individual spheroids measurements of the total area (including all cells exiting the spheroids) were performed followed by subtraction of the spheroid area. Statistical analyses were performed using Microsoft Excel 2008 and GraphPad Prism 4.

The data presented in Figure 3.5 B show that after 3 hours in collagen gel spheroids invaded equally under all conditions tested. After 3 hours all conditions showed comparable invasion areas (DMSO = 2314.036  $\mu$ m<sup>2</sup>, rapamycin = 1549.966  $\mu$ m<sup>2</sup>, CVT-313 = 1940.694  $\mu$ m<sup>2</sup>). 24 hours after seeding CVT-313 displayed a significant reduction of invasive area compared to DMSO ( $p = 0.0017$ ), whereas DMSO (18305.10  $\mu$ m<sup>2</sup>) and rapamycin (18507.16  $\mu$ m<sup>2</sup>) showed almost same invasion areas. After 2 days of cultivation rapamycin treated cells displayed significant reduction of the invasive areas compared to the control ( $p = 0.0012$ ). At that time CVT-313 showed about 50% less invasion than DMSO, rapamycin displayed a 40% reduction of invasive area.

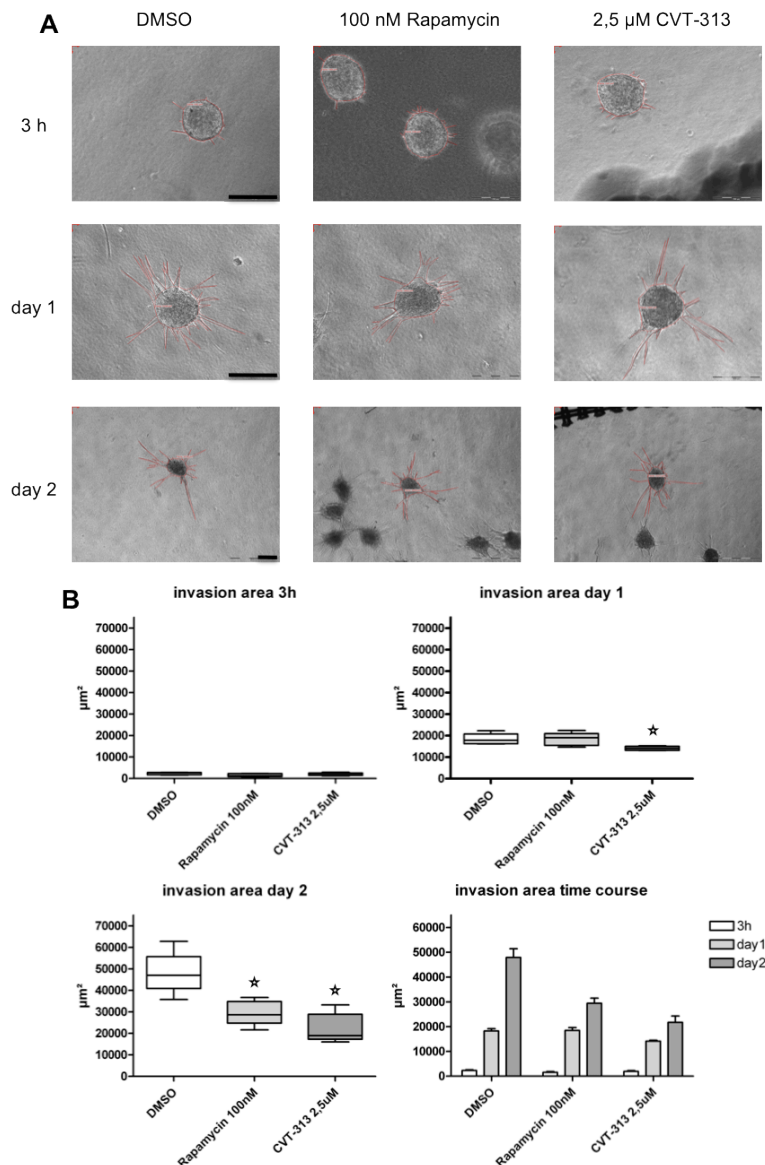


Figure 3.5: Time course experiment of spheroids treated after collagen gel polymerisation with 100 nM rapamycin and 2.5 μM CVT-313, respectively. **A** Microscopic images with invasion areas marked in red. Scale bar represents 200 μm **B** Box plots showing spheroids of the individual conditions. The whiskers represents the highest and lowest outgrowth, the box the middle 50% of the data and the lines the mean values. Significant differences compared with DMSO are marked with stars. (n = 6) The barchart shows a summary of the mean values of invasive area over time.

### 3.4.2 Treatment three hours before harvesting spheroids

Since differences in invasion areas in rapamycin and CVT-313 treated cultures were clearly visible only after two days of incubation, we decided to pretreat the spheroids prior to embedding them into collagen gels with the inhibitors. This pretreatment eliminates potential diffusion problems, which might be present in the previous experiment. Therefore, rapamycin, CVT-313 or DMSO were supplemented to the growth medium three hours before harvesting the spheroids. When cells were embedded into collagen gel they were with 100 nM rapamycin, 2.5 μM CVT-313 and DMSO, respectively. Microscopic pictures were taken at different time points (Figure 3.6 A).



After 16 hours significant differences in invasive areas were detectable between DMSO and rapamycin ( $p = 0.0002$ ) and CVT-313 ( $p < 0.0001$ ), respectively (Figure 3.6 B). Both displayed decrease in invasive area compared to the control cells. Comparison of rapamycin and CVT-313 showed comparable invasion areas (rapamycin =  $21396 \mu\text{m}^2$ , CVT-313 =  $18452 \mu\text{m}^2$ ). At day two there was no increase of invasion area in CVT-313 treated cells, a 5% increase in rapamycin and 25% in DMSO compared to day one. After two days CVT-313 displayed 70% less invasion area, rapamycin 55% compared to DMSO.

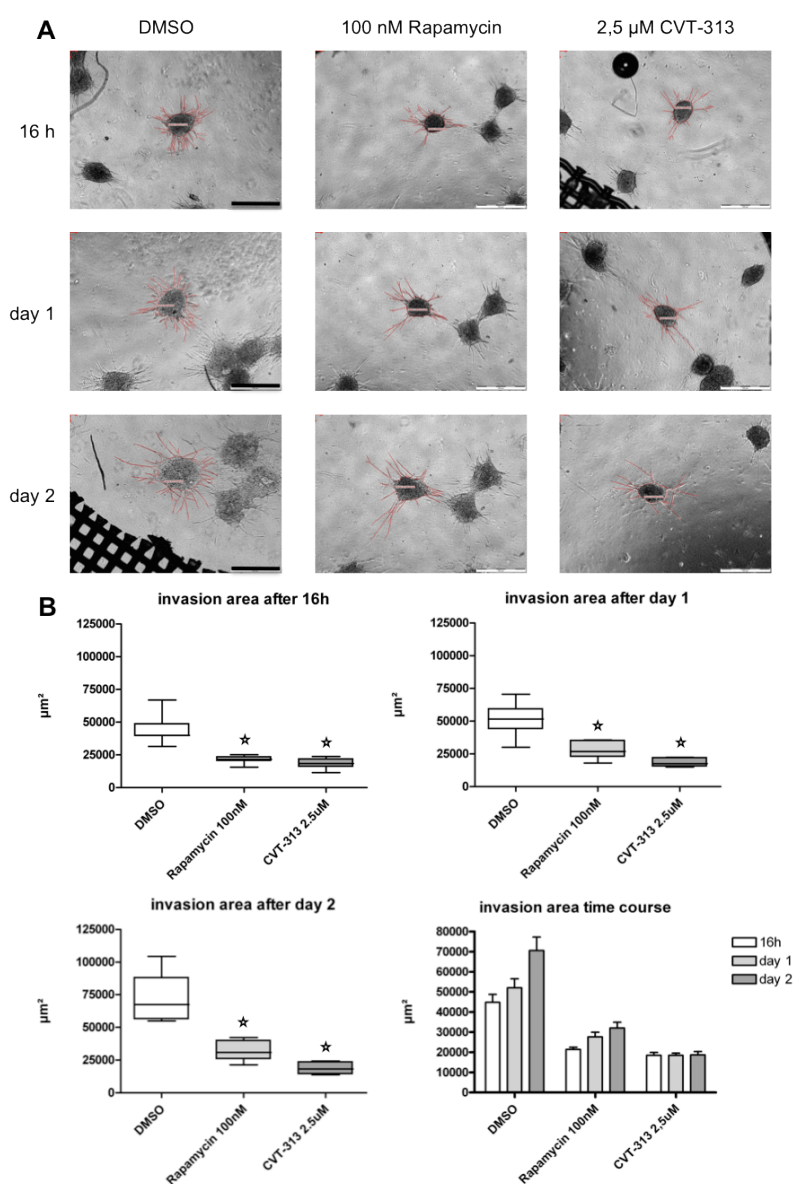


Figure 3.6: Time course of cells treated three hours before harvesting spheroids and after embedding them in collagen gels with 100 nM rapamycin and 2.5 $\mu\text{M}$  CVT-313, respectively. **A** Pictures of the different time points with the measured invasion area in red. Scale bar represents 500  $\mu\text{m}$ . **B** Boxblots show invasive area of all measured spheroids, significant differences to DMSO are marked with stars. ( $n = 7$ ) The barchart shows a summary of the mean values over time.

### *3.4.3 Over night treatment before spheroid aggregation*

To fully rule out that the incubation did not reach every cell in the previous experiments due to the fact that the cells were present as spheroids, we performed pretreatment of the cells before spheroid aggregation. The day before spheroid formation IMR-90 were incubated with 100 nM rapamycin or 2.5  $\mu$ M CVT-313 or DMSO. Spheroid formation and subsequent cultivation in the gels were done in the presence of the inhibitors. Microscopic pictures were taken after 18 hours, 24 hours and 48 hours (Figure 3.7 A). Importantly the aggregation of the fibroblasts to spheroids was not influenced by the pretreatment with the inhibitors.

After 18 hours rapamycin ( $p < 0.0001$ ) and CVT-313 ( $p < 0.0001$ ) showed half the invasion area than DMSO (Figure 3.7 B). While control cells with DMSO invaded constantly more until day 2, both, rapamycin and CVT-313, showed no significant increase in invasion area. In summary, we got 75% less area size in rapamycin and CVT-313 treated cells, than in the control condition.

In general, there were significant differences to the previous experiment, indicating that the over night pretreatment is necessary to efficiently target the cells with the inhibitors. The effects on invasion of the two inhibitors did not rule out that many of the cells died of apoptosis under the culture conditions and as a consequence displayed reduced invasive capacity. Experiments addressing apoptosis are presented below.

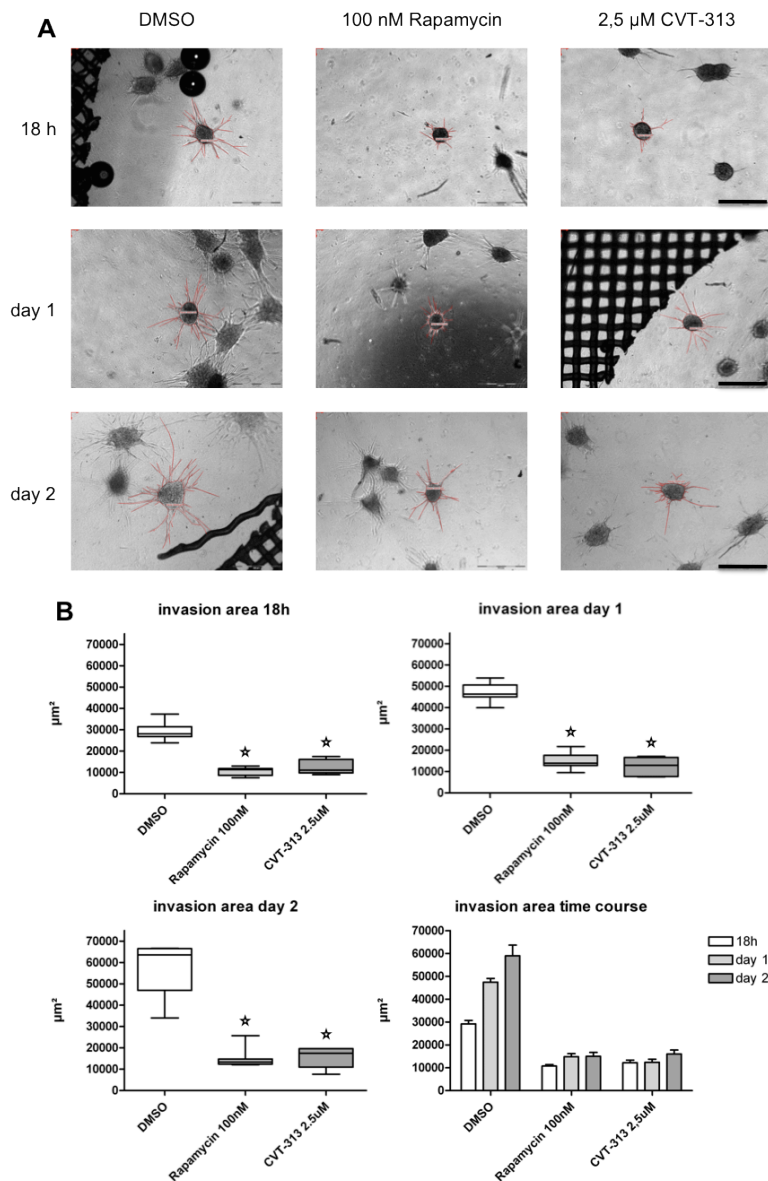


Figure 3.7: Time course of collagen gels treated with 100 nM rapamycin and 2.5  $\mu$ M CVT-313, respectively. Cells were treated over night before spheroid formation and subsequently during aggregation and cultivation in collagen gels. **A** Microscopic images of spheroids with red marked invasion area. Scale bar represents 500  $\mu\text{m}$ . **B** Boxplots showing evaluated data, significant differences compared with DMSO are signalised with stars. (n = 7) Barchart represents the mean values over time.

### 3.5 Collagen gels with siRNA treated cells

Rapamycin is an inhibitor of mTORC1 activity and affects mTORC2 activity indirectly after long term incubation [45, 80, 87]. Therefore, we decided to perform more controlled experiments in which we interfered either with mTORC1 or mTORC2 activity. mTORC1 activity can be inhibited by removing raptor from the mTORC1 complex and for mTORC2 by removing rictor [46]. We transfected the cells with raptor and rictor siRNA and used non-targeting control (NTC) siRNA for comparison. Prior to phenotypic analysis of the invasive behaviour in collagen gels the effectiveness of the individual knockdowns (k-d) was verified by Western blot analysis.

Cells grown on plastic for 72h after transfection were trypsinised, lysed and subjected to Western blot analysis. We detected raptor, rictor, the downstream target phosphorylation sites T389 of p70 S6K for mTORC1 and S473 of AKT for mTORC2 (Figure 3.8 A). The total protein of AKT and p70 S6K served as controls for equal loading. For densitometric quantification the values of NTC condition was set to 100% for the individual antibodies in order to get comparable data.

An efficient knockdown of raptor and rictor protein was detectable (Figure 3.8 B). In accordance to the raptor k-d, downstream signalling of mTORC1 was also affected. The phosphorylation status of p70 S6K in the raptor knockdown is specifically lower than in the other two lysates. Concomitantly, there is a shift in the electrophoretic mobility of the total p70 S6K, which is associated with the dephosphorylated form of p70 S6K. In addition, there is an increase of 80% of AKT S473 phosphorylation in the raptor knockdown cells, which is the expected consequence of the lost negative feedback loop of active mTORC1. In the rictor knockdown phosphorylation of the mTORC2 direct target AKT at S473 is massively decreased. Taken together, these data indicate that rictor and raptor knockdown was efficient and resulted in the expected changes in downstream signalling.

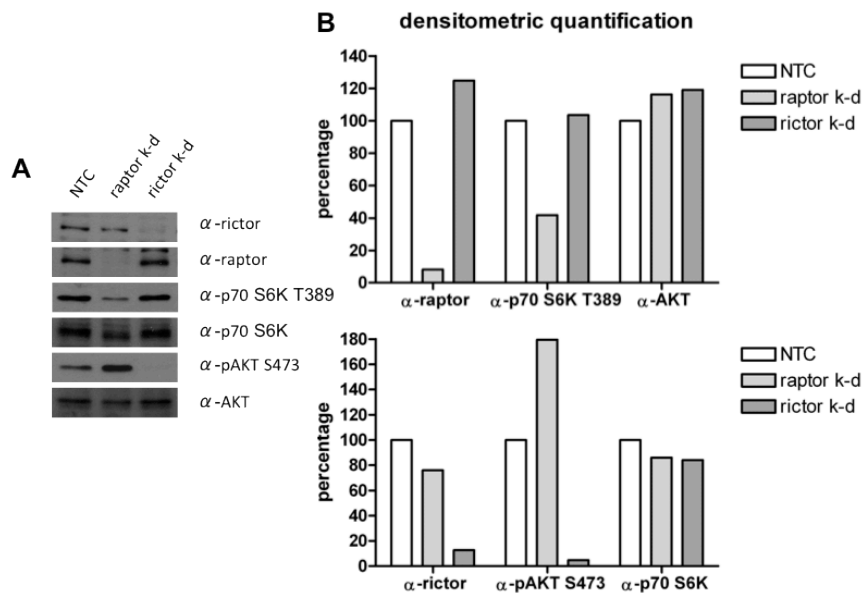


Figure 3.8: **A** Western blot analysis of IMR-90 cells transfected with siRNA for raptor and rictor knockdown, NTC served as control. Samples were tested to determine the effectiveness of the individual knockdowns. **B** For densitometric quantification the measured values were normalised to p70 S6K in the raptor k-d and to AKT in the rictor k-d, respectively. Values of NTC were set to 100% for comparison purpose. The upper bar chart shows the raptor k-d, its downstream target p70 S6K (T389) and AKT, the lower bar chart represents rictor k-d, the downstream target p AKT (S473) and p70 S6K.

In further experiments we tested the consequences of raptor and rictor k-d in the collagen gel invasion assay. Therefore 72 hours after transfection, the cells were splitted and used for spheroid formation 24 hours later and were subsequently embedded into collagen gels. Besides raptor, rictor and NTC siRNA cells were treated only with the transfection reagent Lipofectamine RNAiMAX, determining whether the treatment itself has an effect on the invasiveness of the cells. Pictures were taken after 16 hours, 24 hours and 48 hours (Figure 3.9 A).

After 16 hours of cultivation DMSO ( $41879.96 \mu\text{m}^2$ ) and RNAiMAX ( $43075.53 \mu\text{m}^2$ ) invaded comparably (Figure 3.9 B). Raptor and rictor k-d showed a significant decrease in invasion area (raptor  $p = 0.001$ ; rictor  $p < 0,0001$ ). During the next days they invaded the surrounding matrix slower than the two control samples. After two days raptor k-d cells showed an invasion area 30% less than the control and the rictor k-d a reduction of 60% compared to NTC. RNAiMax displayed no significant decrease compared with NTC during cultivation, indicating that the treatment has no effect on the behaviour of the cells.

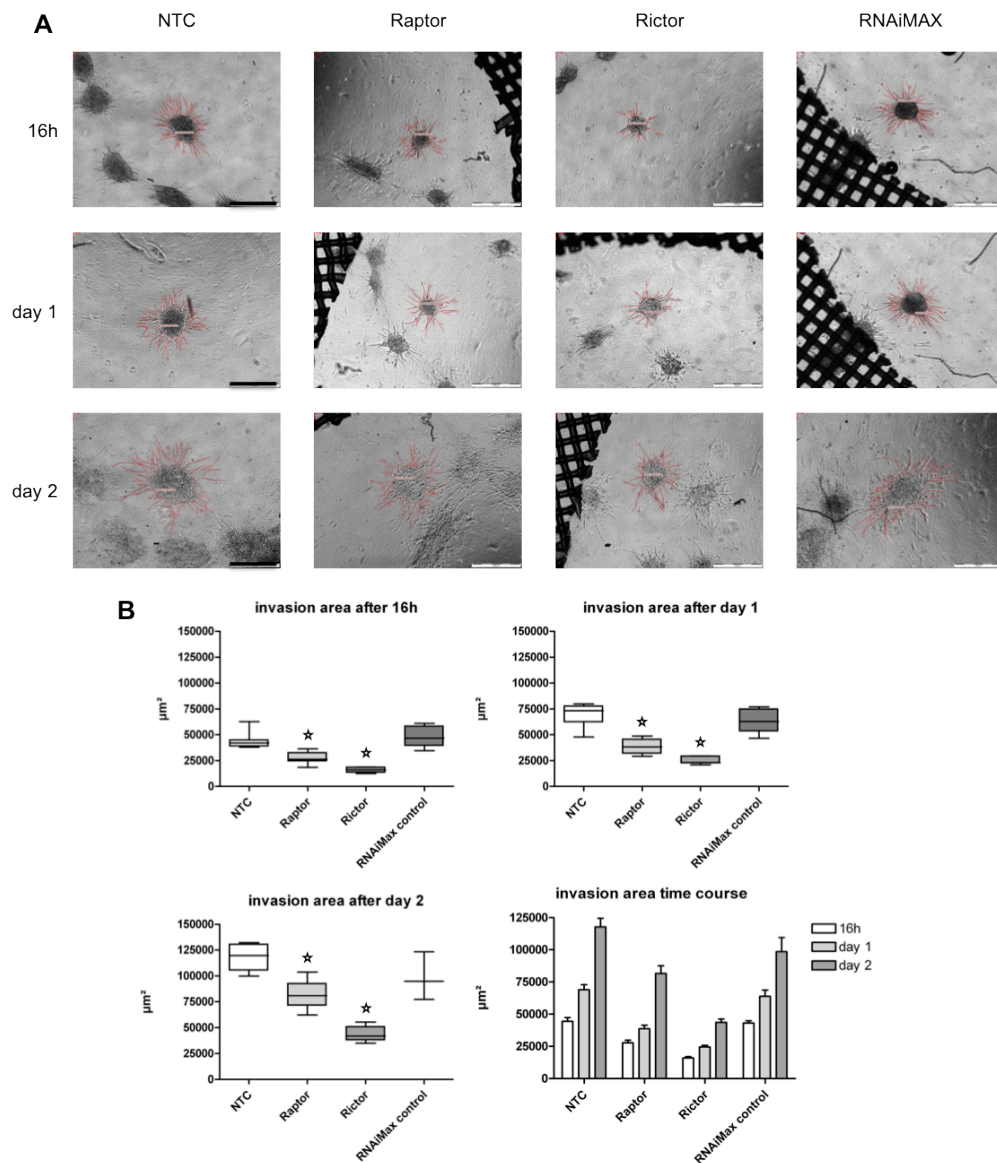


Figure 3.9: Time course experiment with raptor, rictor and NTC siRNA treated cells. Cells were transfected for 72 hours, for control purpose cells were incubated with the transfection reagent Lipofectamine RNAiMAX, instead of siRNA. After transfection cells were trypsinised, aggregated and embedded into collagen gel. **A** Microscopic images of spheroids with red marked outgrowth. Scale bar represents 500  $\mu\text{m}$ . **B** Statistical evaluation presented by boxplots. Significant differences compared to NTC are marked with stars. (n = 7) The data used for the barchart is shown as mean values.

### 3.6 Comparison of the invasion rates

After collecting data from all time course experiments described above (rapamycin and CVT-313, siRNA experiments) we were able to compare the rate of invasion of IMR-90 cells into the collagen gels.

In order to get results, which are directly comparable, the maximum invasion area after 2 days of culture under DMSO and NTC control conditions was set to 100%. Then we composed graphs, which show a time course of the increase of invasion area.

The data presented in Figure 3.10 shows that the effect on invasion area occurred earlier when cells were pretreated over night with rapamycin and CVT-313, treatment after collagen gel polymerisation displayed the lowest effect. Cells, which were treated in the middle of spheroids aggregation with CVT-313, stopped invading the collagen gel after 16 hours of incubation completely; rapamycin treated cells invaded slower but steadily. With siRNA treated cells invaded without stagnation, but never reached the invasion area of NTC or RNAiMAX control.

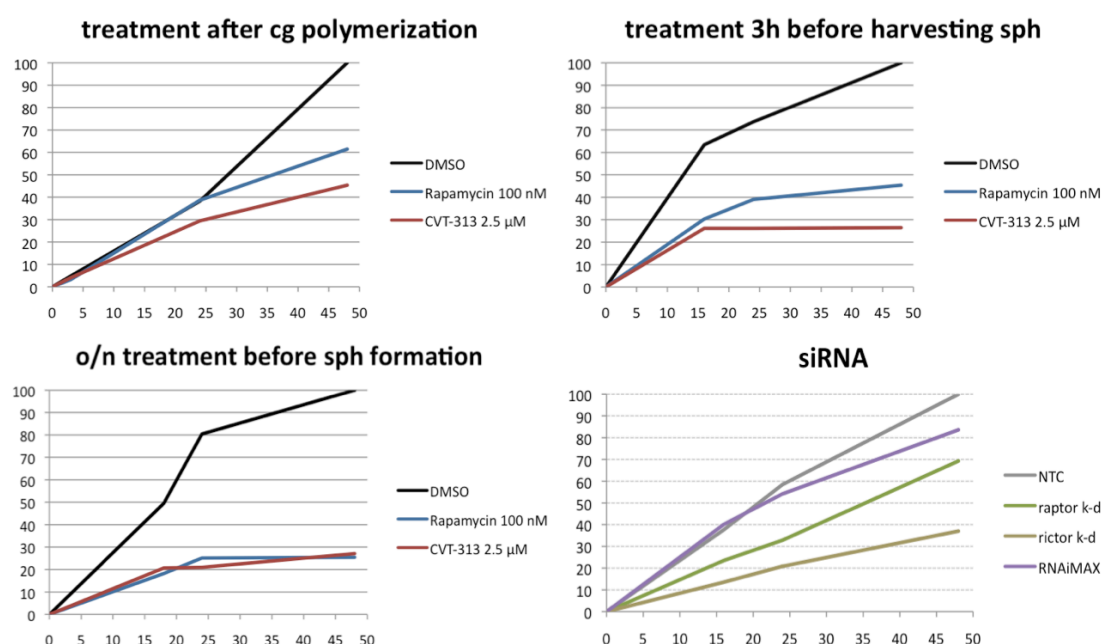


Figure 3.10: Comparison of the invasion rates under different conditions. The x-axis presents the elapsed time in hours, the y-axis the percentage compared to DMSO and NTC after 2 days. Values were taken from the individual experiments from chapter 3.4 and 3.5.

### 3.7 Detection of apoptosis upon mTOR inhibition

As mentioned above, induction of apoptosis in fibroblasts grown in 3D could be the reason for decreased invasion upon mTOR inactivation with rapamycin. Previous experiments have shown that IMR-90 cells cultivated on plastic dishes did not show an increase of apoptosis upon rapamycin treatment [96]. Apoptosis in IMR-90 cells grown in 3D was so far not addressed. Therefore we determined how many cells underwent apoptosis upon rapamycin and CVT-313 treatment in the 3D cell culture setting. After collagen gel fixation cells were stained with  $\alpha$ -cleaved caspase-3 and nuclei were visualized with DAPI. After capturing images with a confocal microscope two different types of DAPI stained nuclei were found within the spheroids, normal shaped nuclei and condensed nuclei. Those condensed nuclei were visible as small dots in between normal shaped nuclei (see Figure 3.11 B).

Next we counted normal nuclei, condensed nuclei and cleaved caspase-3 positive cells, which we separated into the two categories “cleaved caspase-3 positive - normal nuclei” and “cleaved caspase-3 positive - condensed nuclei” (Figure 3.11 B).

The total number of cleaved caspase-3 positive cells (Figure 3.11 C) increased from 2.1% in DMSO to 8.7% upon rapamycin treatment. CVT-313 treated cells revealed 14.5% cleaved caspase-3 positive cells. The analysis of cleaved caspase-3 positive cells, which display condensed nuclei revealed a comparable increase (Figure 3.11 D). In DMSO 77% of the positive cells concomitantly display condensed nuclei, in rapamycin 88.6% and in CVT-313 97.8% showed condensed nuclei. In relation to all counted nuclei, that are all normal nuclei and condensed nuclei, the number of condensed nuclei increased from 13% in DMSO to 44% in rapamycin to 75% in CVT-313 treated spheroids whereas the number of cleaved caspase-3 positive cells is specifically lower (2.1% in DMSO, 8.7% in rapamycin and 14.5% in CVT-313 treated cells) (Figure 3.11 E).

As caspase-3 activation occurs early during apoptosis we defined cleaved caspase-3 positive cells with normal nuclei as early apoptotic cells and cleaved caspase-3 positive cells with condensed nuclei as late apoptotic cells. Cells with condensed nuclei and without positive cleaved caspase-3 signal died due to caspase-3-independent pathways.



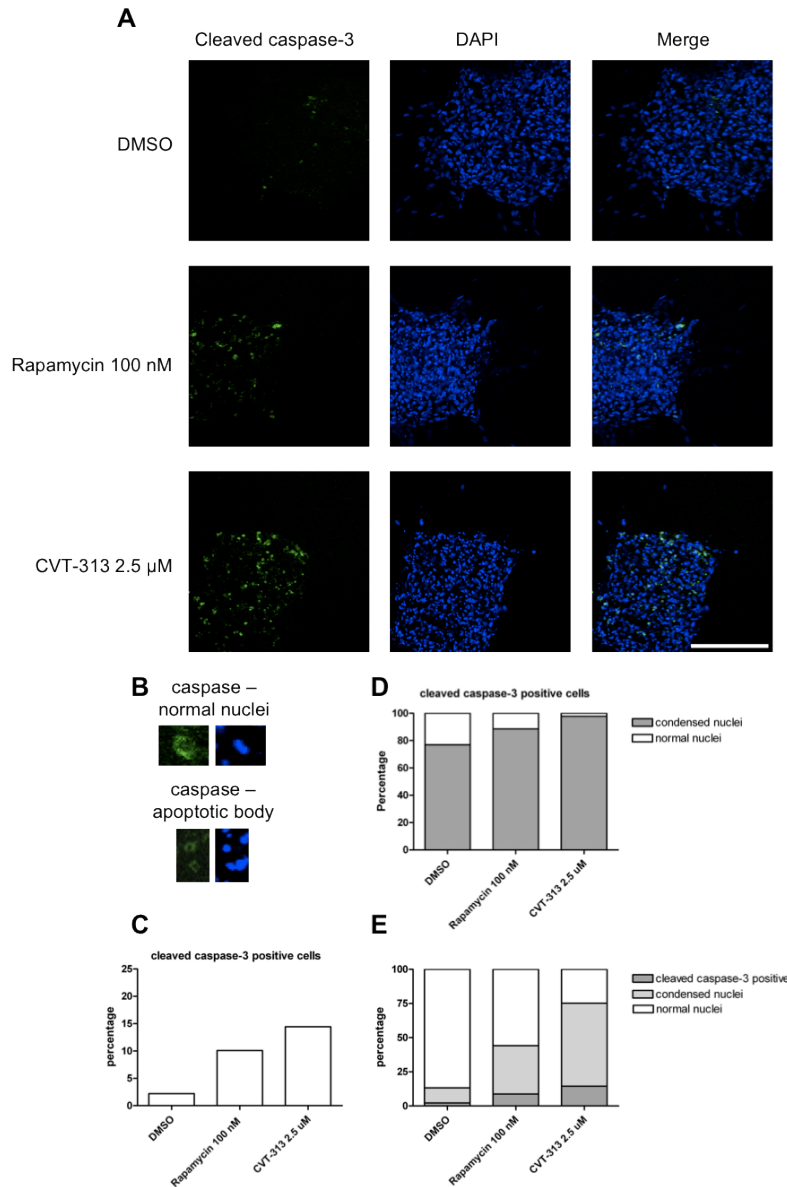


Figure 3.11: Spheroids treated with 100 nM rapamycin, 2.5 μM CVT-313 and DMSO were fixed after 2 days with 4% PFA. They were stained with cleaved caspase-3 and DAPI and microscopic images were taken with a confocal microscope. Thereafter cleaved caspase-3 positive cells and DAPI stained nuclei were counted. (DMSO n=592, rapamycin n=515, CVT-313 n=645) **A** Confocal microscopic images of cleaved caspase-3 and DAPI stained spheroids, which were treated with 100 nM rapamycin and 2.5 μM CVT-313 after embedding into collagen gel. Scale bar represents 200 μm. **B** Two groups of cleaved caspase-3 positive cells were found, one group consists of normal nuclei the other one of condensed nuclei. **C** Barchart of the number of cleaved caspase-3 positive cells compared to all counted nuclei in the individual conditions. **D** Barchart showing the number of cleaved caspase-3 positive cells with condensed nuclei (dark gray) in relation to all positive cells (white) in the individual conditions. **E** Barchart showing a comparison off cleaved caspase-3 positive cells (dark gray), condensed nuclei (light gray) and all counted nuclei (normal nuclei and condensed nuclei) representing 100% (white).

### 3.8 Immunofluorescence stainings

Next we asked whether mTOR components are expressed and where they are located in cells grown in 3D culture compared to cells cultured on plastic. Therefore we cultivated cells on tissue culture slides (2D) and as single-cell suspension collagen gels (3D) both treated with and without 100 nM rapamycin for 48 hours. After fixation cells were stained with various antibodies for mTOR pathway components, nuclei were counterstained with DAPI and the actin cytoskeleton was visualised by staining of F-actin with fluorescently labelled phalloidin.

#### 3.8.1 Secondary antibody control

To evaluate the amount of background staining caused by the secondary antibody, cells were stained with secondary antibody alone, nuclei were counterstained with DAPI and the cell body was visualised with phalloidin in 2D (Figure 3.12). The cells were examined using a confocal microscope. As expected secondary antibody alone showed almost no background staining in 2D as well as in 3D.

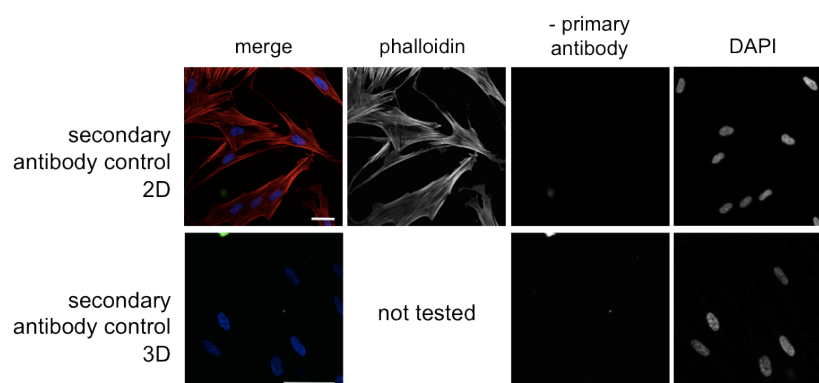


Figure 3.12: Secondary antibody control for background staining in cells cultured on plastic slides and in single-cell suspension collagen gels. Alexa Fluor 546 phalloidin was not tested in 3D. Scale bar represents 50  $\mu\text{m}$ .

#### 3.8.2 mTOR

In cells grown on tissue culture plates mTOR is located in a vesicle-like manner with a predominantly expression in the perinuclear region and a smaller fraction in the periphery, within the nucleus there is no accumulation visible (Figure 3.13). In rapamycin treated cells the staining pattern is similar, despite a more pronounced vesicular appearance. This is in close accordance to data from literature. mTOR predominantly localises to the endoplasmic reticulum and the golgi apparatus and only a small fraction of mTOR is present in the nucleus [97]. The distribution of mTOR in IMR-90 cells grown

in collagen gels show an identical staining pattern. Increased vesicular appearance of mTOR was also present in cells treated with rapamycin.

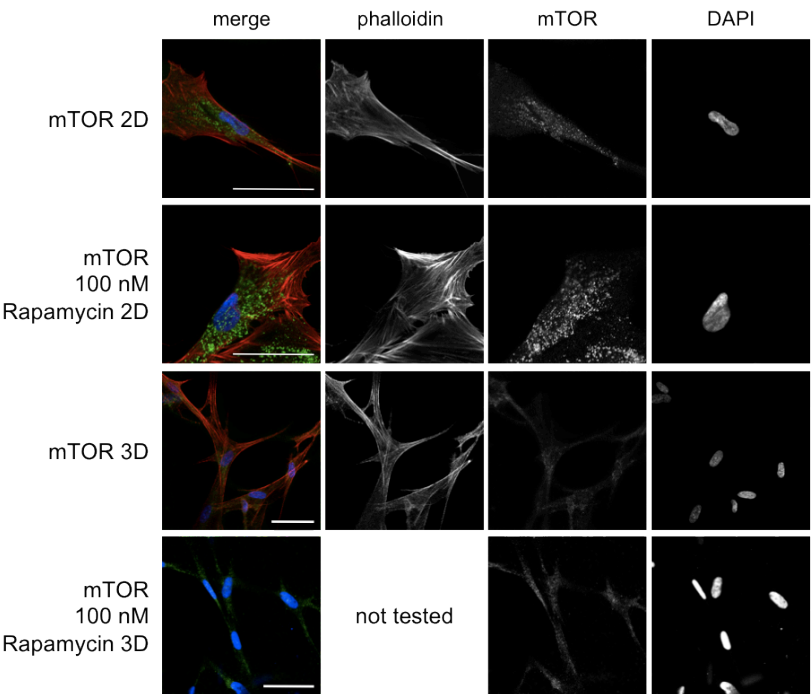


Fig. 3.13: mTOR distribution in cells cultured on tissue plates and in single-cell suspension collagen gels, both treated with and without 100 nM rapamycin. Alexa Fluor 546 phalloidin was not tested in 3D treated with rapamycin. Scale bar represents 50  $\mu$ m.

### 3.8.3 *pAKT S473*

In 2D AKT phosphorylated at S473 is located in the cytoplasm with predominantly accumulation in the cell protrusions in the periphery of the cells (Figure 3.14). This is in accordance to data from the literature [98]. The signal is increased after treatment with rapamycin as expected. This is caused by the loss of the negative feedback-loop of p70 S6K towards IRS1 upon mTOR inhibition (see chapter 1.3.6). In 3D the situation is similar, phospho-Akt-S473 is located in the cytoplasm with increased staining intensities in cell protrusions. The increase of AKT S473 phosphorylation upon rapamycin treatment is also recapitulated in fibroblasts grown in collagen gels.

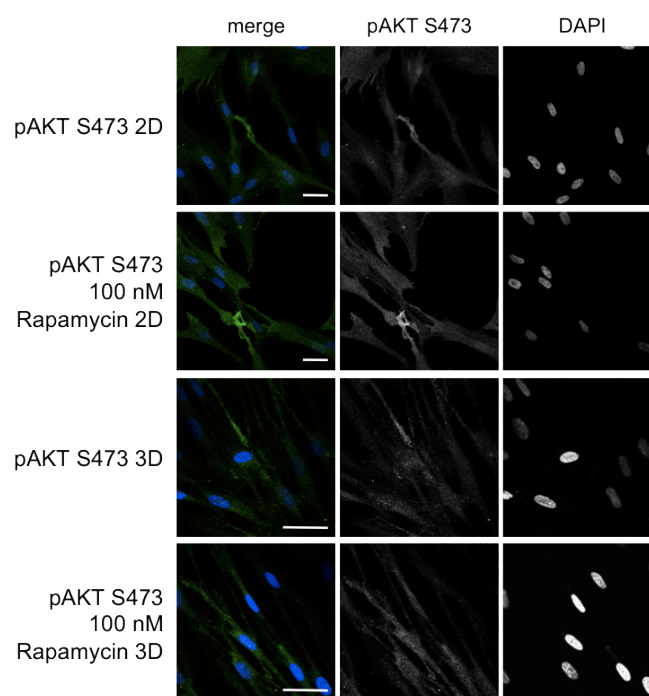


Figure 3.14: pAKT S473 distribution in cells cultured on tissue plates and in single-cell suspension collagen gels treated with and without 100 nM rapamycin. Scale bar represents 50  $\mu$ m.

### 3.8.4 AKT

In 2D AKT is distributed throughout the whole cell with accumulation either within the nucleus or bound on its membrane (Figure 3.15). This is in accordance to data from literature [99]. Treatment with rapamycin does not change its localisation. Whereas AKT localised in the nucleus seems to be increased in 3D culture.

Akt was not tested in collagen gels treated with rapamycin.

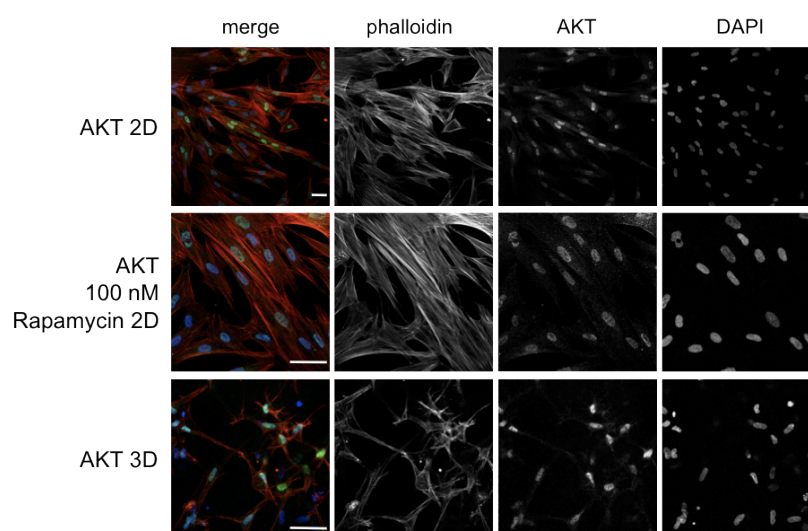


Figure 3.15: Localisation of the total protein of AKT in cells cultured on tissue plates and in single-cell suspension collagen gels with and without 100 nM rapamycin treatment. Scale bar represents 50  $\mu$ m.

### 3.8.5 pS6 S240/244

In fibroblasts grown on a 2D surface S6 phosphorylated at S240/244 is localised in the cytoplasm (Figure 3.16). The nuclei show a weak signal, which is not a proof for pS6 localisation within the nuclei maybe it is residues behind it. After rapamycin treatment the phosphorylation of S6 at S240/244 is undetectable. This is in accordance with biochemical data from IMR-90 cells grown on plastic dishes [46]. The same situation can be observed in 3D culture. Untreated cells show a bright signal with the same distribution compared to 2D and a lack of signal after rapamycin treatment. Biochemical studies in IMR90 cells [100] and immunofluorescence stainings in human Hep2 cells [101] demonstrated that S6 and S6 S240/244 are predominantly localised within the nuclei and the nucleoli. To be sure that the lack of signal in the nucleoli in our IF analysis was not caused by insufficient antibody penetration of the cells we used a fibrillarin antibody. Fibrillarin is a component of a nucleolar ribonucleoprotein particle [102]. Cells from the same experiment were stained with identical protocols with either  $\alpha$ -fibrillarin antibody or  $\alpha$ -pS6 S240/244 (Fig 3.17). The fibrillarin antibody stained the nucleoli of the cells, whereas no pS6 S240/244 staining within the nuclei was observable, indicating that the staining protocol per se was not responsible for the lack of staining and antibodies could diffuse into nucleolar structures.

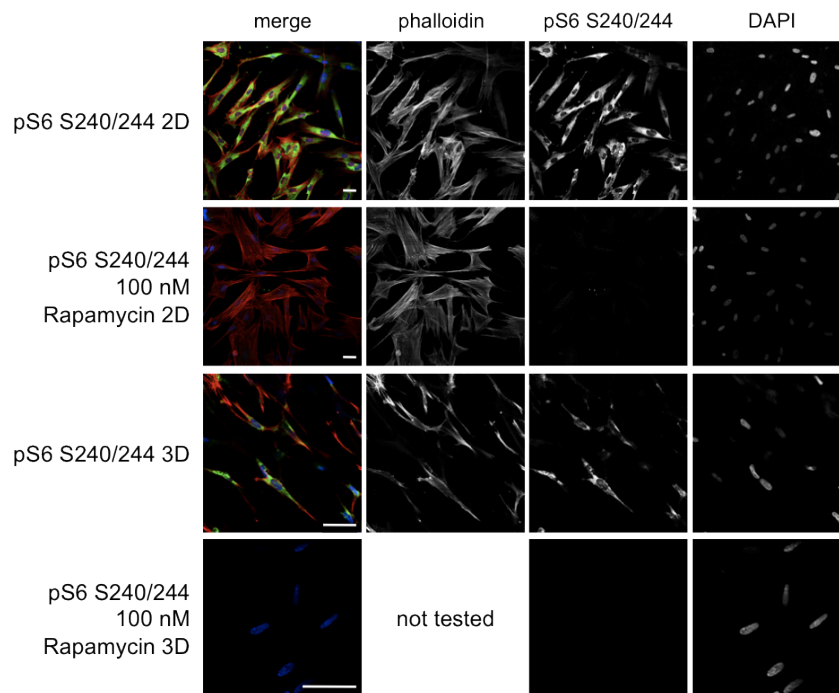


Figure 3.16: Localisation of ribosomal S6 phosphorylated at S240/244 in cells cultured on tissue plates and in single-cell suspension collagen gels with and without 100 nM rapamycin treatment. Alexa Fluor 546 phalloidin was not tested in 3D collagen gels treated with rapamycin. Scale bar represents 50  $\mu$ m.

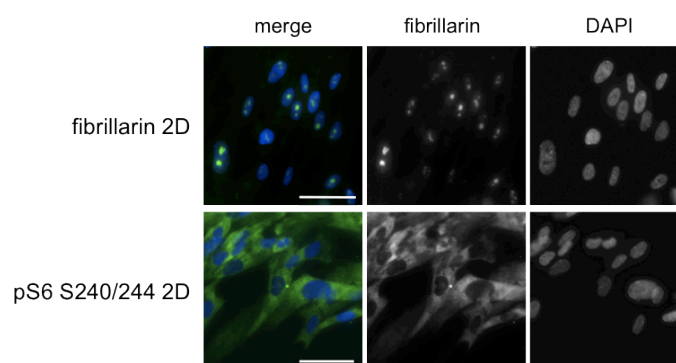


Figure 3.17: Fibrillarin and pS6 S240/244 stained cells grown on plastic slides in order to test the protocol for the ability of nuclear staining. Scale bar represents 50  $\mu\text{m}$ .

### 3.8.6 4E-BP1

In 2D 4E-BP1 is localised throughout the cytoplasm and the nucleus (Figure 3.18). The same distribution is visible in rapamycin treated cells. In 3D the situation is equal to 2D, protein localisation in the cytoplasm and the nucleus. This localisation pattern is also proposed in the literature; furthermore they showed with immunofluorescence analyses that 30% of the total number of protein resides within the nuclei [103].

4E-BP1 was not tested in rapamycin treated collagen gels.

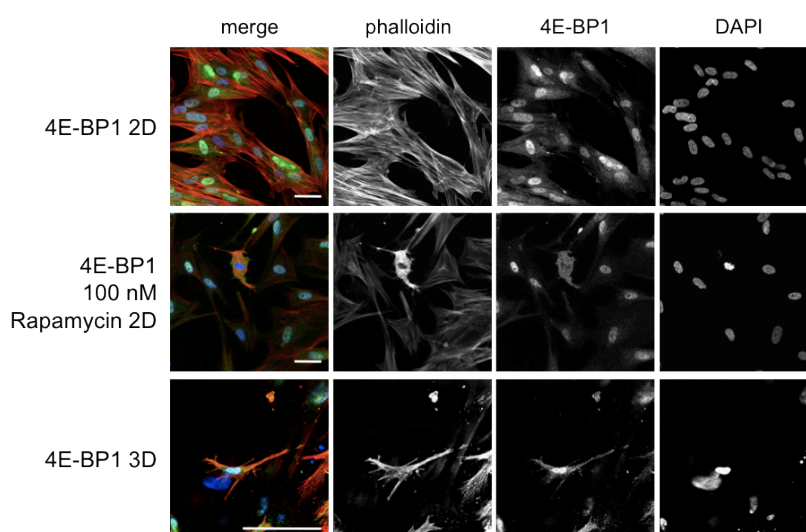


Figure 3.18: Localisation of 4E-BP1 in cells cultured on tissue plates with and without treatment with 100 nM rapamycin and in single-cell suspension collagen gels. Scale bar represents 50  $\mu\text{m}$ .

### 3.8.7 p-H3 S10

Histone H3, H2A, H2B and H4 are part of the core particles of nucleosomes where DNA is wrapped around. Nucleosomes are linked together with H1 for further folding into chromatin fibers. During mitosis all H3 molecules become phosphorylated in the n-tail site at S10 [104, 105]. Therefore, phospho-H3 (p-H3) can be used as a marker for dividing cells. Figure 3.19 shows that in the three tested conditions phosphorylated H3



molecules can be found indicative for cell proliferation. The aim of this staining was to calculate a mitotic index showing how many cells undergo mitosis in the individual conditions, but the number of stained H3 was too small for statistical analyses.

p-H3 was not tested in rapamycin treated collagen gels.

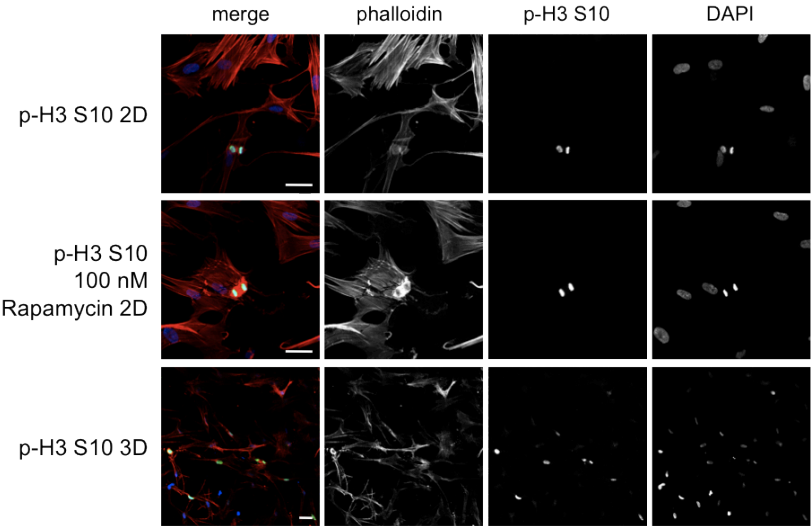


Figure 3.19: Localisation of phosphorylated histone H3 at S10 in cells cultured on tissue plates and in single-cell suspension collagen gels with and without 100 nM rapamycin treatment. Scale bar represents 50  $\mu\text{m}$ .

### 3.8.8 Cleaved caspase-3

Caspases are responsible for apoptosis. They can be classified as initiator or executor molecules. To activate the executor caspase-3, leading to apoptosis, cleavage mediated by initiator caspases is needed [106]. Figure 3.20 shows staining of the activated form cleaved caspase-3. The number of apoptotic cells was too small to calculate an apoptotic index. Cleaved caspase-3 was not tested in 2D.

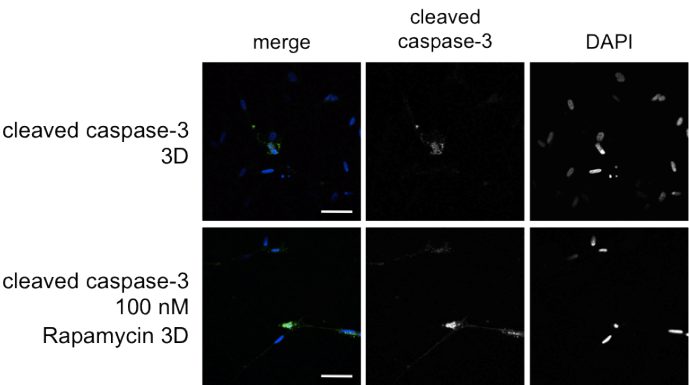


Figure 3.20: Localisation of cleaved caspase-3 in cells cultured on tissue plates with and without treatment with 100 nM rapamycin and in single-cell suspension collagen gels. Scale bar represents 50  $\mu\text{m}$ .





## **4. Discussion**

Threedimensional (3D) cell culture is a useful tool to study physiological aspects of many cellular features under *in-vitro* conditions; for example to investigate the biomechanical functions or cell-matrix interactions. It is supposed to resemble a tissue like environment mimicking extracellular matrix (ECM) features, which are found *in-vivo*, since environment and shape of a cell can determine its behaviour and gene expression [14]. We are interested in molecular changes of mTOR signalling during 3D culture of IMR-90 lung fibroblasts and the effects of mTOR pathway inhibition in this experimental setting. Therefore we produced collagen gels with collagen I as a main component since our cells are derived from a fetal lung and the lung interstitium contains collagen type I [3]. Our intent was to analyse the differences between 2D and 3D culture due to the fact that IMR-90 were isolated, they resided in a 3D environment and were put in flat tissue culture plates afterwards. Furthermore we were interested in the invasion of these cells, when they were embedded into collagen gels.

#### **4.1 Setup of a 3D model system**

We wanted to use a novel approach to study the behaviour and invasive properties of fibroblasts in collagen gels. Therefore we decided to form spheroids from fibroblasts and to embed these spherical structures into collagen gels. The invasive capacity could then be determined by measuring the area of cells, which left the spheroids and migrated in an astral manner away from the spheroid surface through the extracellular matrix. Our first intent was to establish appropriate culture conditions for IMR-90 in collagen gels, since they have not been cultured in 3D in our lab before. We cultivated them as single-cell suspension collagen gels and for invasion assays as spheroids embedded into collagen gels. One problem we had to deal with was the induction of a process called nemosis in the fibroblasts when cultivated in aggregates. Vaheri, et al. described that culturing fibroblasts in aggregates activates a programmed necrosis-like pathway called nemosis (chapter 1.2.1) leading to decomposition of the spheroids and the cells within them [25]. We observed very similar features, when IMR-90 cells were incubated as aggregates in 96-well plates. In several optimisation steps we reduced the aggregation time to 6 hours. Using these conditions the spheroids were still formed but the cells did not display apoptotic structures. Many cells invaded the surrounding gel and quantification was possible. Our standard conditions for spheroid invasion assays were as following: 1,500 cells, 6 hours of aggregation and 200 spheroids per collagen gel. Phenotypically there were no signs of cell death detectable, however, it is not clear whether some cells died

due to necrosis or apoptosis triggered by the aggregation process, therefore TUNEL analysis would be necessary to determine the exact number of dying cells in the spheres. As mentioned above IMR-90 were also cultured as single-cell suspension collagen gels. Therefore 300.000 cells in single-cell suspension were embedded into collagen gel. Due to the lack of spheroid formation cells within this culture condition do not undergo necrosis and even after a week of cultivation they look vital. Therefore, these cultivation parameters could be used for further experiments for single-cell suspension collagen gels.

#### **4.2 Cell cycle distribution and cell size of IMR-90 cells in 3D**

Now that we were able to culture IMR-90 in collagen gels, we were interested whether cell cycle distribution and/or cell size was altered by 3D cultivation as compared to 2D culture. We used flow cytometry (FACS) to analyse cell cycle parameters and cell size distributions. For FACS analyses cells have to be available as single-cell suspension, therefore we established a protocol to isolate cells cultured in collagen gels. We could demonstrate that cell size parameters and cell cycle distribution were not affected by the isolation process. After establishing appropriate harvesting conditions for IMR-90 fibroblasts, we were able to address whether 3D culture induced phenotypical as well as functional differences in the cells as compared to 2D culture. As described in chapter 3.3 cell cycle analyses showed an increase of cells in G1 and a decrease in S and G2 phase cells in all collagen gels compared to cells from plastic cell culture dishes (figure 3.4). This is in close accordance to the literature; human skin fibroblasts cultured in collagen gels behaved very similar [48]. Higher fractions of G1 phase cells after 7 days of 3D cultivation were detected, indicating less proliferation [48]. Another study showed that polymerised collagen I suppresses fibroblast proliferation via an integrin - protein phosphatase 2A (PP2A) - TSC2 complex activating TSC2 by repressing its phosphorylation level leading to enhanced GAP activity towards Rheb and consequently to inhibited mTORC1 signalling towards S6K1 [107]. Primary human lung fibroblasts (HLF 210) were cultured on top of polymerised collagen matrices showing reduced levels of S6K1 phosphorylation at T389, increased PP2A activity and reduced numbers of cells entering S-phase compared to fibroblasts cultured on monomeric collagen. Knock-down experiments and inhibition of PP2A revealed that reduced S6K1 phosphorylation is mediated through activated TSC2 [107]. In order to proof if these observations are an explanation for the reduction of proliferation within our experiments Western blot analyses with PP2A and TSC2 antibodies and further spheroid invasion assays with either

TSC2 knock-out cells or with TSC2 siRNA transfected IMR-90 are needed. However, so far the size of fibroblasts cultivated in collagen gels was never determined. FSC analysis demonstrated that all cells cultured in 3D display smaller cell size compared to 2D. Furthermore cells isolated from spheroids/astral outgrowths after two days of cultivation in collagen gels show the smallest cell size compared to all other conditions. This massive size reduction occurs only after long-term cultivation in collagen gels, one hour after embedding into collagen gels cells display the same cell size as after spheroid formation. Due to this observations cell shrinking caused by osmotic changes or isolation artefacts can be ruled out. The decrease in cell size might indicate changes in the mTOR-signalling pathway, as this pathway is involved in many cellular functions like regulating mRNA translation, ribosomal biosynthesis, proliferation and cell size via its downstream targets (see chapter 1.3; reviewed in [44]). As rapamycin is a highly specific inhibitor of mTOR function and has been shown to decrease the cell size and alter cell cycle progression in 2D cultures in IMR-90 fibroblasts [46] this inhibitor is also well suited to study cell size regulation in 3D. Therefore further experiments are needed concerning cell cycle distribution and cell size analyses of rapamycin treated cells cultured in the same conditions as mentioned above and Western blot analyses of mTOR pathway components to identify different phosphorylation states and expression patterns in 2D and 3D.

Due to the above mentioned decreased percentage of cells in S phase under 3D culture conditions we tried to quantify proliferation of cells cultured on tissue culture plates and in collagen gels. First we used phosphorylated histone H3 (p-H3) as a marker for cells undergoing mitosis [105]. Positive p-H3 (S10) cells were found in both culture conditions (Figure 3.19), but the number was too small for statistical analysis, since H3 is only phosphorylated during mitosis, which lasts only for 1-2 hours. For better quantification further experiments are needed using Bromodeoxyuridine (BrdU) incorporation in the individual conditions (tissue culture plates and single-cell suspension collagen gels) analysed by flow cytometry. Another possibility could be to detect incorporated BrdU with immunofluorescence analyses. The advantage of BrdU compared to p-H3 is that cells start to incorporate BrdU during S-phase and that after a complete cell cycle they do not lose the incorporated signal. This leads to a higher number of positive cells and the possibility to calculate the proliferation rates in the individual conditions. Furthermore Western blot analysis could be performed detecting proliferation markers like pRB, cyclin A, cyclin D1 and cdk inhibitors like p21 and p27.

### **4.3 Does mTOR signalling alter invasion?**

IMR-90 cultivated in collagen gels display spindle like bipolar morphology and invade the collagen gel. For quantification of the invasion areas we used a spheroid assay, aggregated cells were embedded into collagen gel and cells start to exit the spheroids and invade the gel. With this assay invasion can be measured in microscopic images determining the area of invasive structures using standard microscopy software.

Our intent was to observe whether the amount of invasion of IMR-90 into the surrounding collagen gel depends on the mTOR pathway or simply on proliferation of the cells, leaving the spheroid. Therefore we used a small molecule cell cycle inhibitor (CVT-313) as control. In collagen gels, which were treated after polymerisation, the effect of the treatment with the cdk-2 inhibitor CVT-313 occurred after one day (Figure 3.5), effects of rapamycin were visible two days after treatment. The reason for the late onset of the rapamycin and CVT-313 effects, respectively, might be explained with a diffusion effect. It could take longer until the inhibitors diffuse through the collagen gels and reach the cells compared to the situation in tissue culture plates.

To eliminate these potential diffusion problems, cells were pretreated during spheroid formation (Figure 3.6) and effects occurred earlier compared to the treatment after collagen gel polymerisation. The mTOR and cdk2 inhibition showed less invasion 16 hours after embedding the pretreated spheroids in the collagen gels. This effect could be explained with an already inhibited mTORC1 complex, when cells were embedded, however mTORC2 activity is not affected at that time. Rosner et al. showed that even one hour after rapamycin treatment the first effects on mTORC1 dependent downstream signalling (phosphorylation of p70 S6K at T389) were visible [46].

To rule out, that the inhibitors did not reach every cell within the spheroids to the same extend, cells were pretreated in tissue culture plates the day before aggregation. This experiment showed that spheroid formation does not depend on the mTOR pathway; the spheroids displayed the same morphology compared to untreated spheroids. This experiment revealed the strongest inhibitory effect in rapamycin treated cells. CVT-313 treated cells showed no difference compared to the previous mentioned experiment. Due to the prolonged treatment within this experiment mTORC1 activity is decreased and the assembly of mTORC2 complexes is diminished, when spheroids were embedded into collagen gels [45]. It seems that the effect of rapamycin is more prominent, when both complexes are affected. Since rapamycin is an inhibitor of mTORC1 activity and affects mTORC2 after prolonged treatment, we decided to perform more controlled experiments

by interfering the assembly of the individual complexes via knock-down (k-d) experiments.

We used specific siRNA's against raptor and rictor to determine the effect of independently inhibited mTORC1 and mTORC2 activities. Removing raptor from the complex inhibited mTORC1 activity and removing rictor inhibited mTORC2 [46]. Western blot analyses of lysates from siRNA treated cells showed significant knock-downs of raptor and rictor (Figure 3.8). Furthermore the main downstream target of mTORC1; p70 S6K (T389) and one target of mTORC2; pAKT (S473) displayed decreased activity in the respective knock-downs. In the raptor knock-down fibroblasts, there was a mobility shift of p70 S6K visible, which is associated with the electrophoretic mobility of its dephosphorylated form and concomitantly there was an induction of phosphorylated AKT, caused by the loss of the negative feedback loop via IRS (see chapter 1.3.6). These data indicated that raptor and rictor knock-downs were efficient and resulted in the expected changes in downstream signalling.

Our next intent was to test the migratory potential of siRNA treated cells, which we used in the spheroid-based invasion assay (Figure 3.9). We looked at effects at 16 hours after embedding the spheroids into the collagen gels. The invasion areas of rictor k-d spheroids were smaller as compared to that of raptor k-d spheroids. This indicates a dependence of invasion rather on mTORC2 than on mTORC1. However, the minor invasion rate of rictor siRNA transfected cells could also be explained with a higher apoptosis rate within those cells. mTORC2 and PDK1 activate AKT through phosphorylation of S473 and T308 leading to phosphorylation of its downstream target BAD, thereby inhibiting its pro-apoptotic function (see chapter 1.3.4). Reduced AKT activity caused by the rictor k-d could result in decreased BAD phosphorylation and increased pro-apoptotic function. To verify this thesis further experiments like Western blot analyses are needed.

In general the reduction of invasion within the knock-down experiments is not as high as in rapamycin treated cells. This fact can be explained with two different effects of rapamycin on the mTOR pathway, it inhibits mTORC1 kinase activity and activates PP2A leading to active dephosphorylation of p70 S6K and 4E-BP1 [83]. This accelerates the effect, so that the decrease of p70 S6K activity is visible as soon as 30 min. after treatment [46]. Whereas in knock-down experiments there is always a fraction of intact protein left.

#### *4.3.1. Cell death and apoptosis*

In spite of the shortened aggregation time the spheroids embedded in collagen gels looked condensed and dark structured after two days of cultivation by rapamycin and CVT-313 treatment. It was not clear how many cells died due to the culture conditions and the additional rapamycin and CVT-313 treatment, respectively. Previous experiments have shown that IMR-90 cultured on tissue culture plates do not show increased apoptosis after rapamycin treatment [96], however these experiments were not addressed in cells cultured in 3D so far. Therefore we determined how many cells underwent apoptosis in collagen gels treated with rapamycin and CVT-313 (Figure 3.11). DNA staining of spheroids revealed two morphological different types of nuclei, normal shaped nuclei and condensed nuclei (Figure 3.11 B). Chromatin condensation occurs in cells, which undergo apoptosis due to stepwise DNA fragmentation. For differentiation between early and late apoptotic cells additional propidium iodide (PI) staining is necessary since late apoptotic cells lose their membrane integrity so that PI can intrude the cells and chromatin stains pink-white, caused by the merging of the colours red (PI) and blue (DAPI) [108]. Execution of DNA degradation can be achieved caspase-dependent or caspase-independent [108]. We found a higher apoptosis rate in CVT-313 treated cells compared to rapamycin treated and control spheroids. Furthermore in all three conditions there were more condensed nuclei than cells, which were positive for cleaved caspase-3 and not all caspase-3 positive cells displayed condensed nuclei. Since caspase-3 activation occurs early during apoptosis [109] and DNA condensation is a later event, our data could show early and late apoptotic cells. Early apoptotic cells could be defined as cleaved caspase-3 positive showing normal nuclei and late apoptotic cells as cleaved caspase-3 positive displaying condensed chromatin. Consequently, negative cleaved caspase-3 staining and condensed nuclei might indicate a caspase-3-independent pathway, like necrosis [25]. For further differentiation of late apoptotic cells additional PI staining is necessary to observe intact membrane integrity or its loss.

Additional experiments addressing the role of apoptosis in invasion could be a treatment of cells with Z-VAD-FMK, a broad range caspase inhibitor, which binds irreversible to the catalytic site of caspases [110]. Thereafter these cells could be analysed in the spheroid-based invasion assay. This experiment would show if the decrease in invasion area after CVT-313 and rapamycin treatment occurs due to the high apoptosis rate or due to the inhibition of cdk2 and mTOR. Furthermore cleaved caspase-3 expression could be determined by Western blot analysis.

#### *4.3.2 Expression and localisation of mTOR pathway components in IMR-90 in 3D*

Since there is a massive decrease in cell size within cultivation in collagen gels Western blot analyses of mTOR pathway components are needed for further understanding of the differences in the individual culture conditions. As first hints cells cultivated in 2D and in 3D were stained with antibodies against pathway components (see chapter 2.6.2) to detect the amount and localisation of mTOR pathway components

mTOR was located within the cytoplasm in vesicle-like structures near the nucleus in all tested conditions. No signal was detectable within the nuclei. After rapamycin treatment an increase of the vesicle-like structures is visible. This is in close accordance to the literature, where it is known that only a small fraction of mTOR is localised within the nucleus and that it is predominantly bound to the endoplasmic reticulum and the golgi apparatus in the cytoplasm [97].

Phosphorylated AKT at S473 was localised preferentially in the lamellipodial protrusions, but without nucleus' signals in 2D and in 3D. After rapamycin treatment the signal increased especially in the protrusions, which is the expected consequence of the lost negative feedback loop (reviewed in [44, 49]). The only difference is that the distribution within cells cultured in collagen gels was not as even as in 2D, it looked like vesicle-like structures. It is described in the literature that phosphorylated AKT at S473 is localised predominantly in the protrusions of the human breast cancer cell line MCF-7, which is in accordance to our data [98].

Total AKT is distributed throughout the whole cells, with accumulation in or around the nuclei in all tested conditions and without changes after rapamycin treatment (Figure 3.15). In 3D the signal within the nuclei seems to be accumulation increased. Our data is in accordance to the literature [99].

In 2D and in 3D the phosphorylation of S6 at S240/244 is located throughout the cytoplasm (Figure 3.16). As expected after rapamycin treatment there is no signal left. This is in accordance with biochemical data from IMR-90 cells grown on plastic dishes [46]. Immunofluorescence staining in human Hep2 cells [101] and biochemical studies in IMR-90 cells [100] showed a S6 and pS6 S240/244 localisation within the nuclei [100, 101]. In our samples there were no stained pS6 proteins within the nuclei visible, whereas a  $\alpha$ -fibrillarin antibody stained the nucleoli as described in the literature [102]. New data in our laboratory indicate that the lack of staining is a fixation artefact, since pS6 signal within nucleoli in acetone/methanol (1:2) fixed IMR-90 is clearly visible (unpublished data).



4E-BP1 is localised in 2D and 3D in the whole cells showing accumulations within the nuclei, which is in close accordance to the literature [103]. Furthermore it was calculated that 30% of the total 4E-BP1 protein amount is localised within the nuclei [103]. Rapamycin treatment did not change its distribution.

In summary there were two differences between cells cultured on tissue plates and cells from single-cell suspension collagen gels. The first one concerns the total protein AKT. In 3D it seems as if more protein is resided within the nuclei. The second one is that pAKT displayed more vesicle-like structures in 3D compared to 2D. All these data do not show severe differences in mTOR signalling components and cannot explain the size reduction when IMR-90 are cultivated in collagen gels, however these are only microscopic observations and quantitative changes are had to evaluate in this setting. For evaluation of the localisation within the nuclei in 3D of the total protein AKT a fractionation of cytoplasm and nuclei would be necessary with following Western blot analyses.

In summary, the cell size of IMR-90 fibroblasts is drastically reduced when cells are cultured on 2D compared to 3D culture. After two days of cultivation in collagen gels the cell size is dramatically decreased and we can see changes in the granularity of the cells. Furthermore cells slow down proliferation. These data indicate changes in the mTOR pathway, since it is involved in regulation of cell size and cell cycle (reviewed in [44]). Immunofluorescence analyses of pathway components in 2D and in 3D do not show any massive differences in the distribution of the proteins, but for quantification of the protein amount we need to perform Western blot analyses. So far we only have preliminary data on Western blots, because protein lysates of cells out of collagen gels are technically demanding and so far the amount of protein was too less to warrant proper analyses.

When IMR-90 are cultured as spheroids in collagen gels they start to invade the surrounding gel. After treatment with rapamycin they display less invasion. The amount of reduction depends on the time when the treatment starts. The biggest effect is visible when cells were treated the day before aggregation, due to inhibition of mTORC1 [51] and diminished mTORC2 activity [55, 56]. Accordingly, knock-down experiments show that the effect is more severe when mTORC2 is down regulated compared to knock-downs of mTORC1. Until now the reasons for this results are unexplained and further investigation is needed. The cdk-2 inhibitor CVT-313 achieves a decrease of invasive area. Immunofluorescence analysis of collagen gels treated with DMSO, rapamycin and CVT-313 shows that CVT-313 treated spheroids display the highest number of cleaved

caspase-3 positive cells. Concomitantly the number of condensed nuclei with negative caspase-3 staining increased, indicating that they died due to caspase-3-independent pathways. The explanation for the low invasion rate of CVT-313 treated cells could be the high amount of dead cells within the spheroids, since there are only few cells left to invade the collagen gel.

To fully address which cellular function is altered upon mTOR inhibition in fibroblasts grown in collagen gels, we need further cell cycle analysis (FACS, BrdU incorporation), migration analysis and apoptosis analysis.

#### **4.4 Perspectives**

Since there are many unexplained observations our next intent will be to establish a harvesting method for NP40 lysis of collagen gels. Thereafter lysates of cells cultured in tissue culture plates and in collagen gels will be used for Western blot analyses of mTOR pathway components, proliferation markers and apoptosis marker.

Further experiments will concern FACS analyses of the above mentioned culture conditions which will be treated with 100 nM Rapamycin.

For quantification of proliferation in cells grown on tissue culture plates and cells cultured in collagen gels will use BrdU incorporation assays with FACS analyses or with immunofluorescence analyses.

## **5 References**

1. Welsch, U., *Lehrbuch Histologie*. 2nd ed. 2006, München: Elsevier GmbH, Urban & Fischer Verlag.
2. Buckley, C.D., et al., *Fibroblasts regulate the switch from acute resolving to chronic persistent inflammation*. Trends Immunol, 2001. **22**(4): p. 199-204.
3. Darby, I.A. and T.D. Hewitson, *Fibroblast differentiation in wound healing and fibrosis*. Int Rev Cytol, 2007. **257**: p. 143-79.
4. Kalluri, R. and M. Zeisberg, *Fibroblasts in cancer*. Nat Rev Cancer, 2006. **6**(5): p. 392-401.
5. Thornton, S.C., et al., *Fibroblast growth factors in connective tissue disease associated interstitial lung disease*. Clin Exp Immunol, 1992. **90**(3): p. 447-52.
6. Russell, S.B., et al., *Epigenetically altered wound healing in keloid fibroblasts*. J Invest Dermatol, 2010. **130**(10): p. 2489-96.
7. Levene, C.I., C.D. Ockleford, and C.L. Barber, *Scurvy; a comparison between ultrastructural and biochemical changes observed in cultured fibroblasts and the collagen they synthesise*. Virchows Arch B Cell Pathol, 1977. **23**(4): p. 325-38.
8. Nanayakkara, P.W., et al., *Vascular type of Ehlers-Danlos syndrome in a patient with ruptured aneurysm of the splenic artery*. Neth J Med, 2006. **64**(10): p. 374-6.
9. Chang, H.Y., et al., *Diversity, topographic differentiation, and positional memory in human fibroblasts*. Proc Natl Acad Sci U S A, 2002. **99**(20): p. 12877-82.
10. Snider, P., et al., *Origin of cardiac fibroblasts and the role of periostin*. Circ Res, 2009. **105**(10): p. 934-47.
11. Elsdale, T. and J. Bard, *Collagen substrata for studies on cell behavior*. J Cell Biol, 1972. **54**(3): p. 626-37.
12. Nichols, W.W., et al., *Characterization of a new human diploid cell strain, IMR-90*. Science, 1977. **196**(4285): p. 60-3.
13. Warburton, D., et al., *Lung organogenesis*. Curr Top Dev Biol, 2010. **90**: p. 73-158.
14. Rhee, S., *Fibroblasts in three dimensional matrices: cell migration and matrix remodeling*. Exp Mol Med, 2009. **41**(12): p. 858-65.
15. Wozniak, M.A. and P.J. Keely, *Use of three-dimensional collagen gels to study mechanotransduction in T47D breast epithelial cells*. Biol Proced Online, 2005. **7**: p. 144-61.
16. Handler, J.S., A.S. Preston, and R.E. Steele, *Factors affecting the differentiation of epithelial transport and responsiveness to hormones*. Fed Proc, 1984. **43**(8): p. 2221-4.
17. Cereijido, M., et al., *Polarized monolayers formed by epithelial cells on a permeable and translucent support*. J Cell Biol, 1978. **77**(3): p. 853-80.
18. Justice, B.A., N.A. Badr, and R.A. Felder, *3D cell culture opens new dimensions in cell-based assays*. Drug Discov Today, 2009. **14**(1-2): p. 102-7.
19. Walpita, D. and E. Hay, *Studying actin-dependent processes in tissue culture*. Nat Rev Mol Cell Biol, 2002. **3**(2): p. 137-41.
20. Ghosh, S., et al., *Three-dimensional culture of melanoma cells profoundly affects gene expression profile: a high density oligonucleotide array study*. J Cell Physiol, 2005. **204**(2): p. 522-31.
21. Kim, J.B., *Three-dimensional tissue culture models in cancer biology*. Seminars in Cancer Biology, 2005. **15**: p. 365-377.
22. Grinnell, F., *Fibroblast biology in three-dimensional collagen matrices*. Trends Cell Biol, 2003. **13**(5): p. 264-9.

23. Grinnell, F., *Fibroblast mechanics in three-dimensional collagen matrices*. J Bodyw Mov Ther, 2008. **12**(3): p. 191-3.
24. Bell, E., B. Ivarsson, and C. Merrill, *Production of a tissue-like structure by contraction of collagen lattices by human fibroblasts of different proliferative potential in vitro*. Proc Natl Acad Sci U S A, 1979. **76**(3): p. 1274-8.
25. Vaheri, A., et al., *Nemosis, a novel way of fibroblast activation, in inflammation and cancer*. Exp Cell Res, 2009. **315**(10): p. 1633-8.
26. Bizik, J., et al., *Cell-cell contacts trigger programmed necrosis and induce cyclooxygenase-2 expression*. Cell Death Differ, 2004. **11**(2): p. 183-95.
27. Hirschhaeuser, F., et al., *Multicellular tumor spheroids: an underestimated tool is catching up again*. J Biotechnol, 2010. **148**(1): p. 3-15.
28. Wright, T.C., et al., *The role of negative charge in spontaneous aggregation of transformed and untransformed cell lines*. J Cell Sci, 1980. **45**: p. 99-117.
29. Yuhas, J.M., et al., *A simplified method for production and growth of multicellular tumor spheroids*. Cancer Res, 1977. **37**(10): p. 3639-43.
30. Becker, J.L. and D.K. Blanchard, *Characterization of primary breast carcinomas grown in three-dimensional cultures*. J Surg Res, 2007. **142**(2): p. 256-62.
31. Bell, E., *Strategy for the selection of scaffolds for tissue engineering*. Tissue Eng, 1995. **1**(2): p. 163-79.
32. van Zijl, F., et al., *Hepatic tumor-stroma crosstalk guides epithelial to mesenchymal transition at the tumor edge*. Oncogene, 2009. **28**(45): p. 4022-33.
33. Albini, A. and R. Benelli, *The chemoinvasion assay: a method to assess tumor and endothelial cell invasion and its modulation*. Nat Protoc, 2007. **2**(3): p. 504-11.
34. Boyden, S., *The chemotactic effect of mixtures of antibody and antigen on polymorphonuclear leucocytes*. J Exp Med, 1962. **115**: p. 453-66.
35. Albini, A., et al., *A rapid in vitro assay for quantitating the invasive potential of tumor cells*. Cancer Res, 1987. **47**(12): p. 3239-45.
36. Freytag, J., et al., *PAI-1 mediates the TGF-beta1+EGF-induced "scatter" response in transformed human keratinocytes*. J Invest Dermatol, 2010. **130**(9): p. 2179-90.
37. Timmins, N.E. and L.K. Nielsen, *Generation of multicellular tumor spheroids by the hanging-drop method*. Methods Mol Med, 2007. **140**: p. 141-51.
38. Sabeh, F., et al., *Tumor cell traffic through the extracellular matrix is controlled by the membrane-anchored collagenase MT1-MMP*. J Cell Biol, 2004. **167**(4): p. 769-81.
39. Sabeh, F., R. Shimizu-Hirota, and S.J. Weiss, *Protease-dependent versus -independent cancer cell invasion programs: three-dimensional amoeboid movement revisited*. J Cell Biol, 2009. **185**(1): p. 11-9.
40. Grinnell, F., et al., *Nested collagen matrices: a new model to study migration of human fibroblast populations in three dimensions*. Exp Cell Res, 2006. **312**(1): p. 86-94.
41. Dallan, J.C. and H.P. Ehrlich, *A review of fibroblast-populated collagen lattices*. Wound Repair Regen, 2008. **16**(4): p. 472-9.
42. Kunz-Schughart, L.A., et al., *A heterologous 3-D coculture model of breast tumor cells and fibroblasts to study tumor-associated fibroblast differentiation*. Exp Cell Res, 2001. **266**(1): p. 74-86.
43. Oxmann, D., et al., *Endoglin expression in metastatic breast cancer cells enhances their invasive phenotype*. Oncogene, 2008. **27**(25): p. 3567-75.

44. Foster, K.G. and D.C. Fingar, *mTOR: Conducting the cellular signaling symphony*. J Biol Chem, 2010.
45. Rosner, M. and M. Hengstschlager, *Cytoplasmic and nuclear distribution of the protein complexes mTORC1 and mTORC2: rapamycin triggers dephosphorylation and delocalization of the mTORC2 components rictor and sin1*. Hum Mol Genet, 2008. **17**(19): p. 2934-48.
46. Rosner, M., et al., *Functional interaction of mammalian target of rapamycin complexes in regulating mammalian cell size and cell cycle*. Hum Mol Genet, 2009. **18**(17): p. 3298-310.
47. Laragione, T. and P.S. Gulko, *mTOR Regulates the Invasive Properties of Synovial Fibroblasts in Rheumatoid Arthritis*. Mol Med, 2010. **16**(9-10): p. 352-358.
48. Liu, Z.G., et al., *[Experimental study of human skin fibroblasts cultured in three-dimension(3D)]*. Zhonghua Zheng Xing Wai Ke Za Zhi, 2004. **20**(6): p. 443-6.
49. Ma, X.M. and J. Blenis, *Molecular mechanisms of mTOR-mediated translational control*. Nat Rev Mol Cell Biol, 2009. **10**(5): p. 307-18.
50. Vezina, C., A. Kudelski, and S.N. Sehgal, *Rapamycin (AY-22,989), a new antifungal antibiotic. I. Taxonomy of the producing streptomycete and isolation of the active principle*. J Antibiot (Tokyo), 1975. **28**(10): p. 721-6.
51. Sabatini, D.M., et al., *RAFT1: a mammalian protein that binds to FKBP12 in a rapamycin-dependent fashion and is homologous to yeast TORs*. Cell, 1994. **78**(1): p. 35-43.
52. Tee, A.R. and J. Blenis, *mTOR, translational control and human disease*. Semin Cell Dev Biol, 2005. **16**(1): p. 29-37.
53. Kim, D.H., et al., *mTOR interacts with raptor to form a nutrient-sensitive complex that signals to the cell growth machinery*. Cell, 2002. **110**(2): p. 163-75.
54. Kim, D.H., et al., *GbetaL, a positive regulator of the rapamycin-sensitive pathway required for the nutrient-sensitive interaction between raptor and mTOR*. Mol Cell, 2003. **11**(4): p. 895-904.
55. Sarbassov, D.D., et al., *Rictor, a novel binding partner of mTOR, defines a rapamycin-insensitive and raptor-independent pathway that regulates the cytoskeleton*. Curr Biol, 2004. **14**(14): p. 1296-302.
56. Jacinto, E., et al., *Mammalian TOR complex 2 controls the actin cytoskeleton and is rapamycin insensitive*. Nat Cell Biol, 2004. **6**(11): p. 1122-8.
57. Sancak, Y., et al., *PRAS40 is an insulin-regulated inhibitor of the mTORC1 protein kinase*. Mol Cell, 2007. **25**(6): p. 903-15.
58. Peterson, T.R., et al., *DEPTOR is an mTOR inhibitor frequently overexpressed in multiple myeloma cells and required for their survival*. Cell, 2009. **137**(5): p. 873-86.
59. Foster, K.G., et al., *Regulation of mTOR complex 1 (mTORC1) by raptor Ser863 and multisite phosphorylation*. J Biol Chem, 2009. **285**(1): p. 80-94.
60. Frias, M.A., et al., *mSin1 is necessary for Akt/PKB phosphorylation, and its isoforms define three distinct mTORC2s*. Curr Biol, 2006. **16**(18): p. 1865-70.
61. Choo, A.Y., et al., *Rapamycin differentially inhibits S6Ks and 4E-BP1 to mediate cell-type-specific repression of mRNA translation*. Proc Natl Acad Sci U S A, 2008. **105**(45): p. 17414-9.
62. Cybulski, N., et al., *mTOR complex 2 in adipose tissue negatively controls whole-body growth*. Proc Natl Acad Sci U S A, 2009. **106**(24): p. 9902-7.

63. Pearson, R.B., et al., *The principal target of rapamycin-induced p70s6k inactivation is a novel phosphorylation site within a conserved hydrophobic domain*. EMBO J, 1995. **14**(21): p. 5279-87.
64. Ferrari, S., et al., *Mitogen-activated 70K S6 kinase. Identification of in vitro 40 S ribosomal S6 phosphorylation sites*. J Biol Chem, 1991. **266**(33): p. 22770-5.
65. Fingar, D.C., et al., *mTOR controls cell cycle progression through its cell growth effectors S6K1 and 4E-BP1/eukaryotic translation initiation factor 4E*. Mol Cell Biol, 2004. **24**(1): p. 200-16.
66. Sarbassov, D.D., et al., *Phosphorylation and regulation of Akt/PKB by the rictor-mTOR complex*. Science, 2005. **307**(5712): p. 1098-101.
67. Jacinto, E., et al., *SIN1/MIP1 maintains rictor-mTOR complex integrity and regulates Akt phosphorylation and substrate specificity*. Cell, 2006. **127**(1): p. 125-37.
68. Manning, B.D. and L.C. Cantley, *AKT/PKB signaling: navigating downstream*. Cell, 2007. **129**(7): p. 1261-74.
69. Inoki, K., T. Zhu, and K.L. Guan, *TSC2 mediates cellular energy response to control cell growth and survival*. Cell, 2003. **115**(5): p. 577-90.
70. Inoki, K., et al., *Rheb GTPase is a direct target of TSC2 GAP activity and regulates mTOR signaling*. Genes Dev, 2003. **17**(15): p. 1829-34.
71. Orlova, K.A. and P.B. Crino, *The tuberous sclerosis complex*. Ann N Y Acad Sci, 2009. **1184**: p. 87-105.
72. Manning, B.D., et al., *Identification of the tuberous sclerosis complex-2 tumor suppressor gene product tuberlin as a target of the phosphoinositide 3-kinase/akt pathway*. Mol Cell, 2002. **10**(1): p. 151-62.
73. Vander Haar, E., et al., *Insulin signalling to mTOR mediated by the Akt/PKB substrate PRAS40*. Nat Cell Biol, 2007. **9**(3): p. 316-23.
74. Ma, L., et al., *Phosphorylation and functional inactivation of TSC2 by Erk implications for tuberous sclerosis and cancer pathogenesis*. Cell, 2005. **121**(2): p. 179-93.
75. Guertin, D.A. and D.M. Sabatini, *Defining the role of mTOR in cancer*. Cancer Cell, 2007. **12**(1): p. 9-22.
76. Gwinn, D.M., et al., *AMPK phosphorylation of raptor mediates a metabolic checkpoint*. Mol Cell, 2008. **30**(2): p. 214-26.
77. Huang, J., et al., *The TSC1-TSC2 complex is required for proper activation of mTOR complex 2*. Mol Cell Biol, 2008. **28**(12): p. 4104-15.
78. Tzatsos, A., *Raptor binds the SAIN (Shc and IRS-1 NPXY binding) domain of insulin receptor substrate-1 (IRS-1) and regulates the phosphorylation of IRS-1 at Ser-636/639 by mTOR*. J Biol Chem, 2009. **284**(34): p. 22525-34.
79. Um, S.H., et al., *Absence of S6K1 protects against age- and diet-induced obesity while enhancing insulin sensitivity*. Nature, 2004. **431**(7005): p. 200-5.
80. Dibble, C.C., J.M. Asara, and B.D. Manning, *Characterization of Rictor phosphorylation sites reveals direct regulation of mTOR complex 2 by S6K1*. Mol Cell Biol, 2009. **29**(21): p. 5657-70.
81. Oshiro, N., et al., *Dissociation of raptor from mTOR is a mechanism of rapamycin-induced inhibition of mTOR function*. Genes Cells, 2004. **9**(4): p. 359-66.
82. Beretta, L., et al., *Rapamycin blocks the phosphorylation of 4E-BP1 and inhibits cap-dependent initiation of translation*. EMBO J, 1996. **15**(3): p. 658-64.

83. Peterson, R.T., et al., *Protein phosphatase 2A interacts with the 70-kDa S6 kinase and is activated by inhibition of FKBP12-rapamycin-associated protein*. Proc Natl Acad Sci U S A, 1999. **96**(8): p. 4438-42.
84. Chen, X.G., et al., *Rapamycin regulates Akt and ERK phosphorylation through mTORC1 and mTORC2 signaling pathways*. Mol Carcinog, 2010. **49**(6): p. 603-10.
85. Meric-Bernstam, F. and A.M. Gonzalez-Angulo, *Targeting the mTOR signaling network for cancer therapy*. J Clin Oncol, 2009. **27**(13): p. 2278-87.
86. Yang, Q. and K.L. Guan, *Expanding mTOR signaling*. Cell Res, 2007. **17**(8): p. 666-81.
87. Sarbassov, D.D., et al., *Prolonged rapamycin treatment inhibits mTORC2 assembly and Akt/PKB*. Mol Cell, 2006. **22**(2): p. 159-68.
88. Shi, Y., et al., *Mammalian target of rapamycin inhibitors activate the AKT kinase in multiple myeloma cells by up-regulating the insulin-like growth factor receptor/insulin receptor substrate-1/phosphatidylinositol 3-kinase cascade*. Mol Cancer Ther, 2005. **4**(10): p. 1533-40.
89. Cheadle, J.P., et al., *Molecular genetic advances in tuberous sclerosis*. Hum Genet, 2000. **107**(2): p. 97-114.
90. Rosner, M., et al., *The mTOR pathway and its role in human genetic diseases*. Mutat Res, 2008. **659**(3): p. 284-92.
91. Goncharova, E.A., et al., *Tuberin regulates p70 S6 kinase activation and ribosomal protein S6 phosphorylation. A role for the TSC2 tumor suppressor gene in pulmonary lymphangioleiomyomatosis (LAM)*. J Biol Chem, 2002. **277**(34): p. 30958-67.
92. Taylor, J.R., et al., *Lymphangioleiomyomatosis. Clinical course in 32 patients*. N Engl J Med, 1990. **323**(18): p. 1254-60.
93. Gallagher, A.R., G.G. Germino, and S. Somlo, *Molecular advances in autosomal dominant polycystic kidney disease*. Adv Chronic Kidney Dis, 2010. **17**(2): p. 118-30.
94. Foley, T.R., T.J. McGarrity, and A.B. Abt, *Peutz-Jeghers syndrome: a clinicopathologic survey of the "Harrisburg family" with a 49-year follow-up*. Gastroenterology, 1988. **95**(6): p. 1535-40.
95. Brooks, E.E., et al., *CVT-313, a specific and potent inhibitor of CDK2 that prevents neointimal proliferation*. J Biol Chem, 1997. **272**(46): p. 29207-11.
96. Valli, A., et al., *Embryoid body formation of human amniotic fluid stem cells depends on mTOR*. Oncogene, 2010. **29**(7): p. 966-77.
97. Drenan, R.M., et al., *FKBP12-rapamycin-associated protein or mammalian target of rapamycin (FRAP/mTOR) localization in the endoplasmic reticulum and the Golgi apparatus*. J Biol Chem, 2004. **279**(1): p. 772-8.
98. de Gunst, M.M., et al., *Functional analysis of cancer-associated EGFR mutants using a cellular assay with YFP-tagged EGFR intracellular domain*. Mol Cancer, 2007. **6**: p. 56.
99. Stratford, S., et al., *Regulation of insulin action by ceramide: dual mechanisms linking ceramide accumulation to the inhibition of Akt/protein kinase B*. J Biol Chem, 2004. **279**(35): p. 36608-15.
100. Rosner, M., et al., *Different cytoplasmic/nuclear distribution of S6 protein phosphorylated at S240/244 and S235/236*. Amino Acids, 2010.
101. Kruger, T., H. Zentgraf, and U. Scheer, *Intranucleolar sites of ribosome biogenesis defined by the localization of early binding ribosomal proteins*. J Cell Biol, 2007. **177**(4): p. 573-8.



102. Aris, J.P. and G. Blobel, *cDNA cloning and sequencing of human fibrillarin, a conserved nucleolar protein recognized by autoimmune antisera*. Proc Natl Acad Sci U S A, 1991. **88**(3): p. 931-5.
103. Rong, L., et al., *Control of eIF4E cellular localization by eIF4E-binding proteins, 4E-BPs*. RNA, 2008. **14**(7): p. 1318-27.
104. Sauve, D.M., et al., *Phosphorylation-induced rearrangement of the histone H3 NH2-terminal domain during mitotic chromosome condensation*. J Cell Biol, 1999. **145**(2): p. 225-35.
105. Li, D.W., et al., *Dynamic distribution of Ser-10 phosphorylated histone H3 in cytoplasm of MCF-7 and CHO cells during mitosis*. Cell Res, 2005. **15**(2): p. 120-6.
106. Boatright, K.M. and G.S. Salvesen, *Mechanisms of caspase activation*. Curr Opin Cell Biol, 2003. **15**(6): p. 725-31.
107. Xia, H., et al., *Polymerized collagen inhibits fibroblast proliferation via a mechanism involving the formation of a beta1 integrin-protein phosphatase 2A-tuberous sclerosis complex 2 complex that suppresses S6K1 activity*. J Biol Chem, 2008. **283**(29): p. 20350-60.
108. Huettenbrenner, S., et al., *The evolution of cell death programs as prerequisites of multicellularity*. Mutat Res, 2003. **543**(3): p. 235-49.
109. Lavrik, I.N., A. Golks, and P.H. Krammer, *Caspases: pharmacological manipulation of cell death*. J Clin Invest, 2005. **115**(10): p. 2665-72.
110. Van Noorden, C.J., *The history of Z-VAD-FMK, a tool for understanding the significance of caspase inhibition*. Acta Histochem, 2001. **103**(3): p. 241-51.



## **6 Appendix**

## 6.1 Reagents

| <i>product name</i>                                   | <i>company</i>                           | <i>article no.</i> |
|---|--|--------------------|
| 2-Glycerophosphate disodium salt hydrate              | Sigma-Aldrich, St. Louis, MO, USA        | G6251              |
| 2-Mercaptoethanol, min. 98%                           | Sigma-Aldrich, St. Louis, MO, USA        | M3148              |
| 30% Acrylamide/ Bis-Solution 37.5:1 (2.6% C)          | BioRad, Hercules, CA, USA                | 1610158            |
| 4',6-Diamidino-2-phenylindole dihydrochloride (DAPI ) | Sigma-Aldrich, St. Louis, MO, USA        | 32670              |
| 5-Sulfosalicylic acid dihydrate                       | Sigma-Aldrich, St. Louis, MO, USA        | S2130              |
| 5x siRNA buffer                                       | Dharmacon, Lafayette, CO, USA            | B-002000-UB-015    |
| Acetic acid   | Sigma-Aldrich, St. Louise, Mo, USA       | 695092             |
| Alexa Fluor® 546 phalloidin                           | Invitrogen, Carlsbad, CA, USA            | A 22283            |
| Ammonium persulfate (APS)                             | BioRad, Hercules, CA, USA                | 1610700            |
| Aprotinin   | Sigma-Aldrich, St. Louis, MO, USA        | A1153              |
| Benzamidinium chloride Hydrochloride Hydrate          | Sigma-Aldrich, St. Louis, MO, USA        | B6506              |
| BioRad - Protein Assay                                | BioRad, Hercules, CA, USA                | 500-0006           |
| Blotting Grade Blocker, non-fat dry milk              | BioRad, Hercules, CA, USA                | 170-6404           |
| Bovine serum albumin (BSA) Albumin, Fraction V        | USB, Cleveland, OH, USA                  | 10857              |
| Bromophenol blue                                      | Merck, Darmstadt, Germany                | L961422            |
| Calcium chloride dihydrate (CaCl <sub>2</sub> )       | Merck, Darmstadt, Germany                | 2382               |
| Collagen I  | Gibco-Invitrogen, Carlsbad, CA, USA      | A10483-01          |
| Collagenase B   | Roche Diagnostics, Indianapolis, IN, USA | 11 088 807 001     |
| CVT-313   | Calbiochem, La Jolla, CA, USA            | 238803             |
| DEPC treated water                                    | Invitrogen, Carlsbad, CA, USA            | 10813-012          |
| Dimethyl sulfoxide (DMSO)                             | Sigma-Aldrich, St. Louis, MO, USA        | D5879              |
| Dithiothreitol (DTT)                                  | Sigma-Aldrich, St. Louis, MO, USA        | 646563             |
| DMEM High Glucose (4.5g/l)                            | PAA, Pasching, Austria                   | E15-011            |
| Dulbecco's 10x PBS                                    | PAA, Pasching, Austria                   | H15-011            |
| Dulbecco's 1x PBS                                     | PAA, Pasching, Austria                   | H15-002            |

|   |  |                       |
|---|--|-----------------------|
| Ethanol absolute for analysis                       | VWR, West Chester, PA, USA                       | 20821.310             |
| Ethylenediaminetetraacetic acid (EDTA)              | Sigma-Aldrich, St. Louis, MO, USA                | E5134                 |
| Fetal calf serum (FCS)                              | PAA, Pasching, Austria                           | A15-101               |
| Glycerol  | Merck, Darmstadt, Germany                        | 1.04093               |
| Glycin  | Sigma-Aldrich, St. Louis, MO, USA                | G8898                 |
| Goat- $\alpha$ -mouse Alexa Fluor® 594              | Invitrogen, Carlsbad, CA, USA                    | A 11032               |
| Goat- $\alpha$ -rabbit Alexa Fluor® 488             | Invitrogen, Carlsbad, CA, USA                    | A 11034               |
| Goat- $\alpha$ -rabbit IgG-h+l                      | Bethyl Laboratories Inc.,<br>Montgomery, TX, USA | A120-101P             |
| HEPES   | USB, Cleveland, OH, USA                          | 16926                 |
| L-glutamine   | PAA, Pasching, Austria                           | M11-004               |
| Leupeptin   | Sigma-Aldrich, St. Louis, MO, USA                | L2023                 |
| Lipofectamine RNAiMAX                               | Invitrogen, Carlsbad, CA, USA                    | 13778075              |
| Magnesium chloride hexahydrate (MgCl <sub>2</sub> ) | Merck, Darmstadt, Germany                        | 5833                  |
| Methylcellulose (4000 centipoises)                  | Sigma-Aldrich, St. Louis, MO, USA                | M0512                 |
| Mounting medium                                     | Vector Laboratories Inc.,<br>Burlingame, CA, USA | H-1000                |
| Nonidet-P40 (NP40)                                  | USB, Cleveland, OH, USA                          | 19628                 |
| OptiMEM I   | Gibco-Invitrogen, Carlsbad, CA, USA              | 31985                 |
| PageRuler Prestained Protein Ladder                 | Fermentas  | SM0671                |
| Paraformaldehyde (PFA)                              | Sigma-Aldrich, St. Louis, MO, USA                | P6148                 |
| Penicillin  | Sigma-Aldrich, St. Louis, MO, USA                | P3032                 |
| Phenyl-methyl-sulfonyl-fluorid (PMSF)               | Sigma-Aldrich, St. Louis, MO, USA                | P7626                 |
| Ponceau S   | Sigma-Aldrich, St. Louis, MO, USA                | P3504                 |
| Potassium chloride (KCl)                            | Merck, Darmstadt, Germany                        | 1.04936               |
| Propidium iodide                                    | Sigma-Aldrich, St. Louis, MO, USA                | P4170                 |
| Rapamycin   | Calbiochem, La Jolla, CA, USA                    | 553211                |
| RNAse A   | Sigma-Aldrich, St. Louis, MO, USA                | R5125                 |
| siRNA   | Dharmacon, Lafayette, CO, USA                    | see<br>chapter<br>6.3 |
| Sodium chloride (NaCl)                              | Sigma-Aldrich, St. Louis, MO, USA                | S9625                 |

|   |   |           |
|---|---|-----------|
| Sodium citrate tribasic dihydrate                       | Sigma-Aldrich, St. Louis, MO, USA             | C7254     |
| Sodium dodecyl sulfate (SDS)                            | Sigma-Aldrich, St. Louis, MO, USA             | L4390     |
| Sodium fluoride (NaF)                                   | Fluka-Sigma-Aldrich, St. Louis, MO, USA       | 71519     |
| Sodium hydroxide (NaOH) pellets                         | Merck, Darmstadt, Germany                     | 1.06498   |
| Sodium orthovanadate (Na <sub>3</sub> VO <sub>4</sub> ) | Sigma-Aldrich, St. Louis, MO, USA             | S6508     |
| Streptomycin sulfate                                    | Sigma-Aldrich, St. Louis, MO, USA             | S6501     |
| Tetramethylethylenediamine (TEMED)                      | Sigma-Aldrich, St. Louis, MO, USA             | T9281     |
| Trichloroacetic acid                                    | Merck, Darmstadt, Germany                     | 807       |
| Tris Base   | Sigma-Aldrich, St. Louis, MO, USA             | T1503     |
| Triton X 100  | Sigma-Aldrich, St. Louis, MO, USA             | T8787     |
| Trypan blue   | STEMCELL Technologies Inc., Vancouver, Canada | 07050     |
| Trypsin 1:250 2.2 U/mg                                  | Serva, Heidelberg, Germany                    | 37290     |
| Trypsin inhibitor                                       | Sigma-Aldrich, St. Louis, MO, USA             | T9003     |
| Tween 20  | BioRad, Hercules, CA, USA                     | 170-6531  |
| $\alpha$ -4E-BP1  | Cell signaling, Danvers, MA, USA              | 9452      |
| $\alpha$ -Akt   | Cell signaling, Danvers, MA, USA              | 9272      |
| $\alpha$ -cleaved caspase-3 (D175) (5A1E)               | Cell signaling, Danvers, MA, USA              | 9664      |
| $\alpha$ -fibrillarin (C13C3)                           | Cell signaling, Danvers, MA, USA              | 2639      |
| $\alpha$ -mTOR  | Cell signaling, Danvers, MA, USA              | 2972      |
| $\alpha$ -p70 S6K                                       | Cell signaling, Danvers, MA, USA              | 9202      |
| $\alpha$ -p70 S6K T389 (108D2)                          | Cell signaling, Danvers, MA, USA              | 9234      |
| $\alpha$ -pAkt S473 (D9E) XP                            | Cell signaling, Danvers, MA, USA              | 4060      |
| $\alpha$ -p-H3 S10                                      | Cell signaling, Danvers, MA, USA              | 9701      |
| $\alpha$ -pS6 240/244                                   | Cell signaling, Danvers, MA, USA              | 2215      |
| $\alpha$ -Raptor  | Bethyl Laboratories Inc., Montgomery, TX, USA | A300-506A |
| $\alpha$ -Rictor  | Bethyl Laboratories Inc., Montgomery, TX, USA | A300-459A |

## 6.2 Equipment

| <i>product name</i>          | <i>company</i>  | <i>article no.</i>                             |
|------------------------------|---|--|
| 1.5 ml microcentrifuge tubes | VWR, West Chester, PA, USA                              | 211-0015 (Europe)<br>20170-038 (North America) |
| 100 mm tissue culture plates | Iwaki, Asahi Glass Co LTD, Tokyo, Japan                 | 3020-100                                       |
| 15 ml centrifuge tubes       | Sarstedt, Nümbrecht, Germany                            | 62.554.502                                     |
| 15-slots comb                | BioRad, Hercules, CA, USA                               | 165-3355                                       |
| 3MM Chr sheets               | Whatman, Dassel, Germany                                | 3030 917                                       |
| 4-well chamber slide         | Lab-Tek®, Nalge Nunc International, Naperville, IL, USA | 177437   |
| 500 µl microcentrifuge tubes | Eppendorf, Hamburg, Germany                             | 0030 121.023                                   |
| 6-well plate                 | PAA, Pasching, Austria                                  | PAA30006X                                      |
| 96-well plates               | Sterillin, Aberbargoed, Caerphilly, UK                  | microtiter plate<br>612V96<br>lid 642000       |
| BioPhotometer                | Eppendorf, Hamburg, Germany                             |  |
| Bright-Line hemacytometer    | Hausser Scientific, Horsham, PA, USA                    | 3120   |
| Cellquest Version 6.0        | BD Immunocytometry Systems                              |  |
| CL-XPosure films             | Thermo Scientific, Rockford, IL, USA                    | 34089  |
| cover slide                  | Thermo Scientific, Waltham, MA, USA                     | DXD-10143263<br>24x60 mm #1                    |
| CryoTubes™                   | Nalge Nunc International, Naperville, IL, USA           | 343958   |
| cuvette                      | Sarstedt, Nümbrecht, Germany                            | 67.746   |
| Eppendorf Centrifuge 5417R   | Eppendorf, Hamburg, Germany                             |  |
| FACS-tube                    | BD Falcon™, BD Biosciences, Erembodegem, Belgium        | 352054   |
| FACSCalibur                  | Beckton Dickinson, Franklin Lakes, NJ, USA              |  |
| FlowJo Version 7.5.5         | Tree Star Inc., Ashland, OR, USA                        |  |

|   |   |   |
|---|---|---|
| glass slide                                   | Thermo Scientific, Waltham, MA, USA         | DXD-10143560  |
| GraphPad Prism 4                              | GraphPad Software Inc., La Jolla, CA, USA   |   |
| Heraeus BBD 6220 incubators                   | Thermo Scientific, Waltham, MA, USA         |   |
| Kodak Medical X-ray Processor 2000            | Kodak, Stuttgart, Germany                   |   |
| light-sensitive Amersham Hyperfilms           | GE Healthcare, Buckinghamshire, UK          | 28906837  |
| Microsoft Excel 2008                          | Microsoft Corporation, Redmond WA, USA      |   |
| Mini-PROTEAN Tetra Electrophoresis System     | Hercules, CA, USA                           | 165-8002  |
| Mini-Trans-Blot Module                        | BioRad, Hercules, CA, USA                   | 170-3935  |
| nitrocellulose membrane                       | Watman, Dassel, Germany                     | 10401396  |
| orbital shaker                                | Rocky® 3D                                   |   |
| Parafilm “M”®                                 | VWR, West Chester, Pa, USA                  | 291-1213  |
| PET mesh with 120 µm mesh size                | Bückmann, Mönchengladbach, Germany          | PET-100/77-32   |
| pipette-tips                                  | Starlab, Ahrensburg, Germany                | 0,1-10 µl S1111-3000<br>1-200 µl S1111-1006<br>101-1000 µl S1111-2021 |
| rocking platform                              | VWR, West Chester, Pa, USA                  | 40000300  |
| single-use syringe                            | B Braun, Bethlehem, PA, USA                 | 460 6051 V)   |
| sterile filtration unit with 0.2 µm pore size | Sarstedt, Nümbrecht, Germany                | 83.1822.001   |
| syringe filter with 0,2 µm pore size          | Whatman, Dassel, Germany                    | 6809-2122)  |
| thermomixer comfort                           | Eppendorf, Hamburg, Germany                 |   |
| v-shaped reservoir                            | Eppendorf, Hamburg, Deutschland             | D5063-85  |
| watherbath shaker Julabo W22                  | JULABO Labortechnik GmbH, Seelbach, Germany |   |



### 6.3 Used siRNA-pools

optained from Dharmacon, Lafayette, CO, USA

|   |  |
|---|--|
| <b>ON-TARGETplus SMARTpool L-004107-00-0005, Human RAPTOR, NM_020761 5nmol</b>  |  |
| ON-TARGETplus SMARTpool siRNA J-004107-05, RAPTOR                               |  |
| Target Sequence   | UGGCUAGUCUGUUUCGAAA                                |
| Mol. Wt.  | 13.414,7 g/mol                                     |
| ON-TARGETplus SMARTpool siRNA J-004107-06, RAPTOR                               |  |
| Target Sequence   | CACGGAAGAUGUUCGACAA                                |
| Mol. Wt.  | 13.429,8 g/mol                                     |
| ON-TARGETplus SMARTpool siRNA J-004107-07, RAPTOR                               |  |
| Target Sequence   | AGAAGGGCAUACGAGAUU                                 |
| Mol. Wt.  | 13.414,9 g/mol                                     |
| ON-TARGETplus SMARTpool siRNA J-004107-08, RAPTOR                               |  |
| Target Sequence   | UGGAGAAGCGUGUCAGAU                                 |
| Mol. Wt.  | 13.429,8 g/mol                                     |
| <b>ON-TARGETplus SMARTpool L-016984-00-0005, Human RICTOR, NM_152756, 5nmol</b> |  |
| ON-TARGETplus SMARTpool siRNA J-016984-05, RICTOR                               |  |
| Target Sequence   | GACACAAGCACUUCGAUUA                                |
| Mol. Wt.  | 13.414,9 g/mol                                     |
| ON-TARGETplus SMARTpool siRNA J-016984-06, RICTOR                               |  |
| Target Sequence   | GAAGAUUUAUUGAGUCCUA                                |
| Mol. Wt.  | 13.384,9 g/mol                                     |
| ON-TARGETplus SMARTpool siRNA J-016984-07, RICTOR                               |  |
| Target Sequence   | GCGAGCUGAUGUAGAAUUA                                |
| Mol. Wt.  | 13.414,9 g/mol                                     |
| ON-TARGETplus SMARTpool siRNA J-016984-08, RICTOR                               |  |
| Target Sequence   | GGGAAUACAACUCCAAUA                                 |
| Mol. Wt.  | 13.399,9 g/mol                                     |
| <b>ON-TARGETplus Non-targeting Pool D-001810-10-05, 5nmol</b>                   |  |
| Catalog Item  | D-001810-10-05<br>ON-TARGETplus Non targeting Pool |

## 6.4 Buffers and solutions

|                                    |  |
|------------------------------------|--|
| Trypsin EDTA solution (TE):        | 2200 U trypsin<br>2% Na EDTA pH 7.4  |
| Antibiotics stock solution:        | 10 g/l streptomycin sulfate<br>6 g/l penicillin<br>10% 10x PBS   |
| DMEM with 10% FCS:                 | DMEM high glucose (4.8 g glucose/l)<br>10% FCS<br>60 mg/l penicillin<br>100 mg/l streptomycin sulfate<br>2 mM l-glutamine                          |
| Methylcellulose:                   | 1.5% (w/v) Methylcellulose<br>in DMEM supplemented with 2 mM l-glutamine   |
| DMEM with 2% FCS:                  | DMEM high glucose (4.8 g glucose/l)<br>2% FCS<br>60 mg/l penicillin<br>100 mg/l streptomycin sulfate<br>2 mM l-glutamine                           |
| DMEM with 10% FCS w/o antibiotics: | DMEM high glucose (4.8 g glucose/l)<br>10% FCS<br>2 mM l-glutamine   |
| NP40 lysis buffer:                 | 40 mM Hepes pH 7.5<br>120 mM NaCl<br>1 mM EDTA pH 8.0<br>10 mM 2-glycerophosphate<br>50 mM NaF<br>0.5mM Na <sub>3</sub> VO <sub>4</sub><br>1% NP40 |

|                             |   |
|-----------------------------|---|
| PIM:                        | 2 µg/ml Leupeptin<br>2 µg/ml Aprotinin<br>0,3 µg/ml Benzamidine chloride<br>10µg/ml Trypsin inhibitor |
| 4x protein sample buffer:   | 200 mM Tris pH 6.8<br>400 mM DTT<br>8% SDS<br>0.4% Bromphenol blue<br>40% Glycerol                    |
| Buffer B pH 8.8:            | 1.5 M Tris pH 8.8<br>0.4% (v/v) SDS   |
| APS:                        | 10% (w/v) APS   |
| Buffer C pH 6.8:            | 0.5 M Tris pH 6.8<br>0.4% (v/v) SDS   |
| 10x electrophoresis buffer: | 250 mM Tris<br>1.94 M glycine<br>1% (w/v) SDS   |
| 1x electrophoresis buffer:  | 10% (v/v) 10x electrophoresis buffer  |
| Harlow 1:                   | 48 mM Tris<br>386 mM glycine<br>0,1% (w/v) SDS<br>20% (v/v) methanol                                  |
| 10x Ponceau S:              | 2% (w/v) Ponceau S<br>30% (w/v) trichlor acetic acid<br>30% (w/v) sulfosalicylic acid                 |

|                             |  |
|-----------------------------|--|
| 1x Ponceau S:               | 10% (v/v) 10x Ponceau S  |
| 10x TBS:                    | 1.5 M NaCl<br>0.5 M Tris pH 7.4  |
| 1x TBS-T:                   | 10% (v/v) 10x TBS<br>0.1% (v/v) Triton X-100   |
| 5% blocking solution:       | 5% (w/v) milk powder<br>1x TBS-T   |
| TBS-T, 5% BSA:              | 5% (w/v) bovine serum albumine<br>1x TBS-T   |
| stripping buffer:           | 60 mM Tris pH 6.7<br>2% SDS<br>0.7% 2-mercaptoethanol  |
| collagenase B:              | 0,10 g/l CaCl <sub>2</sub><br>0,10 g/l MgCl <sub>2</sub> hexahydrate<br>0,20 g/l KCl<br>1x PBS w/o Ca <sup>2+</sup> , Mg <sup>2+</sup> , K |
| PI:                         | 1.176 mg/ml of trisodiumcitrat<br>0.25 mg/ml of RNase A<br>0.05 mg/ml of propidium iodide<br>0.1% Triton X-100                             |
| 4% Paraformaldehyde pH 7.4: | 4% (w/v) PFA<br>1% 1M NaOH<br>10% 10x PBS  |
| 1x TBS-Tween:               | 0.5% Tween-20<br>1x TBS  |

|                           |                                       |
|---------------------------|---------------------------------------|
| 1x PBS-Tween:             | 0.5% Tween-20<br>1x PBS               |
| Blocking buffer:          | 5% FCS<br>0.3% Triton X-100<br>1x PBS |
| Antibody Dilution Buffer: | 1% BSA<br>0,3% Triton X-100<br>1x PBS |

## 6.5 List of abbreviations

|            |   |
|------------|---|
| %          | percentage  |
| °C         | degree Celsius  |
| 2D         | two-dimensional   |
| 3D         | three-dimensional   |
| 4E-BP1     | eukaryotic initiation factor 4E (eIF4E) binding protein 1 |
| ADPKD      | autosomal recessive polycystic kidney disease             |
| AKT        | v-Akt murine thymoma viral oncogene homolog               |
| AMP        | adenosine monophosphate                                   |
| AMPK       | AMP kinase  |
| APS        | ammonium persulfate                                       |
| ATCC       | American Type Culture Collection                          |
| BAD        | Bcl-2-associated death promoter                           |
| BM         | basement membrane   |
| BME        | basement membrane extract                                 |
| BrdU       | Bromodeoxyuridine   |
| BSA        | bovine serum albumin                                      |
| c          | cells   |
| cDNA       | chromosomal DNA   |
| cm         | centimeter  |
| COX-2      | cyclooxygenase-2  |
| DAPI       | 4',6-diamidin-2'-phenylindol- dihydrochlorid              |
| DMEM       | Dulbecco's Modified Eagle Medium                          |
| DMSO       | dimethylsulfoxide   |
| DNA        | deoxyribonucleic acid                                     |
| DTT        | dithiothreitol  |
| ECL        | enhanced chemilumescence                                  |
| ECM        | extracellular matrix                                      |
| EDTA       | ethylene  |
| EGF        | epithelial growth factor                                  |
| eIF4E      | eukaryotic translation initiation factor 4E               |
| ERK        | extracellular-signal-regulated kinase                     |
| FACS       | fluorescence activated cell sorting                       |
| FCS        | fetal calf serum  |
| FKBP12     | FK506-binding protein 12                                  |
| FOXO       | forkhead box protein                                      |
| FRB domain | FKBP12-rapamycin binding domain                           |
| FSC        | forward scatter   |
| g          | gram  |
| g          | g-force   |
| GAP        | GTPase activating protein                                 |

|                                   |   |
|-----------------------------------|---|
| GβI/mLST8                         | G-protein β-subunit like protein/mammalian LST8                 |
| H2A                               | Histone H2A   |
| H2B                               | Histone H2B   |
| H <sub>2</sub> O <sub>dest.</sub> | Aqua dest.  |
| H3                                | Histone H3  |
| H4                                | Histone H4  |
| HEPES                             | 4-(2-hydroxyethyl)-1-piperazineethanesulfonic acid              |
| IMR90-2D-dense                    | IMR-90 cultured dense in 2D                                     |
| IMR90-2D-sparse                   | IMR-90 cultured sparse in 2D                                    |
| IMR90-cell-CG                     | IMR-90 cultured as single-cell suspension collagen gel          |
| IMR90-sph                         | IMR-90 cultured as spheroids                                    |
| IMR90-sph-CG-1h                   | spheroids cultured for 1 hour in collagen gel                   |
| IMR90-sph-CG-2d                   | spheroids cultured for 2 days in collagen gel                   |
| IRS                               | insulin receptor substrate                                      |
| k-d                               | knock down  |
| kDa                               | kilodalton  |
| l                                 | litre   |
| LAM                               | lymphangioliomyomatosis   |
| M                                 | Mol   |
| mA                                | milli ampere  |
| MAPK                              | mitogen-activated protein kinase                                |
| MC                                | Methylcellulose   |
| mg                                | milligram   |
| min.                              | minutes   |
| ml                                | millilitre  |
| mM                                | millimol  |
| mm                                | millimetre  |
| mm <sup>2</sup>                   | square millimetres  |
| mm <sup>3</sup>                   | cubic millimetres   |
| mRNA                              | messenger RNA   |
| mSin1                             | mammalian stress-activated protein kinase interacting protein 1 |
| MT1-MMP                           | Matrix metalloproteinase-14                                     |
| mTOR                              | mammalian target of rapamycin                                   |
| mTORC 1                           | mammalian target of rapamycin complex 1                         |
| mTORC 2                           | mammalian target of rapamycin complex 2                         |
| MW                                | molecular weight  |
| nMol                              | nano mol  |
| NP40                              | Nonidet P40   |
| NTC                               | non-targeting control   |
| p70 S6K                           | ribosomal protein S6-kinase, 70 kDa                             |
| pAKT                              | phosphorylated v-Akt murine thymoma viral oncogene homolog      |

|             |   |
|-------------|---|
| PBS         | phosphate buffered saline                                 |
| PDGF        | platelet derived growth factor                            |
| PDK1        | 3-phosphoinositide dependent protein kinase-1             |
| PET         | polyethylene terephthalate                                |
| PFA         | paraformaldehyde  |
| pH          | potentiometric hydrogen ion concentration                 |
| PI          | propidium iodide  |
| PI3K        | phosphatidylinositol 3-kinase                             |
| PIKK        | phosphoinositide 3-kinase related kinase                  |
| PIM         | protease inhibitor mix                                    |
| PMSF        | phenylmethylsulfonyl fluoride                             |
| PP2A        | protein phosphatase 2A                                    |
| PRAS40      | proline-rich AKT substrate of 40 kDa                      |
| PRR5/protor | proline-rich protein 5/protein observed with rictor       |
| pS6         | phosphorylated ribosomal protein S6                       |
| raptor      | regulatory associated protein of mTOR                     |
| Ras         | rat sarcoma   |
| rH          | relative humidity   |
| Rheb        | ras-homologue enriched in brain                           |
| rictor      | rapamycin insensitive companion of mTOR                   |
| RNA         | ribonucleic acid  |
| rpm         | rounds per minute   |
| S           | serine  |
| S6          | ribosomal protein S6                                      |
| S6K1        | ribosomal protein S6 kinase 1                             |
| S6K2        | ribosomal protein S6 kinase 2                             |
| SDS         | sodium dodecyl sulfate                                    |
| SDS-PAGE    | sodium dodecyl sulfate polyacrylamide gel electrophoresis |
| sec.        | seconds   |
| siRNA       | small interfering RNA                                     |
| sph         | spheroid  |
| SSC         | side scatter  |
| STK11/LKB1  | Serine/threonine kinase 11                                |
| T           | threonine   |
| TBS         | tris buffered saline                                      |
| TBS-T       | tris buffer saline + Triton X-100                         |
| TE          | trypsin-EDTA  |
| TEMED       | N, N, N', N'-tetramethylethylenediamine                   |
| TOS motif   | TOR signalling motif                                      |
| TSC         | tuberous sclerosis complex                                |
| TSC1        | tuberous sclerosis complex 1                              |



|      |                                    |
|------|------------------------------------|
| TSC2 | tuberous sclerosis complex 2       |
| U    | enzyme unit                        |
| V    | volt                               |
| v/v  | volume/volume                      |
| VEGF | vascular endothelial growth factor |
| w/v  | weight/volume                      |
| μ    | micro                              |
| μg   | microgram                          |
| μl   | microliter                         |
| μm   | micrometer                         |
| μM   | micromol                           |



## 6.6 Curriculum vitae

Name: Nina Kramer, nee Slabina

Date of birth: 18. August 1986

Place of birth: Vienna

Nationality: Austria

### Education:

1992-1996 Volksschule Bendagasse, Vienna, Austria

1996-2000 Hauptschule Sta. Christiana, Vienna, Austria

2000-2004 Oberstufenrealgymnasium Anton Kriegergasse, Vienna, Austria

2004-2005 study of veterinary medicine at the Veterinary University of Vienna, Austria

2005-2010 study of biology at the University of Vienna, Austria with focus on anthropology and population genetics

09.2009-08.2010 diploma thesis at the Institute of Medical Genetics, Medical University of Vienna, Austria

### List of publications:

Rosner M, Siegel N, Fuchs C, **Slabina N**, Dolznig H, and Hengstschläger M.  
Efficient siRNA-mediated prolonged gene silencing in human amniotic fluid stem cells.  
*Nat Protoc* 5: 1081-1095, 2010.

Siegel N, Rosner M, Unbekandt M, Fuchs C, **Slabina N**, Dolznig H, Davies JA, Lubec G, and Hengstschläger M.  
Contribution of human amniotic fluid stem cells to renal tissue formation depends on mTOR. *Hum Mol Genet* 19: 3320-3331, 2010